

## CURRICULUM VITAE

**Stephanie Shiffka**  
SShiffka@gmail.com  
(443) 553 9102

### Education

**Doctor of Philosophy** May 2021  
Pharmaceutical Sciences  
University of Maryland, School of Pharmacy

**Bachelor of Science, *cum laude*** 15 May 2015  
Pharmaceutical Sciences, minor in Biological Sciences  
University of Rhode Island

### Relevant Work Experience

**Peter Swaan, PhD and Maureen Kane, PhD** 12 January 2016 – 26 April 2021  
Graduate Research Assistant (Doctoral dissertation research)  
Conducted independent research relating to:

- Transporter (SLC10A2) structure, function, and evolution as compared to bile salts
- Bile acid signaling and homeostasis in hepatocytes as measured by gene product(s) protein and RNA changes
- Individual bile acid profiles as related to human and experimental non-human primate injury models measured by LC-MS/MS

**Amanda Oglesby-Sherrouse, PhD** 1 October 2015 – 20 December 2016  
Graduate Research Assistant (Additional rotation research)  
Conducted independent research pertaining to iron regulation and virulence pathways in *Pseudomonas aeruginosa* and *Staphylococcus aureus* in cystic fibrosis

**Hongbing Wang, PhD** 15 July 2015 – 30 September 2015  
Graduate Research Assistant (Additional rotation research)  
Conducted and advised on research regarding regulation of expression of the bile salt export pump (ABCB11)

**Ruitang Deng, PhD, DVM** 15  
January 2014 – 15 June 2015  
Undergraduate Faculty Research Fellowship  
University of Rhode Island  
Performed independent research on liver enzymology related to bile acid synthesis in human and murine tissue

### Applicable Skills

- Accomplished the adaption, optimization, and validation of LC-MS/MS methodology and sample preparation for quantitation of numerous bile acid, bile salt, and sterol analytes from multiple tissue and biofluid matrices
- Developed, optimized, and validated several quantitative LC-MS/MS methods in collaboration with other laboratories
- Experienced in FDA bioanalytical method validation
- Trained in Waters MassLynx and ThermoFischer Xcalibur LC-MS data analysis software
- Practiced in dissection and tissue collection of laboratory mice (esp. gall bladder, serum, liver lobules, digestive tissues)
- Accomplished the development of bacterial co-culture systems (*P. aeruginosa* and *S. aureus*)
- Proficient in mRNA collection from cells and tissues and measurement by qRT-PCR
- Proficient in protein extraction from cells and tissues and measurement by electrophoresis and chemiluminescence
- Skilled in plasmid creation, vector annealing, and plasmid DNA transformation and transfection with mammalian cells
- Proficient in maintenance and experimental use of immortalized cultured cells
- Independent supervision and maintenance of laboratory radiation safety and LC-MS/MS instrumentation
- Mentored several graduate and undergraduate students in laboratory techniques, including many of the above
- Proficient in independent experimental design and introduction
- Trained in statistical techniques and data analysis
- Talented written and oral communicator

### **Publications and Presentations**

- **Shiffka, SJ**; Jones, J; Li, L; Farese, AM; MacVittie, TJ; Wang, H; Swaan, PW; Kane, MA. “Quantification of common and planar bile acids in tissues and cultured cells.” *Journal of Lipid Research*. 2020 June.
- **Shiffka, SJ**; Kane, MA; Swaan, PW. “Planar bile acids in health and disease.” *BBA – Biomembranes*. Nov 2017; Vol 1859 (11); pp. 2269-2276.
- Valanejad, L; Ghareeb, M; **Shiffka, S**; Nadolny, C; Chen, Y; Guo, L; Verma, R; You, S; Akhlaghi, F; Deng, R. “Dysregulation of  $\Delta^4$ -3-oxosteroid 5 $\beta$ -reductase in diabetic patients: Implications and mechanisms.” *Molecular and Cellular Endocrinology*. Jul 2018; Vol 470; pp. 127-141.
- Valanejad L; Nadolny C; **Shiffka S**; Chen Y; You S; Deng R. “Differential Feedback Regulation of  $\Delta^4$ -3-Oxosteroid 5 $\beta$ -Reductase Expression by Bile Acids.” *PLoS ONE*. Jan 2017; Vol 12 (1), pp. 1-19.
- Chen, Y; Vasilenko, A; Song, X; Valanejad, L; Verma, R; You, S; Yan, B; **Shiffka, S**; Hargreaves, L; Nadolny, C; Deng, R. “Estrogen and Estrogen Receptor- $\alpha$ -Mediated Transrepression of Bile Salt Export Pump.” *Molecular Endocrinology*. Apr 2015; Vol 29 (4), pp. 613-26.

- **Shiffka, S;** Kane, MA; Swaan, PW. “Investigating the Co-evolution of ASBT and Bile Salts.” Poster presented at: AAPS PharmSci 360. 4-7 Nov 2018; Washington, D.C.
- Valanejad L; **Shiffka, S;** Verma, R; Deng, R. “Transcriptional Regulation of AKR1D1 in Bile Acid Synthesis.” Poster presented at: Pharmacogenomic Interplay in Biotransformation and Pharmacokinetics. 4-8 Aug 2014; Kingston, RI.

#### **Awards and Affiliations:**

- American Foundation for Pharmaceutical Education (AFPE) Pre-Doctoral Fellowship in Pharmaceutical Sciences (2019-2021)
- Dr. Gerald P. and Margaret M. Polli Graduate Student Travel Award (2018)
- University of Maryland, Baltimore, Department of Pharmaceutical Sciences (PSC) Fellowship and Merit Award (2018-2019)
- University of Rhode Island, College of Pharmacy Research Excellence Award (2015)
- Graduate and Undergraduate Memorial Scholarship (2014 - 2015)
- National Association of Chain Drug Stores Scholarship (2014 - 2015)
- Rho Chi Society (2017 – )
- Dean’s List (2011 - 2015)
- American Association of Pharmaceutical Sciences (2015 – )
- National Society of Collegiate Scholars (2012 – )

#### **References**

Peter W. Swaan, Ph. D.

University of Maryland, School of Pharmacy, Professor and Department Chair  
Health Sciences Facility II, 20 Penn Street, Room 621, Baltimore MD 21201

Office phone: (410) 706 0103

Email: [pswaan@rx.umaryland.edu](mailto:pswaan@rx.umaryland.edu)

Maureen A. Kane, Ph.D.

University of Maryland, School of Pharmacy, Associate Professor  
University of Maryland Mass Spectrometry Center, Executive Director  
Pharmacy Hall, 20 North Pine Street, Room 723N, Baltimore MD 21201

Office phone: (410) 706 5097

Email: [mkane@rx.umaryland.edu](mailto:mkane@rx.umaryland.edu)

## **Abstract**

**Title of Dissertation**

Bile Acids as Biomarkers and Evolutionary Phenotypes

**Author**

Stephanie J. Shiffka, Doctor of Philosophy, 2021

**Dissertation Directed by**

Maureen Kane, PhD  
Associate Professor  
Department of Pharmaceutical Sciences  
Executive Director  
Mass Spectrometry Center  
University of Maryland, Baltimore, School of  
Pharmacy

Peter Swaan, PhD  
Professor and Chair  
Associate Dean for Research  
Department of Pharmaceutical Sciences  
University of Maryland, Baltimore, School of  
Pharmacy

Bile acids (BAs) are the amphipathic end products of cholesterol metabolism and represent a critical means of cholesterol excretion. BAs have a plethora of functions, including digestive roles, homeostatic feedback loops, energy metabolism, regulation of the microbiome, inflammation, and more. These effects implicate BAs in physiological and pathological processes throughout the body, not just within the enterohepatic circuit. To date, BAs have been linked to the pathogenesis of multiple types of cancer, type 2 diabetes mellitus, metabolic syndrome, and neurological disorders, among others. In health, BA homeostasis is precisely regulated by a process termed enterohepatic circulation (EHC). Several transport proteins are instrumental to this process, and disruptions in any of these transport systems lead to dysregulation of BA homeostasis, further leading to complications such as cholestasis and liver disease. BA metabolism and the EHC are

conserved throughout vertebrate evolution, but the BA pool of more modern species has been modified to be more hydrophilic while still retaining properties of digestive surfactants. Though EHC is well-characterized, the understanding of eukaryotic transporters in this process is lacking, especially at the molecular level.

Despite the recognition of bile acids as signaling molecules involved in disease progression, there remain numerous BAs that are poorly characterized. This is especially important because BAs are an extremely diverse group of molecules that represent the effects of host and microbiome metabolism. Furthermore, the unique physicochemical properties of these variations confer these molecules with differential levels of cytotoxicity and divergent, sometimes opposing, activation of cell signaling pathways.

Thus, the scope of this dissertation is two-fold: first, to further characterize the BA pool in health and injury using cell and animal models; secondly, to use this information in order to probe the transporter responsible for the first step of the enterohepatic circulation, ASBT (SLC10A2). Completion of the first objective yielded improved understanding of BA metabolism in cell culture models and non-human primate laboratory models, as well as in radiation injury in the latter model. Accomplishment of the second objective returned insight into ASBT and BA evolution through the use of multiple vertebrate orthologs.

Bile Acids as Biomarkers and Evolutionary Phenotypes

by  
Stephanie J. Shiffka

Dissertation submitted to the Faculty of the Graduate School of the  
University of Maryland, Baltimore in partial fulfillment  
of the requirements for the degree of  
Doctor of Philosophy  
2021

© Copyright 2021 by Stephanie Shiffka  
All rights Reserved

To my mom:

I owe all of my accomplishments to your unending love and support

## **Acknowledgements**

I must start by thanking my advisors, Drs. Peter Swaan and Maureen Kane, who have provided me with endless guidance and opportunity throughout my mentorship. I believe special thanks is due to Dr. Kane, who has been an extraordinary role model to me as a female scientist since day one.

On that note, I would also like to thank the entire Department of Pharmaceutical Sciences and its leadership for constantly surrounding me with truly impressive scientific minds. Thank you especially to my committee members in the department, Drs. Hongbing Wang, James Polli, and Jace Jones, who have always kept their doors open. Thank you also to Dr. Kathleen Hillgren for serving as my external committee member and for providing me with another impressive female role model within science.

Thank you to postdocs and my fellow students within the department and especially to my lab mates, from whom I have learned so much. Thank you to friends within the department – Will, Jess, Joel, Brandon, Steph, and Amy – for keeping me going when science wasn't as fun. Thanks to Kristina San Juan, without whom we would all be lost and who is a constant beam of sunshine.

I would like to extend a very belated thank you to my undergraduate advisor – Dr. Ruitang Deng – and labmates – Leila, Chrissy, and Jessie, who ignited my passion for science and led me to this path. I am endlessly grateful that I stumbled into a research opportunity and discovered a career, and it would not have happened without you all.

Finally, my family deserves the biggest thanks. Mom, Donny, Keilly – you have never doubted me, and that must be why I rarely doubt myself. I can't imagine a life without your love, support, and unconditional confidence in me.

I must also thank my fuzzy friends, who give me purpose and joy when science does not.

To anyone I have left out, you are not forgotten. I am so grateful to every professor, teacher, mentor, friend, and classmate that has brought me to where I am today.

## Table of Contents

Acknowledgements.....	iv
Table of Contents.....	v
List of Tables.....	viii
List of Figures .....	x
List of Abbreviations .....	xi
1. Bile Acids as Digestive Molecules and Hormonal Messengers .....	1
1.1 Bile Acid Homeostasis.....	1
1.1.1 Synthesis of bile acids .....	1
1.1.2 Enterohepatic circulation of bile acids.....	3
1.3.1 Cholestasis.....	12
1.3.2 BA dysregulation in cancer.....	13
1.3.3 NAFLD, NASH, and metabolic diseases .....	15
1.3.4 BA dysregulation in other disease and injury states.....	17
1.4 Conclusions and Thesis Introduction .....	18
2. Significance and Research Objectives.....	23
2.1 Background.....	23
2.2 Research Objectives.....	26
3. Development, Optimization, and Validation of a Quantitative LC-MS/MS Assay for the Detection of Bile Acids <i>in vivo</i> and <i>in vitro</i> .....	30
3.1 Introduction.....	30
3.2 Materials and Methods.....	32
3.2.1 Chemicals and reagents. ....	32
3.2.2 Preparation of standard solutions and calibrants.....	33
3.2.3 Immortalized cell lines and culture conditions .....	33

3.2.4 Animal model .....	34
3.2.5 Sample preparation.....	34
3.2.6 Liquid chromatography-tandem mass spectrometry (LC-MS/MS) .....	37
3.3.1 Method development.....	40
4. Investigating the Co-Evolution of SLC10A2 and Bile Salts .....	71
4.1 Introduction.....	71
4.1.1 Bile acids as phenotypes of evolution.....	71
4.1.2 Planar bile acids in human health and disease.....	73
4.2 Materials and methods.....	74
4.2.1 Materials.....	74
4.2.2 Uptake assay and transporter kinetics.....	75
4.2.3 LC-MS/MS uptake analysis.....	75
4.2.4 Data analysis.....	76
4.3 Results.....	76
4.3.1 Determining sodium-dependent uptake by multiple ASBT/Asbt orthologs.....	76
4.3.2 Characterizing transport kinetics of ASBT/Asbt orthologs .....	78
4.4 Discussion.....	81
4.5 Conclusions and Future Directions.....	83
4.6 References.....	84
5. Disruption of Bile Acid Homeostasis in A Non-Human Primate Model of Radiation Injury .....	86
5.1 Introduction.....	86
5.2 Materials and Methods.....	88
5.2.1 Radiation Animal Model .....	88
5.2.2 Quantification of Bile Acids .....	90
5.2.3 qRT-PCR.....	91
5.2.4 Statistics .....	93
5.3 Results.....	93
5.3.1 Plasma.....	93
5.3.2 Bile.....	97

5.3.3 Liver Tissue .....	98
5.3.4 Planar Bile Acids .....	98
5.3.5 mRNA .....	99
5.4 Discussion.....	106
5.6 References.....	111
6. Conclusions and Future Directions .....	114
7. References.....	117

## List of Tables

<b>Table 1.1</b> Summary of the currently recognized functions and effects of bile acids.....	7
<b>Table 3.1</b> Summary of $m/z$ transitions, retention times, and collision energies used for analyte detection.....	38
<b>Table 3.2</b> Summary of linear ranges and LODs and LLOQs for BAs in this assay. These values were determined using authentic standards dissolved in mobile phase. LOD is defined as analyte peak area having $S/N > 3$ . LLOQ is represented as the lower end of the linear range and is defined as analyte peak area having $S/N > 10$ and deviation from the nominal value less than $\pm 20\%$ . The $r^2$ value reflects fit to linear regression with $1/x$ weighting. ....	43
<b>Table 3.3</b> Values are presented as mean $\pm$ standard deviation. $n \geq 5$ for all validation experiments. Recovery was obtained from the ratio of response from samples spiked with IS pre-extraction to responses from samples spiked with IS post-extraction for each matrix. Intra-day studies were performed using 4 hour intervals for each matrix. Inter-day studies were performed using 24 hour intervals for each matrix. Benchtop stability was evaluated by leaving specified matrix with spiked IS at ambient room temperature ( $23 \pm 2^\circ\text{C}$ ) for 4 hours before performing extraction. COS-1 cells grown with DMEM were used for method validation. ....	44
<b>Table 3.4</b> Concentrations of BAs found in cultured cell lysates. Determined concentration is displayed as mean $\pm$ SD.....	48
<b>Table 3.5</b> Concentrations of BAs found in medium removed from cultured cells. Determined concentration is displayed as mean $\pm$ SD.....	49
<b>Table 3.6</b> Concentrations of BAs discovered in NHP tissues. Determined concentration is displayed as mean $\pm$ SD. Units are specified separately within the table due to the wide range of concentrations.....	53
<b>Table 4.1</b> Chromatographic run used for LC-MS/MS analysis of uptake studies. ....	76
<b>Table 5.1</b> Animal identifiers, euthanasia day and type, and groupings used during analysis. ....	89
<b>Table 5.2</b> Experimental NHP groupings used for qRT-PCR.....	92
<b>Table 5.3</b> Primer sequences used in qRT-PCR.....	92
<b>Table 5.4</b> Summary of total bile acids (TBI) and conjugation in each tissue compartment. ....	96
<b>Table 5.5</b> Summary of total bile acids (A) and conjugation profiles (B) in NHP plasma. ....	100

**Table 5.6** Summary of total bile acids (A) and conjugation profiles (B) in NHP liver tissue.  
.....102

**Table 5.7** Summary of total bile acids (A) and conjugation profiles (B) in NHP bile...104

## List of Figures

<b>Figure 1.1</b> The biosynthesis of bile acids from cholesterol. ....	1
<b>Figure 1.2</b> A crude representation of the enterohepatic circulation of bile acids. ....	4
<b>Figure 2.1</b> Representative models of cholesterol and the three classes of bile salts:.....	24
<b>Figure 2.2</b> A simplified schematic of cholesterol metabolism.....	27
<b>Figure 3.1</b> Total ion chromatogram of included analytes.....	41
<b>Figure 3.2</b> Concentrations of BAs determined in human primary hepatocytes.....	47
<b>Figure 3.3</b> BA pool in immortalized cells and media .....	51
<b>Figure 3.4</b> BA pools and amidation summaries in <i>M. mulatta</i> tissue and biofluids. ....	54
<b>Figure 4.1</b> A simplified flowchart of the different types of bile acids and alcohols.....	72
<b>Figure 4.2</b> Relative amount of bile acid or derivative transported into ASBT/Asbt-transfected COS-1 cells.....	77
<b>Figure 4.3</b> Substrate kinetics studies demonstrating sodium-dependent uptake of bile acids in hASBT-transfected COS-1 cells. ....	78
<b>Figure 4.4</b> Substrate kinetics studies demonstrating sodium-dependent uptake of bile acids in pmASBT-transfected COS-1 cells. ....	79
<b>Figure 4.5</b> Substrate kinetics studies demonstrating sodium-dependent uptake of bile acids in leASBT-transfected COS-1 cells. e.....	80
<b>Figure 5.1</b> Summary of total bile acids (A) and conjugation profiles (B) in each tissue compartment of NHP.....	94
<b>Figure 5.2</b> Summary of statistically significant changes in bile acid concentration (left) and proportion of total bile acids (right) demonstrated following PBI. ....	97
<b>Figure 5.3</b> Relative changes in mRNA determined by qRT-PCR.....	99

## List of Abbreviations

3 $\beta$ -HSD	cholest-5-ene-3 $\beta$ ,7 $\alpha$ -diol-3 $\beta$ -dehydrogenase
ACA	allocholic acid
ACN	Acetonitrile
AD	Alzheimer's disease
AKR1D1	$\Delta^4$ -3-oxosteroid-5 $\beta$ -reductase
ALS	amyotrophic lateral sclerosis
ASBT	apical sodium-dependent bile salt transporter (SLC10A2)
BA	bile acid
BAAT	bile acid-CoA:amino acid N-acyltransferase
BAD	bile acid diarrhea
BAM	bile acid malabsorption
BAS	bile acid coenzyme-A synthetase
BEH	ethylene bridged hybrid
BM2.5	2.5% bone marrow sparring
BSEP	bile salt export pump (ABCB11)
CA	cholic acid

CAD	coronary artery disease
CDCA	chenodeoxycholic acid
ChREBP	carbohydrate responsive element-binding protein
CRC	colorectal cancer
CSF	cerebrospinal fluid
CTX	cerebrotendinous xanthomatosis
CYP	cytochrome P450
DCA	deoxycholic acid
DILI	drug-induced liver injury
dmAsbt	Asbt ortholog from fruit fly ( <i>Drosophila melanogaster</i> )
DMEM	Dulbecco's modified Eagle's medium
DPBS	Dulbecco's phosphate-buffered saline
EGFR	epidermal growth factor receptor
EHC	enterohepatic circulation
ESI	electrospray ionization
FBS	fetal bovine serum
FGF	fibroblast growth factor
FXR	farnesoid X receptor (NR1H4)

G	Glycine
G6Pase	glucose-6-phosphatase
GC	gas chromatography
GCA	glycocholic acid
GCDCA	glychochenodeoxycholic acid
GDCA	glycodeoxycholic acid
GI-ARS	gastrointestinal acute radiation syndrome
GLCA	glycolithocholic acid
GUDCA	glycoursodeoxycholic acid
HCC	hepatocellular carcinoma
HCM	hepatocyte culture medium
HM	high mass
HNF	hepatocyte nuclear factor
HPH	human primary hepatocyte
IACUC	institutional animal care and use committee
IALCA	isoallolithocholic acid
IBABP	ileal bile acid binding protein (FAPB6)
JNK	c-Jun N-terminal kinase

LCA	lithocholic acid
LC-MS/MS	liquid chromatography coupled to tandem mass spectrometry
leAsbt	Asbt ortholog from little skate ( <i>Leucoraja erinacea</i> )
LLOQ	lower limit of quantification
LM	low mass
LOD	limit of detection
LRH	liver receptor homolog
M-BAR	membrane bile acid receptor (TGR5/GPBAR1)
MDR	multidrug resistance protein
MHBSS	modified Hank's balanced salt solution
MOI	multi-organ injury
MRM	multiple reaction monitoring
MRP	multidrug resistance-associated protein
MS	multiple sclerosis
NAFLD	nonalcoholic fatty liver disease
NASH	nonalcoholic steatohepatitis
NHP	non-human primate
NR	nuclear receptor

NTCP	sodium-taurocholate cotransporting polypeptide (SLC10A1)
OST	organic solute transporter (SLC51)
PBC	primary biliary cholangitis
PBI	partial-body irradiation
PBS	phosphate-buffered saline
PEPCK	phosphoenolpyruvate carboxykinase
PFIC	primarily familial infantile cholestasis
PKA	protein kinase A
pmAsbt	Asbt ortholog from sea lamprey ( <i>Petromyzon marinus</i> )
PSC	primary sclerosing cholangitis
PXR	pregnane X receptor (NR1I2)
SHP	small heterodimer partner (NR0B2)
SIM	selected ion monitoring
SLC	solute carrier
SPE	solid-phase extraction
SREBP	sterol responsive element-binding protein
T	Taurine
TBA	total bile acids

TCA	taurocholic acid
TCDC	taurochenodeoxycholic acid
TDCA	taurodeoxycholic acid
TLCA	tauroolithocholic acid
UDCA	ursodeoxycholic acid
ULOQ	upper limit of quantification
UPLC	ultra-high pressure liquid chromatography
VDR	vitamin D receptor (NR1H1)

# 1. Bile Acids as Digestive Molecules and Hormonal Messengers

## 1.1 Bile Acid Homeostasis

### 1.1.1 Synthesis of bile acids

Bile acids (BAs) are synthesized in the hepatocytes from cholesterol, a C<sub>27</sub> steroid containing an alcohol group at C3, a double bond at C5, and an isooctane side chain (figure

1.1) (1, 2). Two pathways have been characterized for BA biosynthesis in humans: the neutral or classic pathway and the alternative or acidic pathway (1). The neutral pathway begins with the hydroxylation of cholesterol at

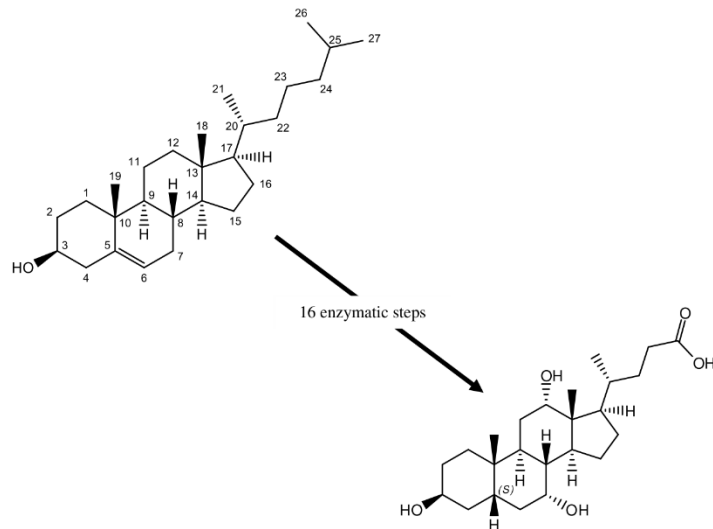


**Figure 1.1** The biosynthesis of bile acids from cholesterol through the classical pathway requires at least 16 enzymatic reactions.

(1). This enzyme is also the rate-limiting step of the classical pathway of BA biosynthesis (2, 3). Next, the planar steroidal backbone of the cholesterol molecule becomes “bent” via isomerization and subsequent saturation of the C5-C6 double bond by two enzymes: microsomal cholest-5-ene-3 $\beta$ ,7 $\alpha$ -diol-3 $\beta$ -dehydrogenase (3 $\beta$ -HSD) and cytosolic  $\Delta^4$ -3-oxosteroid-5 $\beta$ -reductase. (AKR1D1), respectively (1). These two steps result in epimerization of the A/B ring system from the *trans* to the *cis* conformation, effectively bending the steroidal backbone of the molecule (1, 4). The resultant product can be hydroxylated at the 12 $\alpha$  position by CYP8B1 or proceed without 12 $\alpha$ -hydroxylation to reduction of the C4-C5 double bond and C3 oxo group (1). Intermediates that undergo 12 $\alpha$ -

hydroxylation before this step will ultimately produce cholic acid (CA), and those that do not will become chenodeoxycholic acid (CDCA), the two primary bile acids in humans (1). Following the reduction step at the C4-C5 bond and the C3 oxo group, intermediates are hydroxylated and oxidized by CYP27A1 at the C27 position, producing a carboxylic acid group (1). The side chain is then ligated to coenzyme A by the bile acid coenzyme-A synthetase (BAS) and shortened to 24 carbon atoms by  $\beta$ -oxidation (1). Finally, BAs are amidated to either glycine or taurine via BA-CoA:amino acid N-acyltransferase (BAAT) (1). This step increases the acidity and overall solubility of BAs, allowing them to more efficiently mix with the digestive contents and preventing cytotoxicity due to their amphipathic nature (1-3). Though amidation to either glycine or taurine predominates in health by a wide margin, BAs can also be conjugate to sulfate or glucuronidated to small sugar residues (5).

The alternative pathway of BA biosynthesis is also called the acidic pathway due to the increased production of acidic intermediates in comparison to the classical pathway (5). In this pathway, cholesterol is oxidized at C27 by CYP27A1, then converted via hydroxylation by CYP7B1 into 7 $\alpha$ ,27-dihydroxycholesterol (1, 5). These intermediates then feed into the classical pathway. The alternative pathway produces mostly CDCA, while the classical pathway of BA biosynthesis produces approximately equal amounts of CDCA and CA (1, 5). Though the classical pathway predominates in health, the alternative pathway may become more active during disease or in cases of deficient CYP7A1 activity, such as during infancy (1, 5, 6). Additionally, other pathways of BA biosynthesis may be found in extrahepatic tissues; for example, oxidation of cholesterol at C24 or C25 produces

metabolites that feed into the BA synthetic pathway and represents an important mechanism of cholesterol elimination in the brain (5).

### 1.1.2 Enterohepatic circulation of bile acids

Following biosynthesis, BAs are actively transported into the bile and stored in the gall bladder (in animals that are equipped with one), then secreted into the small intestine when a fatty meal is ingested (2). Instead of being excreted with the feces, bile acids are efficiently reclaimed at the terminal end of the small intestine and transported back to the liver through the portal circulation via a series of highly specific transporters (figure 1.2) (2, 5). This cycle is termed the enterohepatic circulation (EHC) of bile acids and allows BAs to be recycled many times per day, resulting in a minute loss of approximately 0.5 grams of BAs daily (5). The total available quantity of bile acids throughout the enterohepatic tissues of the body is known as the bile acid pool and totals 2-4 grams in the human adult (2, 5).

The EHC of bile acids is made possible by multiple transporters in the bile duct, intestine, and liver epithelia acting in concert to efficiently recycle BAs. Once BAs have synthesized and amidated in the hepatocytes, they are effluxed from the liver into the bile canaliculi via the bile salt export pump (BSEP/ABCB11). Additional transporters that are primarily responsible for the efflux of phospholipids, cholesterol, and organic anions such as the MRPs (multidrug resistance-associated proteins) and MDRs (multidrug resistance proteins) can also transport BAs to a lesser extent (2, 7). From the bile canaliculi, bile acids, phospholipids, cholesterol, electrolytes, minerals, and bilirubin and biliverdin pigments are combined and concentrated in the gall bladder (6). Within the gall bladder, the amphipathic nature of bile acids allows the formation of mixed micelles

with phospholipids, solubilizing cholesterol and preventing the formation of gall stones (6).

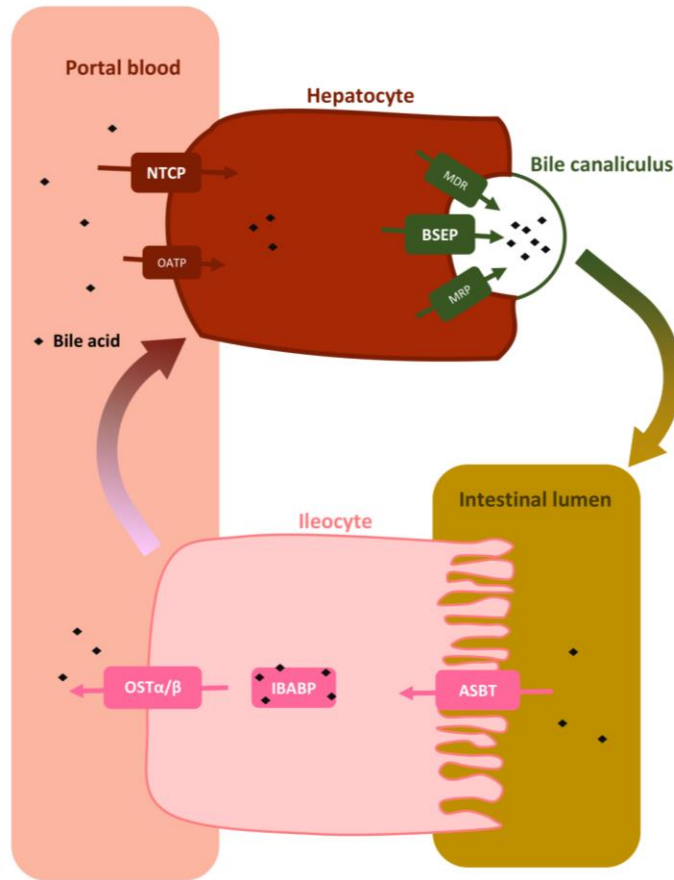


**Figure 1.2** A crude representation of the enterohepatic circulation of bile acids (represented as small diamond shapes). Major physiological compartments and transporters involved in EHC are highlighted.

The presence of dietary fats in the proximal small intestine trigger contraction of smooth muscle in the gall bladder, releasing bile into the duodenum (6). Upon reaching the distal small intestine, conjugated BAs are taken up by the secondary active transporter ASBT (apical sodium-dependent bile salt transporter/SLC10A2) (7). A minority of BAs in the intestinal lumen will be unionized and therefore subject to passive diffusion without needing ASBT-mediated transport (6, 7). Within enterocytes, BAs are thought to be

shuttled to the basolateral membrane by the ileal bile acid binding protein (IBABP) where they are exported into the portal vein via the organic solute transporter (OST)  $\alpha/\beta$  heterodimer (7). As in the hepatocytes, MRPs may also play a minor role in transporting modified BAs through the intestinal membrane (7).

From the portal bloodstream, BAs are transported across the hepatocyte sinusoidal membrane by the sodium-taurocholate cotransporting polypeptide (NTCP/SLC10A1) and the organic anion transporting polypeptide (OATP/SLCO) (7). BAs are then redirected to the bile canaliculi to begin the process anew (2, 6, 7). Under cholestatic conditions – i.e. when the hepatocyte is overloaded with BAs and risks hepatotoxicity – BAs may spill over into systemic circulation via OST $\alpha/\beta$  and MRPs (7). When this happens, free BAs are filtered by the renal glomerulus and taken up by renal ASBT for delivery back to the liver, thus minimizing urinary excretion of BAs (7).

Because BAs are exposed to the intestinal microbiota multiple times per day via the EHC, they are subjected to microbial metabolism, resulting in the formation of so-called secondary bile acids. In humans, the quantitatively most important secondary BAs are lithocholic acid (LCA) and deoxycholic acid (DCA), but the term secondary bile acid refers to any BA species that is not synthesized from the host metabolism and encompasses hundreds of potential metabolites and intermediate species (8). The formation of LCA and DCA occurs through dehydroxylation of primary BAs at C7 (7). These processes result in the conversion of CA to DCA and CDCA to LCA (7). Intestinal metabolism of primary and secondary BAs yields a wide variety of possible isomers and steroidal derivatives, all of which can vary in their micellar and hormonal capabilities (7). Notably, because it

usually includes dehydroxylation, intestinal metabolism tends to result in a more hydrophobic and, therefore, more cytotoxic BA metabolite (6, 7).

## 1.2 Functions of Bile Acids

The following functions of bile acids have been summarized in table 1.1.

### 1.2.1 Bile acids as digestive surfactants

Bile acids are first and foremost known as digestive surfactants that aid in the solubilization of dietary fats (6). The amphipathic nature of bile acids allows them to form simple micelles at high concentrations; however, because BAs are rarely circulating on their own, it is more common for them to form mixed micelles with phosphatidylcholine in the bile and with fatty acids and glycerols in the small intestine (2). In these mixed micelles, BAs are able to solubilize membrane lipids, which is critical for the digestion and absorption of dietary fats and fat-soluble vitamins A, D, E, and K (2, 6).

Bile acids have additional roles in the digestive tract that expand beyond their formation of mixed micelles. For example, BAs accelerate the digestion of dietary proteins by proteases via binding to these proteins and causing denaturation (2). Bile acids have also been found to improve calcium absorption and affect pancreatic enzyme secretion (9). Furthermore, BAs serve as antimicrobial agents that regulate the amount and species of bacteria in the intestines (9). Within the biliary tree, the transport of BAs into the bile canaliculus generates osmotic pressure that stimulates bile flow (5, 9). Similarly, certain bile acids (CDCA and DCA) act as osmosensors within the colon, stimulating secretion of water and electrolytes and colonic motility (2).

Function	Mechanism	Location
Elimination of cholesterol	Biosynthesis	Whole body
Stimulation of bile flow	Osmotic gradient driven by active transport	Bile canaliculi
Solubilization of cholesterol and prevention of gall stone formation	Micelle formation	Bile canaliculi and gall bladder
Solubilization of heavy metals	Micelle formation	Bile canaliculi and gall bladder
Secretion of fluid and electrolytes	M-BAR activation	Bile canaliculi
Solubilization of dietary fats and fat-soluble vitamins	Micelle formation	Small intestine
Feedback regulation of biosynthesis and transport	FXR activation	Small intestine and liver
Antimicrobial effects	Physiochemical/detergent properties FXR activation	Bile canaliculi, small intestine, and large intestine
Maintenance of lipid and lipoprotein metabolism	FXR activation	Whole body
Maintenance of gluconeogenesis, glycolysis, and insulin sensitivity	FXR and M-BAR activation	Liver and pancreas
Induction of phase I-III metabolic enzymes and transport proteins	FXR, VDR, and PXR activation	Liver
Maintenance of intestinal motility	M-BAR activation	Small and large intestine
Inception of anti-inflammatory cascades	M-BAR activation	Macrophages
Thermogenesis	M-BAR activation	Brown adipose tissue

**Table 1.1** Summary of the currently recognized functions and effects of bile acids.

### 1.2.2 Bile acids as signaling molecules

Bile acids have been discovered to activate a number of nuclear and cell membrane receptors and are significant players in multiple physiological signaling cascades. These include regulation of their own synthesis and transport via feedback mechanisms, glucose and energy homeostasis, lipid metabolism, and inflammation, among others (6).

#### Bile acid feedback

As demonstrated by the enterohepatic circulation, BA homeostasis is tightly regulated to minimize loss and maintain an appropriate concentration of BAs within the bile acid pool. This regulation is accomplished through a number of mechanisms. The nuclear receptor (NR) FXR (farnesoid X receptor/NR1H4) is found at the highest levels in hepatic, renal, and enteric cells and is differentially responsive to multiple BAs (2, 6, 7).

CDCA is the most efficient endogenous activator of FXR, followed by LCA and DCA, then CA (7). Activation of FXR causes repression of CYP7A1 and CYP8B1, important enzymes in the BA biosynthetic pathway, through at least two mechanisms. The first mechanism begins with the activation of hepatic FXR, causing increased expression of the small heterodimer partner (SHP/NR0B2). SHP then disrupts the positive regulatory effects of liver receptor homolog 1 (LRH-1) and hepatocyte nuclear factor 4 alpha (HNF4 $\alpha$ ) on CYP7A1 and CYP8B1 (2, 6). The second mechanism for FXR-mediated BA feedback involves the activation of ileal FXR by bile acids that have been reabsorbed from the intestinal lumen. Ileal FXR activation causes production of fibroblast growth factor 19 (FGF19), which is secreted into the circulation and, upon reaching the hepatocyte membrane, binds to the FGFR4/ $\beta$ -Klotho receptor complex (2, 6). This activates a JNK signaling cascade that represses CYP7A1 expression (6).

BA activation of FXR also modulates the expression and function of transporters involved in EHC. Hepatic FXR activation leads to increased expression of BSEP, MDR3/MDR2, and ABCG5/ABCG8 and decreased expression of NTCP, thereby increasing the efflux of bile acids and other components of bile into the biliary canaliculi while decreasing the influx of bile acids from the blood (6). Similarly, activation of ileal FXR represses the expression of ASBT, which limits the amount of bile acids in the ileocyte, while increasing expression of IBABP, presumably to aid in expedited shuttling of BAs across the cell (6, 7). As mentioned in the above section, renal FXR and ASBT play a similar role in regulating the amount of bile acids lost to the urine (7).

Bile acids in glucose and energy metabolism

Bile acid signaling is known to affect glucose and energy metabolism, mainly through activation of FXR and the membrane bile acid receptor (M-BAR/TGR5/GPBAR1) (6, 10). These effects have been demonstrated in both enterohepatic and peripheral tissues, highlighting the importance of BAs as more than just digestive molecules (10). As such, targeting BA signaling represents a potential treatment for type 2 diabetes mellitus (T2DM) and dyslipidemia.

BA-mediated hepatic FXR signaling modulates glucose levels following a meal through repression of gluconeogenesis and simultaneous induction of glycogen synthesis (10). Specifically, genes involved in lipogenesis and glycolysis, including carbohydrate responsive element-binding protein (ChREBP) and sterol responsive element-binding protein 1 (SREBP1c), are inhibited, along with gluconeogenesis genes such as phosphoenolpyruvate carboxykinase (PEPCK) and glucose-6-phosphatase (G6Pase) (10). Additionally, activation of the intestinal FXR/FGF19/FGFR4 pathway contributes to hepatic glycogen synthesis (10). There is also recent evidence that peripheral secretion of FGF19 by extraenterohepatic BAs leads to repressed glucagon secretion from the pancreas (10).

M-BAR is a G protein-coupled receptor that can be found in multiple tissues throughout the body (10). BA-mediated activation of M-BAR activates protein kinase A (PKA) pathways in these compartments. In intestinal L cells, M-BAR activation promotes secretion of glucagon-like peptide 1 (GLP-1), which further acts on the pancreas to regulate insulin secretion (10). This effect is antagonized by activation of FXR, which suppresses GLP-1 secretion in L cells but does so in a delayed fashion, causing a temporal separation between BA-mediated GLP-1 signaling (10).

M-BAR activation also induces the thyroid hormone-activating enzyme type 2 iodothyronine deiodinase, which further induces energy expenditure in brown adipose and skeletal tissue (10). Pancreatic  $\beta$  cells are equipped with both M-BAR and FXR, and activation promotes glucose-stimulated insulin secretion, while FXR activation leads to induction of insulin transcription (10).

Overall, most studies have demonstrated negative effects of intestinal FXR activation on hyperglycemia and positive effects of M-BAR signaling. Thus, one potential approach to T2DM is the combined activation of M-BAR signaling and simultaneous antagonism of intestinal FXR signaling; however, precautions would need to be taken in order to prevent peripheral effects of M-BAR activation (10).

#### The role of bile acids in inflammation

BA signaling is believed to play a part in anti-inflammatory responses with most evidence pointing towards this effect being M-BAR-mediated. Though the exact mechanisms have not been elucidated as of yet, it has been shown that M-BAR activation suppresses lipid polysaccharide (LPS)-induced production of proinflammatory cytokines and NF- $\kappa$ B phosphorylation and signaling (10). This may be especially important because M-BAR is especially present on macrophages and Kupffer cells in the liver (5). Activation of another bile acid-responsive nuclear receptor, the pregnane X receptor (PXR), also attenuates expression of NF- $\kappa$ B and proinflammatory cytokines (6). Additional studies suggest that M-BAR activation decreases macrophage infiltration into adipose tissue, leading to improved glucose and insulin sensitivity (10). Thus, there may be a link between BA-mediated glucose and energy signaling and anti-inflammatory signaling.

## Additional roles of bile acids in signaling

Multiple avenues of research regarding BA signaling are being followed and continue to reveal new discoveries. For example, it is possible that BAs affect xenobiotic or at least their own metabolism through the activation of PXR in the liver. PXR is most responsive to activation by hydrophobic secondary bile acid LCA and its metabolite, 3-keto-LCA (6). PXR activation leads to production of phase I-III enzymes and transporters that are involved in the metabolism and excretion of xenobiotics and more hydrophobic bile acids like LCA (6). As mentioned above, PXR activation also attenuates the inflammatory response by inhibiting the NF- $\kappa$ B pathway; thus, this effect may be part of the hepatic defense mechanism in cholestatic conditions.

Like PXR, LCA and its metabolite 3-keto-LCA are capable of activating another nuclear receptor, the vitamin D receptor (VDR) (6). VDR is present in the kidney, intestine, and macrophages, as well as multiple other tissues. Activation of VDR by LCA induces target genes including the CYP3A family of enzymes, which are responsible for the detoxification of hydrophobic secondary BAs and a wide array of xenobiotics (6). In addition, vitamins A and D are capable of activating separate feedback mechanisms that repress BA biosynthesis, indicating a possible balance between BAs and vitamins A and/or D (6).

### 1.3 Dysregulation of Bile Acids during Disease and Injury

Dysregulation of normally tightly regulated bile acid homeostasis has been noted in a plethora of disease and injury states, including maladies of enterohepatic and peripheral tissues. In some cases, this dysregulation is a symptom of the causative disease;

in others, BA dysregulation can cause and exacerbate related issues. In most of these cases, this is due to the aforementioned hydrophobicity and thus cytotoxicity of BAs; however, deleterious effects can also arise from skewed BA signaling.

### 1.3.1 Cholestasis

One of the most common and well-known complications of BA dysregulation is cholestasis, or buildup of bile acids within the liver and/or bile. This can occur for a number of reasons but usually is due to the absence or inhibition of BSEP at the canalicular membrane. Absence of BSEP is found as a congenital defect, so named Primary Familial Infantile Cholestasis (PFIC) type 2, and presents as severe infantile cholestasis, i.e. bile acid buildup in the hepatocytes, with accompanying jaundice (2). In these cases, the only viable treatment option is total liver transplantation (2). Less severe phenotypes can be seen in patients with mutations in other EHC transporters (11).

Inhibition of BSEP by xenobiotics can cause drug-induced liver injury (DILI), which is sometimes so severe that the injury can be fatal or require organ transplantation to save the patient. Multiple drugs can inhibit BSEP, including rifampicin, cyclosporine A, and troglitazone, the latter of which required market withdrawal due to DILI (11). Thus, preclinical studies of new drug candidates screen for cholestatic potential, and BSEP inhibition is one of the leading causes new drug candidates are pulled before or during clinical trials (11). These studies are complicated by the differences between the bile acid pools between laboratory animal models and humans; however, advances in pharmacological modeling have proven to be a potential workaround (11).

In most cases of nonfatal cholestasis and/or BSEP inhibition, regulatory feedback pathways can compensate for the nonfunctional transporter with other mechanisms of BA

excretion, preventing liver injury. As mentioned in an earlier section, sulfation and glucuronidation represent minor pathways of BA metabolism in health, but these may become more important during cholestasis (1, 11). Similarly, transporters that normally carry a very small BA load, such as MDRs, MRPs, P-GP, OATPs, and OSTs, may be able to shoulder some of the burden when the classical transporter's function is repressed.

Cholestasis can also be caused by physical blockage of the bile ducts. Primary biliary cholangitis (PBC) is a progressive autoimmune disease that causes inflammation in the intrahepatic bile duct, preventing proper bile flow (12). Primary sclerosing cholangitis (PSC) presents as a similar disease but is idiopathic and causes progressive inflammation in both intra- and extrahepatic bile ducts (12).

Regardless of the underlying cause of cholestasis, hepatocytes become overloaded with cytotoxic bile acids, which leads to inflammation, mitochondrial dysfunction, formation of reactive oxygen species, and apoptosis, all of which may also be added to by the underlying cause of the cholestatic insult (5, 11). As mentioned, untreated cholestasis that cannot be remedied through the liver's compensatory mechanisms can be fatal. Moreover, cholestasis is a common complication of other liver diseases, as detailed in the following sections.

### 1.3.2 BA dysregulation in cancer

Multiple types of cancer – including gastrointestinal, esophageal, stomach, liver, biliary, pancreatic, and intestinal cancers – are associated with dysregulation in the BA pool and/or EHC (5). Besides their cytotoxic effects, BAs are also of interest due to their activation of FXR, which may influence cell proliferation (5). The more hydrophobic bile acids have been shown to be teratogenic and carcinogenic or co-carcinogenic (5).

Hepatocellular carcinoma (HCC) is the most common type of liver cancer and one of the most deadly cancers overall (13). HCC risk factors include heavy alcohol use, hepatitis C infection, and obesity or metabolic disorder (13). Multiple studies have identified skewed BA profiles in HCC patients versus those with other types of liver injury (13, 14). Specifically, glycine-conjugated CA, DCA, and CDCA, taurine-conjugated CA, and unconjugated CDCA were decreased in HCC patients when compared with healthy controls (14). A separate study discovered similar trends with decreases seen in GCA, GDCA, TCA, and TCDCA in comparison to patients with cirrhosis (13). It is still unclear if the modified BA profile plays a causative or exacerbating role in the pathogenesis of HCC, if it plays a role at all. Efforts continue to be made to establish these changes in the BA pool as biomarkers of HCC; however, confounding factors such as diet, concomitant medications, and genetics prove to be substantial hurdles.

Colorectal cancer (CRC) is another common cancer whose development is rooted in lifestyle choices such as alcohol consumption and diet (15). The development of CRC and most of its risk factors (e.g. diet, alcohol consumption, physical activity, etc.) can profoundly modify the intestinal microbiome; in turn, the microbiome is known to influence the members of the bile acid pool (15). As noted in an above section, production of secondary bile acids by bacterial dehydroxylation creates stronger activators of VDR, M-BAR, and PXR. An overabundance of dietary fat leads to increased synthesis and circulation of primary bile acids (CA and CDCA) in order to properly digest the lipids. Increased primary BA delivery to the intestines then leads to increased bacterial metabolism of these compounds, resulting in the increased formation of secondary bile acids (LCA and DCA). Because LCA is more efficiently excreted and metabolized, DCA

is more likely to reside in the body and cause changes (15). It has been established for several decades that CRC patients have increased serum and fecal levels of DCA; furthermore, the increased proliferation of colonic mucosa is correlated with the amount of DCA in circulation (15). This is possibly through a number of mechanisms, including release of arachidonic acid due to the solubilization of local membranes by the detergent BAs (15). DCA has also been shown to be involved in transactivation of the epidermal growth factor receptor (EGFR), causing cell proliferation through the  $\beta$ -catenin signaling pathway (15). Finally, DCA can induce degradation of the tumor suppressor gene p53, thus disrupting an important defense against cancer cell proliferation (15).

In stomach and esophageal cancers, bile acids are proposed to have a contributing role due to the combination of BAs and stomach acid refluxing from the duodenum into the stomach and/or esophagus (16). Chronic esophageal and/or duodenogastric reflux is already thought to be a major risk factor for these cancers, but BAs may be an unknown mechanistic factor. In addition, the ingestion of a high animal protein and high fat diet, as with colorectal cancer, is a major risk factor for the development of other types of cancer in the digestive tract, including pancreatic, gall bladder, bile duct, and small intestinal cancers (16). As above, dietary modulation of the gut microbiome may promote the formation of a more carcinogenic BA pool.

### 1.3.3 NAFLD, NASH, and metabolic diseases

#### NAFLD, NASH, and cirrhosis

Nonalcoholic fatty liver disease (NAFLD) is one of the most common types of liver disease and is associated with metabolic dysregulation and T2DM (17, 18). If NAFLD progresses without treatment, it can develop into nonalcoholic steatohepatitis (NASH),

which further can lead to liver cirrhosis, then cancer. Save for liver transplantation, there are no approved therapies for NASH (18). The BA pool has been shown to shift towards more trihydroxy BAs (i.e. CA versus CDCA) with advancing steatosis, which would result in depressed FXR activation, which has also been demonstrated in NAFLD patients (18). Another study showed an increase in the percent of secondary bile acid DCA, which antagonizes FXR activation, with a simultaneous increase in the percent of circulating CDCA, the strongest endogenous FXR activator (17). Similarly, increased conjugated and unconjugated CA was discovered to directly associate with clinically significant fibrosis (18). Taken together, these data represent compelling evidence that BA dysregulation contributes to NAFLD and NASH progression, likely through inhibition of FXR signaling.

#### Diabetes mellitus and metabolic disorders

Type 2 diabetes mellitus (T2DM) and multiple metabolic disorders share multiple similarities, including insulin resistance and glucose intolerance, which is modulated by bile acid signaling, as reported above. Accordingly, BA metabolism is altered in T2DM, and the BA pool size is increased in this and other metabolic disorders (19, 20). Additionally, glucose and insulin can stimulate transcription of CYP7A1, the rate-limiting step of BA biosynthesis (19). In diabetic and obese patients, serum bile acids are composed of a higher ratio of CA and its bacterial metabolite DCA to CDCA and its bacterial metabolite LCA, leading to decreased FXR signaling, as above (19). This is consistent with decreased circulating FGF19 in diabetic patients (19). Thus, increase  $12\alpha$  BAs stimulate fat and cholesterol absorption and may contribute to dyslipidemia. As in the above section, diet – a major factor in the development of T2DM and metabolic disorders – affects the gut microbiome, which affects the composition of the bile acid pool. Indeed, it has been

shown that the populations of certain gut bacteria are skewed in T1DM and T2DM patients (19).

T2DM is often associated with comorbidities, such as obesity, metabolic syndrome, and cardiovascular disease (19). In obese patients, increased circulating BAs positively correlate with body mass index (BMI) and serum triglycerides (21). Due to the differential ability of BAs to induce or inhibit inflammation, it is also postulated that modifications made to the BA pool caused by changes in the microbiota in metabolic disorders plays a role in the intestinal inflammation present in many of these diseases (21). Finally, BAs are known to differentially modulate lipoprotein metabolism (21). As above, it is unclear the extent to which BAs exacerbate and/or contribute to the pathogenesis of metabolic disorders, but it is clear that they are significant players.

#### 1.3.4 BA dysregulation in other disease and injury states

##### BAs in neurodegenerative and neurological disorders

It is clear that bile acids are ubiquitous molecules that can affect and are affected by more than just the digestive system. Thus, their dysregulation has been noted in a wide variety of diseases. For example, BAs in cerebrospinal fluid (CSF) have been investigated as biomarkers in the development of Alzheimer's disease (AD); CA, CDCA, and ACA (allocholic acid, an epimer of cholic acid) concentrations in CSF distinguished AD patients from those with non-AD neurological diseases, and the concentrations of these correlated with disease severity (22). Similarly, this group reported increased BAs in the plasma of patients with Parkinson's disease (23). Additional evidence exists for the dysregulation of bile acids in other neurodegenerative and neurological disorders, including Huntington's

disease, amyotrophic lateral sclerosis (ALS), prion diseases such as Creutzfeldt-Jakob disease, multiple sclerosis (MS), and cerebrotendinous xanthomatosis (CTX) (24).

#### BAs as biomarkers for lung transplant rejection

Preclinical studies have demonstrated the utility of bile acids in predicting inflammation in lung allografts following transplantation (25). In these studies, the presence of certain BAs in bronchoalveolar lavage correlated with gastroesophageal reflux, amount of proinflammatory markers, and predictive of chronic lung allograft dysfunction (25-27). Thus, these authors have suggested the use of TCA and inflammatory factors as biomarkers to predict lung allograft inflammation and rejection.

#### BAs in cardiovascular diseases

As mentioned above, BAs are involved in glucose, lipid, and energy metabolism and are dysregulated in obesity and metabolic disorders; thus, it follows that BA homeostasis is also modified in cardiovascular diseases. Multiple studies have demonstrated the depressed fecal excretion of BAs in patients with coronary artery disease (CAD), which agrees with a lower concentration of circulating bile acids in this group (28). Moreover, decreased presence of total bile acids in serum is associated with severity of CAD and myocardial infarction (28).

#### 1.4 Conclusions and Thesis Introduction

It is clear that bile acids are important regulatory, digestive, and pathological molecules with an abundance of functions and effects. Cutting edge research is constantly taking place that furthers the understanding of these versatile compounds. One area that still remains to be explored is the function and properties of unusual subsets of bile acids, those which occupy an infinitesimal part of the BA pool during health but may become

important players during cases of dysregulated bile acid metabolism. Among these subsets are the tetra-hydroxy BAs, the iso- and oxo-BAs, and the planar BAs, which form a large basis of this thesis and will be discussed in more detail in the following chapters.

## 1.5 References

1. Alnouti Y. Bile Acid Sulfation: A Pathway of Bile Acid Elimination and Detoxification. *Toxicological Sciences*. 2009;108(2):225-46.
2. Hofmann AF, Hagey LR. Bile Acids: Chemistry, Pathochemistry, Biology, Pathobiology, and Therapeutics. *Cellular and Molecular Life Sciences*. 2008;65(16):2461-83.
3. Hofmann AF, Hagey LR. Key discoveries in bile acid chemistry and biology and their clinical applications: history of the last eight decades. *Journal of Lipid Research*. 2014;55(8):1553-95.
4. El-mir MY, Badia MD, Luengo N, Monte MJ, Marin JJG. Increased levels of typically fetal bile acid species in patients with hepatocellular carcinoma. *Clin Sci*. 2001;100:499-208.
5. Marin J, Macias R, Briz O, Banales J, Monte M. Bile Acids in Physiology, Pathology and Pharmacology. *Current drug metabolism*. 2015;17.
6. de Aguiar Vallim Thomas Q, Tarling Elizabeth J, Edwards Peter A. Pleiotropic Roles of Bile Acids in Metabolism. *Cell Metabolism*. 2013;17(5):657-69.
7. Dawson PA. Chapter 12 - Bile Acid Metabolism. In: Ridgway ND, McLeod RS, editors. *Biochemistry of Lipids, Lipoproteins and Membranes (Sixth Edition)*. Boston: Elsevier; 2016. p. 359-89.
8. Lan K, Su M, Xie G, Ferslew BC, Brouwer KLR, Rajani C, Liu C, Jia W. Key Role for the 12-Hydroxy Group in the Negative Ion Fragmentation of Unconjugated C24 Bile Acids. *Analytical Chemistry*. 2016;88(14):7041-8.
9. Monte MJ, Marin JJG, Antelo A, Vazquez-Tato J. Bile acids: chemistry, physiology, and pathophysiology. *World J Gastroenterol*. 2009;15(7):804-16.
10. Shapiro H, Kolodziejczyk AA, Halstuch D, Elinav E. Bile acids in glucose metabolism in health and disease. *The Journal of Experimental Medicine*. 2018;215(2):383.
11. Schadt HS, Wolf A, Pognan F, Chibout S-D, Merz M, Kullak-Ublick GA. Bile acids in drug induced liver injury: Key players and surrogate markers. *Clinics and Research in Hepatology and Gastroenterology*. 2016;40(3):257-66.
12. Chiang JYL, Ferrell JM. Bile Acid Metabolism in Liver Pathobiology. *Gene Expr*. 2018;18(2):71-87.
13. Resson HW, Xiao JF, Tuli L, Varghese RS, Zhou B, Tsai T-H, Nezami Ranjbar MR, Zhao Y, Wang J, Di Poto C, Cheema AK, Tadesse MG, Goldman R, Shetty K.

Utilization of metabolomics to identify serum biomarkers for hepatocellular carcinoma in patients with liver cirrhosis. *Analytica Chimica Acta*. 2012;743:90-100.

14. Xiao JF, Varghese RS, Zhou B, Nezami Ranjbar MR, Zhao Y, Tsai T-H, Di Poto C, Wang J, Goerlitz D, Luo Y, Cheema AK, Sarhan N, Soliman H, Tadesse MG, Ziada DH, Resson HW. LC–MS Based Serum Metabolomics for Identification of Hepatocellular Carcinoma Biomarkers in Egyptian Cohort. *Journal of Proteome Research*. 2012;11(12):5914-23.

15. Ridlon JM, Wolf PG, Gaskins HR. Taurocholic acid metabolism by gut microbes and colon cancer. *Gut Microbes*. 2016;7(3):201-15.

16. Bernstein H, Bernstein C, Payne CM, Dvorakova K, Garewal H. Bile acids as carcinogens in human gastrointestinal cancers. *Mutation Research/Reviews in Mutation Research*. 2005;589(1):47-65.

17. Jiao N, Baker SS, Chapa-Rodriguez A, Liu W, Nugent CA, Tsompana M, Mastrandrea L, Buck MJ, Baker RD, Genco RJ, Zhu R, Zhu L. Suppressed hepatic bile acid signalling despite elevated production of primary and secondary bile acids in NAFLD. *Gut*. 2018;67(10):1881-91.

18. Puri P, Daita K, Joyce A, Mirshahi F, Santhekadur PK, Cazanave S, Luketic VA, Siddiqui MS, Boyett S, Min HK, Kumar DP, Kohli R, Zhou H, Hylemon PB, Contos MJ, Idowu M, Sanyal AJ. The presence and severity of nonalcoholic steatohepatitis is associated with specific changes in circulating bile acids. *Hepatology*. 2018;67(2):534-48.

19. Ferrell JM, Chiang JYL. Understanding Bile Acid Signaling in Diabetes: From Pathophysiology to Therapeutic Targets. *Diabetes Metab J*. 2019;43(3):257-72.

20. Lefort C, Cani PD, Crispino M. The Liver under the Spotlight: Bile Acids and Oxysterols as Pivotal Actors Controlling Metabolism. *Cells* (2073-4409). 2021;10(2):400.

21. Agus A, Clément K, Sokol H. Gut microbiota-derived metabolites as central regulators in metabolic disorders. *Gut*. 2020;gutjnl-2020-323071.

22. Yaping Shao YOTLXLXXSLGXWL. Alteration of Metabolic Profile and Potential Biomarkers in the Plasma of Alzheimer's Disease. *Aging and disease*. 2020;11(6):1459-70.

23. Shao Y, Li T, Liu Z, Wang X, Xu X, Li S, Xu G, Le W. Comprehensive metabolic profiling of Parkinson's disease by liquid chromatography-mass spectrometry. *Molecular Neurodegeneration*. 2021;16.

24. Grant SM, DeMorrow S. Bile Acid Signaling in Neurodegenerative and Neurological Disorders. *International Journal of Molecular Sciences*. 2020;21(17):5982-.

25. Ahmed M, Levy L, Hunter SE, Zhang KC, Huszti E, Boonstra KM, Sage AT, Azad S, Zamel R, Ghany R, Yeung JC, Crespino OM, Frankel C, Budev M, Shah P, Snyder LD,

Belperio J, Singer LG, Weigt SS, Todd JL. Lung Bile Acid as Biomarker of Microaspiration and Its Relationship to Lung Inflammation. *Journal of Heart & Lung Transplantation*. 2019;38:S255-S6.

26. Zhang CYK, Ahmed M, Huszti E, Levy L, Hunter SE, Boonstra KM, Moshkelgosh S, Sage AT, Azad S, Zamel R, Ghany R, Yeung JC, Crespín OM, Frankel C, Budev M, Shah P, Reynolds JM, Snyder LD, Belperio JA, Singer LG. Bronchoalveolar bile acid and inflammatory markers to identify high-risk lung transplant recipients with reflux and microaspiration. *Journal of Heart & Lung Transplantation*. 2020;39(9):934-44.

27. Neujahr DC, Uppal K, Force SD, Fernandez F, Lawrence C, Pickens A, Bag R, Lockard C, Kirk AD, Tran V, Lee K, Jones DP, Park Y. Bile acid aspiration associated with lung chemical profile linked to other biomarkers of injury after lung transplantation. *American journal of transplantation : official journal of the American Society of Transplantation and the American Society of Transplant Surgeons*. 2014;14(4):841-8.

28. Li W, Shu S, Cheng L, Hao X, Wang L, Wu Y, Yuan Z, Zhou J. Fasting serum total bile acid level is associated with coronary artery disease, myocardial infarction and severity of coronary lesions. *Atherosclerosis (00219150)*. 2020;292:193-200.

## Chapter 2 2. Significance and Research Objectives

### 2.1 Background

The solute carrier (SLC) superfamily of uptake transporter proteins constitutes an indispensable method of nutrient acquisition, homeostasis, and xenobiotic absorption and disposition; however, many of these proteins are poorly characterized at the molecular level. No crystal structures have been obtained from eukaryotic transport proteins, so structural information has been derived from computational modeling and cellular studies as well as bacterial transporter crystal structures, which may not be an accurate representation of eukaryotic transporters (1). The Swaan laboratory's research is focused on increasing structural and mechanistic understanding of SLC member 10A2, or ASBT, as a prototypical SLC transporter. ASBT, the ileal sodium-dependent bile acid transporter, is responsible for the uptake of bile acids (BAs) from the intestine following their release from the gallbladder after a meal (1, 2). As such, it is an integral component of enterohepatic circulation and BA homeostasis. BAs are molecules produced by the liver from cholesterol with the traditional purpose of solubilizing lipids for increased intestinal absorption (3). BAs are also involved in signaling pathways, antimicrobial activity, intestinal function, and are the major route of elimination of cholesterol (3). Human ASBT exhibits high affinity for BAs, but the extent varies substantially with the structure of each individual BA (1, 2). More hydroxylated (i.e. trihydroxylated species) and unconjugated BAs are recognized with the highest affinity, while conjugated and di- and mono-hydroxylated BAs are recognized with less affinity (1). This structure specificity is important because BAs are a highly diverse group of molecules, exhibiting more structural variation than any other known class of molecules in vertebrates (4). It is currently

estimated that humans can have nearly 400 distinct BAs resulting from the highly diverse bacterial metabolism occurring within the intestine (4).

BAs are especially diverse between species. Three broad classes of bile salts have been acknowledged among vertebrates: the 27-carbon ( $C_{27}$ ) bile alcohols,  $C_{27}$  bile acids, and the 24-carbon ( $C_{24}$ ) bile acids (figure 2.1) (3, 5, 6). These groups differ in the length

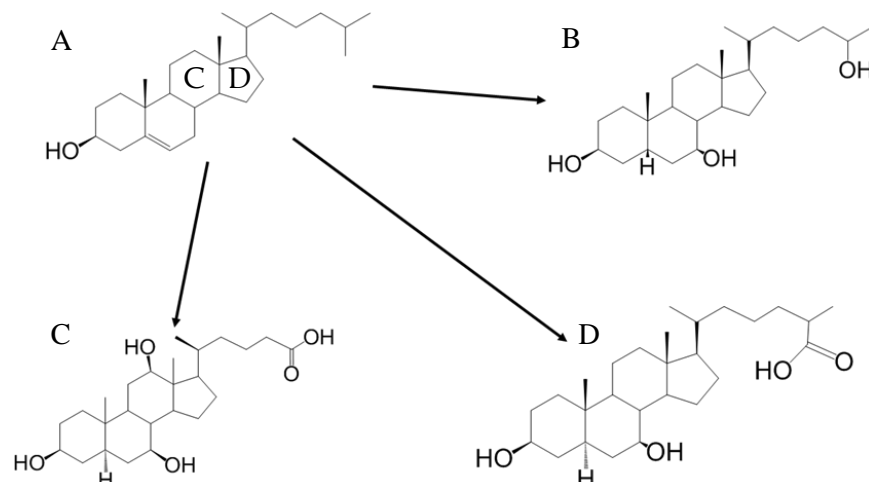


**Figure 2.1** Representative models of cholesterol (A) and the three classes of bile salts: the  $C_{27}$  bile alcohols (B),  $C_{27}$  bile acids (C), and  $C_{24}$  bile acids (D).

of the carbon side chain as well as oxidation state at C-27 (having a carboxylic acid or alcohol group). These classes can be further divided based on hydroxylation points, hydroxyl group orientation, and orientation of the ring system (3). For the most part, an individual species uses just one group or subgroup of bile salts. For example, humans and most mammals utilize  $5\beta$ - $C_{24}$  BAs – molecules with a 19-carbon steroidal ring system in which the A and B rings are *cis* to one another and a 5-carbon side chain with various hydroxylation points specific to the individual bile acid (5, 6). Earlier evolved species, however, utilize  $5\alpha$ - and  $5\beta$ - $C_{27}$  bile alcohols and acids, with the earliest extant vertebrate species using  $5\alpha$ - $C_{27}$  bile alcohols (Figure 2.1). The  $5\alpha$ - $C_{27}$  bile alcohols, unlike the BAs in most mammals, are molecules with an 8-carbon side chain instead of a 5-carbon chain,

less common hydroxylation points and ketone groups, and with an A/B *trans* ring system, as opposed to A/B *cis* (5, 6). Notably, the 5 $\beta$  configuration common in humans and most mammals results in a “bent” or “twisted” bile acid molecule, whereas the 5 $\alpha$ -BAs are planar (5, 7-9). The structural diversity of bile salts confers bile acid transporters and receptors a great deal of specificity. The affinity of ASBT for human bile salts has been previously reported by our lab and others (2).

As mentioned, there is a high degree of diversity among the bile acid pools of different species, especially of those species at distinct points of the phylogenetic tree. The 5 $\alpha$  C<sub>27</sub> bile alcohols are regarded as the ancestral bile salts, used by the evolutionary oldest extant species, whereas the 5 $\beta$  C<sub>24</sub> BAs are the most modern bile salts, used by humans and the most recently evolved mammalian species (5, 6). Thus, over time, BAs have shifted from having an 8-carbon chain and a 5 $\alpha$  A/B ring orientation to a 5-carbon chain and a 5 $\beta$  A/B ring orientation (Figure 2.1). Between these distinct points of the phylogenetic tree, species have also evolved to use 5 $\alpha/\beta$  C<sub>27</sub> BAs and 5 $\alpha$  C<sub>24</sub> BAs. Additional variance in bile salts appear in individual species as specific hydroxylation points (5, 6). For example, early aquatic species, such as lobe-finned and jawless fish use exclusively 5 $\alpha$  C<sub>27</sub> bile alcohols, and many lizards utilize 5 $\alpha$  C<sub>24</sub> BAs. Conversely, healthy humans use exclusively 3 $\alpha$ -, 7 $\alpha$ -, and/or 12 $\alpha$ -hydroxylated 5 $\beta$  C<sub>24</sub> BAs (5, 6). Interestingly, humans are also found to sometimes have the 5 $\alpha$  C<sub>24</sub> bile salts, termed the *allo* or planar bile salts, during gestation and infancy, as well as in certain disease states (10-12). Sufficient information does not exist to explain the recurrence of the *allo* BAs in humans, but a popular theory postulates that the proliferating liver – as is found in infancy, gestation, and in hepatic cancer – has incomplete enzymatic capacity due to retro-differentiation of the hepatocytes and further

that this immature hepatic state is metabolically representative of a less evolved liver (10). Additional putative pathways for the formation of planar bile acids are given in figure 2.2. Simultaneous quantitation of individual BAs is needed to elucidate the changes in the BA pool as a function of the hepatic state. The Kane lab specializes in the development and application of analytical methods for the investigation of putative biomarkers using quantitative mass spectrometry (MS). Presently, LC-MS/MS represents the most sensitive, specific, and robust methodology of quantifying bioactive small molecules such as BAs from complex biological matrices.

With the highly specific nature of ASBT's transport capabilities formerly described, we hypothesize that this transporter has evolved alongside the bile salts previously described herein. That is, the ASBT protein found in human intestine is more suited to transport human BAs and structurally similar molecules, whereas bile acid/alcohol transport proteins found in earlier evolving animals, such as lizards and fish, are specific to the bile salts used by that species. This hypothesis is instrumental to another ongoing effort by our lab: to demonstrate that specific recognition of bile salts by ASBT/SLC10A2 is unique to vertebrates, as this group comprises the only species to synthesize bile salts. Thus, we further hypothesize that eukaryotic SLC10A2 is functionally distinct from prokaryotic homologs. To this effect, we have made efforts to (1) examine the evolution of ASBT as a highly specific BA transporter and to (2) investigate the recurrence of planar BAs in injury models to determine their origin and potential effects.

## 2.2 Research Objectives

This project began with the intention of using the planar bile acids as biomarkers and determining their role in cancer, hepatitis, and/or liver regeneration. For both of these

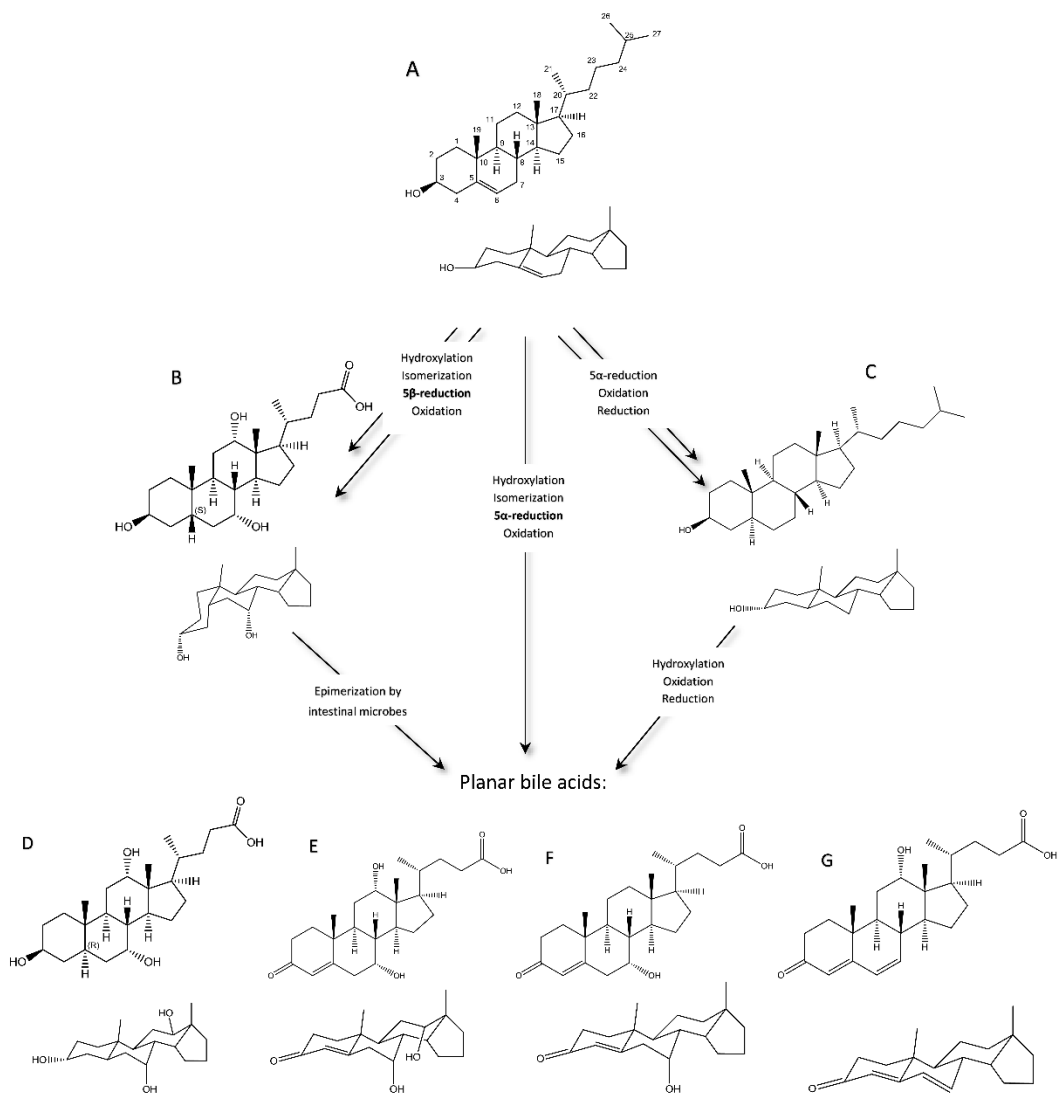


**Figure 2.2** A simplified schematic of cholesterol (A) metabolism highlighting major enzymatic changes. Cholic acid (B) is used here to represent typical human BAs, which constitute most of cholesterol metabolism. Cholestanol (C) is another metabolic product of cholesterol found in small amounts in humans. All three of these are possible precursors to planar bile acids, the most common of which are shown here: (D) allo-cholic acid; (E) 7 $\alpha$ ,12 $\alpha$ -dihydroxy-3-oxochol-4-en-24-oic acid; (F) 7 $\alpha$ -hydroxy-3-oxochol-4-en-24-oic acid; (G) 12 $\alpha$ -hydroxy-3-oxochol-4,6-dien-24-oic acid. The reaction mechanisms shown here summarize the most important enzymatic changes during the conversion of cholesterol to cholestanol or to typical 5 $\beta$  bile acids as well as summarize the likely enzymatic reactions taking place during conversion to the planar bile acids. Structures E, F, and G are also transiently formed within normal bile acid biosynthesis.

goals, it was necessary to establish and validate an analytical method to reliably separate and quantify typical and unusual BAs, preferably simultaneously. Because the planar BAs are a relatively new and unexplored area of bile acid metabolism, it would also be necessary to first benchmark the amount of these molecules in different tissues and biofluids in any laboratory models that would be used. From these requirements came the experiments detailed in Chapter 3 of this dissertation.

When it became clear that the planar bile acids that were commercially available to our laboratory possessed no signaling capacity in our preliminary studies, the focus of this project switched to examining the evolutionary timeline of BAs and their transporters, specifically ASBT. This was fortuitous, as the method developed in Chapter 3 for *in vivo* studies could also be applied to cell culture and transporter experiments, minimizing additional method development. Thus, Chapter 4 presents the investigation of multiple Asbt orthologs using representative BAs and derivatives to probe ancestral and modern BA transport.

Finally, it is clear from past research that BA homeostasis is disturbed in multiple forms of intra- and extrahepatic injury; however, information is lacking regarding changes to planar bile acid production. Chapter 5 investigates perturbation of planar and typical bile acid homeostasis following partial body irradiation in a non-human primate (NHP) model of gastrointestinal acute radiation syndrome (GI-ARS). These studies highlight the importance of examining the less populous members of the bile acid pool, including the planar BAs as well as other less commonly described subsets.

### 2.3 References

1. Swaan PW. Structural biology of the apical bile acid transporter. National Institute of Diabetes and Digestive and Kidney Diseases; 2017.
2. Lionarons DIA, Boyer JL, Cai S-Y. Evolution of substrate specificity for the bile salt transporter ASBT (SLC10A2). *Journal of Lipid Research*. 2012;53(8):1535-42.
3. Hofmann AF, Hagey LR. Bile Acids: Chemistry, Pathochemistry, Biology, Pathobiology, and Therapeutics. *Cell Mol Life Sci*. 2008;65:2461-83.
4. Lan K, Su M, Xie G, Ferslew BC, Brouwer KLR, Rajani C, Liu C, Jia W. Key Role for the 12-Hydroxy Group in the Negative Ion Fragmentation of Unconjugated C24 Bile Acids. *Anal Chem*. 2016;88(14):7041-8.
5. Hofmann AF, Hagey LR, Krasowski MD. Bile salts of vertebrates: structural variation and possible evolutionary significance. *Journal of Lipid Research*. 2010;51:226-46.
6. Hagey LR, Vidal N, Hofmann AF, Krasowski MD. Evolutionary diversity of bile salts in reptiles and mammals, including analysis of ancient human and extinct giant ground sloth coprolites. *BMC Evolutionary Biology*. 2010;10:133.
7. Mendoza ME, Monte MJ, Serrano MA, Pastor-Anglada M, Steiger B, Meier PJ, Medarde M, Marin JJG. Physiological characteristics of *allo*-cholic acid. *J Lipid Res*. 2003;44:84-92.
8. Elliott WH. The *allo* bile acids. *NATO Adv Study Inst Ser, Ser A*. 1976;A7(Hepatobiliary Syst.: Fundam. Pathol. Mech.):469-83.
9. Anderson IG, Haslewood GAD. Comparative studies of 'bile salts'. 15. The natural occurrence and preparation of *allo*cholic acid. *Biochemical Journal*. 1962;85(1):236-42.
10. El-mir MY, Badia MD, Luengo N, Monte MJ, Marin JJG. Increased levels of typically fetal bile acid species in patients with hepatocellular carcinoma. *Clin Sci*. 2001;100:499-208.
11. Kimura A, Mahara R, Inoue T, Nomura Y, Murai T, Kurosawa T, Tohma M, Noguchi K, Hoshima A, Fujisawa T, Kato H. Profile of Urinary Bile Acids in Infants and Children: Developmental Pattern of Excretion of Unsaturated Ketonic Bile Acids and 7 $\beta$ -Hydroxylated Bile Acids. *Ped Res*. 1999;45(4):603-9.
12. Shiffka SJ, Kane MA, Swaan PW. Planar bile acids in health and disease. *Biochimica et Biophysica Acta (BBA) - Biomembranes*. 2017;1859(11):2269-76.

## Chapter 3.3. Development, Optimization, and Validation of a Quantitative LC-MS/MS

### Assay for the Detection of Bile Acids *in vivo* and *in vitro*

#### 3.1 Introduction

Bile acids (BAs), the amphipathic metabolites of cholesterol, have been recognized as having a multitude of regulatory properties that extend beyond the emulsification and absorption of lipids in the gut. These many functions are discussed in detail in several recent reviews (1-5). Furthermore, these roles have implicated this extremely diverse group of molecules in the progression of many disease and injury states, including, among others: hepatic and intestinal cancer (6-8), liver steatosis and associated non-alcoholic steatohepatitis (NASH) and non-alcoholic fatty liver disease (NAFLD) (9-12), diabetes (13-15), metabolic disease (16), and drug-induced liver injury (DILI) (17). Understanding the particular changes in the BA pool that occur in these conditions can aid in diagnostic and prognostic assessments thereof. Moreover, a deeper awareness of the mechanisms that give rise to the perturbations in the BA pool during disease can assist in the understanding of hepatic and gastrointestinal function and pathology.

The biosynthetic pathway of BAs is highly complex, resulting in an exceptionally diverse pool of BAs mostly within the liver, gastrointestinal (GI) tract, bile, plasma, urine, and feces (2, 5). BAs and their derivatives can also accumulate in other tissues, especially in illness (1, 3, 5, 18). In health, the BA pool is mainly made up of conjugated primary BAs; however, in disease and following injury, dysregulation in BA synthesis and/or homeostasis can result in the accumulation of unusual and intermediate species (1, 3, 5, 19-21). Thus, the total amount of possible BA derivatives that circulate in disease is orders of magnitude more diverse than in health, demonstrating the need for a more sensitive

quantification method that captures this high heterogeneity in the multiple compartments of the BA pool.

This phenomenon of distortion in the BA pool has already been demonstrated in numerous studies in human patients in the disease states mentioned above as well as in several animal models (10, 22-28). Nevertheless, there remain multiple subsets of BAs that have yet to be characterized in much detail, if at all. Further investigation is needed to determine if the appearance of these molecules in disease is related to disease progression – either as instigators or byproducts – and if they can be used to aid in clinical detection and prognoses. Because it is still unclear exactly why, how, and which of these BA species develop in various disease states, investigating them is critical for understanding the molecular mechanisms behind these conditions. Unfortunately, due to their high degree of structural similarity, most detection methods are insufficient to simultaneously detect and differentiate the high variety of BAs (29, 30). One such case is the planar BAs, a category that differs in their 3D structure, resulting in a “flat” or “planar” conformation contrary to the more typical “bent” or “twisted” shape of the steroid backbone (1, 25, 31). The planar BAs are of interest due to their resurgence in the circulating BA pool in several types of liver diseases, but the high degree of similarity to the more abundant BAs make them challenging to detect *in vivo* (1, 23-25, 31). Historically, BA heterogeneity was detected with gas chromatography coupled to mass spectrometry (GC-MS). (8, 23, 32-34). Recently, several research groups have taken advantage of the high specificity and selectivity of liquid chromatography coupled to tandem mass spectrometry (LC-MS/MS) to reliably detect and quantify these molecules among their more typical counterparts (18,

30, 35-37). The study herein sought to build upon and extend previous methodologies and simultaneously characterize BAs *in vitro* and *in vivo*.

BA metabolism is often studied using animal models that assume similarity to human systems. Murine BA metabolism is well studied and known to have several discrepancies when compared to that of humans, but mouse and rat models are still used most often (5, 38-45). Nonhuman primate (NHP) models represent an attractive alternative because of their increased genetic resemblance to man; however, BA metabolism in NHPs has not been as well characterized (46, 47). A secondary purpose of this study was to apply the method developed herein to establish a detailed baseline profile of the BA pool in relevant tissues and biofluids in NHP, for the comparison to injury models in this animal and to humans. Similarly, cultured cell systems of human origin are also popular in studying liver physiology and pharmacology, but these models, too, are poorly detailed with regard to BA synthesis and metabolism. Examples of primary and immortalized cell systems were examined. Herein, the development, validation, and application of a sensitive UPLC-MS/MS method for the simultaneous quantification of abundant BAs, as well as uncommon and planar mammalian BA species is demonstrated in human cell lysates and cell culture media and in NHP liver tissue, bile, and plasma.

## 3.2 Materials and Methods

### 3.2.1 Chemicals and reagents.

All solvents used were of LC-MS grade or higher and purchased from Fischer Scientific (Pittsburgh, PA). Solid standards were purchased from either Sigma-Aldrich (St Louis, MO), Toronto Research Chemicals (North York, ON, Canada), Cambridge Isotope Laboratories (Tewksbury, MA), Isosciences (Ambler, PA), Bridge Organics (Vicksburg,

MI), or Steraloids (Newport, RI). 3-oxo-cholic acid was generously provided by Dr. James E. Polli's lab (University of Maryland, Baltimore, MD).

### 3.2.2 Preparation of standard solutions and calibrants

Stock solutions of each BA were prepared at 500  $\mu\text{g/mL}$  by dissolving each solid standard in 100% methanol, then sonicating in a 45°C water bath. Twelve mixed standard solutions containing between 0.05 ng/mL and 2500 ng/mL of each analyte standard (CA, GCA, TCA, CDCA, GCDCA, TCDCA, UDCA, GUDCA, ACA, IALCA, LCA, GLCA, TLCA, DCA, GDCA, TDCA, 3-oxo-CA, 3-oxo-chol-4-enic acid, and 7-alpha-hydroxy-3-oxo-chol-4-en-24-oic acid) and 50 ng/mL of each deuterium-labeled internal standard (CA-d<sub>4</sub> and GCDCA-d<sub>4</sub>) were prepared in mobile phase (1:1 ACN:water with 0.01% FA) by serial dilution. From these, calibration curves for each analyte were constructed.

### 3.2.3 Immortalized cell lines and culture conditions

COS-1 and HepG2 cells were purchased from ATCC (Manassas, VA). HuH-7 cells were a generous gift from Dr. Hongbing Wang (University of Maryland, Baltimore, Maryland). COS-1, HuH-7, and HepG2 cells were cultured in Dulbecco's modification of Eagle's medium (DMEM) supplemented with 10% fetal bovine serum (FBS), penicillin (100 IU/mL), and streptomycin (100  $\mu\text{g/mL}$ ) (Life Technologies, Inc., Rockville, MD). For the analysis of basal BA production in immortalized cell lines, cells were plated at a density of  $2.0 \times 10^6$  cells/10 cm culture dish in DMEM containing no supplements and in Hepatocyte Culture Medium (HCM) and maintained at 37°C with 5% CO<sub>2</sub> for 48 hours (Lonza, Basel, Switzerland). Human primary hepatocytes (HPHs) were obtained from BioIVT (Baltimore, MD). Hepatocytes at  $\geq 90\%$  viability were seeded at  $1.5 \times 10^6$  cells/well in a 6-well collagen coated plate in InVitroGRO CP medium (BioIVT,

Baltimore, MD). After overnight attachment at 37°C in a humidified atmosphere of 5% CO<sub>2</sub>, the culture medium was changed to complete Williams' E medium. The cells were overlaid with 0.25 mg/ml Matrigel (Corning Inc., Corning, NY) for another 24 hours before medium was switched to HCM. Medium was then aspirated and stored at -20°C until further preparation for LC/MS-MS injection. Before lysis, cells were rinsed with cold PBS. If not further processed immediately, culture dishes were stored at -80°C.

#### 3.2.4 Animal model

All animal procedures were conducted in accordance with the NIH guidelines for the care and use of laboratory animals and experiments were performed with prior approval from the University of Maryland Institutional Animal Care and Use Committee (IACUC). Animals were housed and cared for in accordance with the Animal Welfare Act at the University of Maryland's Association for Assessment and Accreditation of Laboratory Animal Care-Accredited Facility. Plasma, bile, and liver tissue were obtained from male rhesus macaques (*Macaca mulatta*) with a mean age = 4.5 y. These NHP samples were derived from a naïve, nonirradiated (no sham treatment) group of multiple irradiation studies (48-51).

#### 3.2.5 Sample preparation

HybridSPE Phospholipid 96-well plates (Sigma-Aldrich, St Louis, MO), ISOLUTE PLD+ protein and phospholipid removal plates, and ISOLUTE PLD+ phospholipid depletion columns (Biotage, Uppsala, Sweden) were used to evaluate different methods of solid-phase extraction. All SPE methods examined use solvent crash/filtration protocols to filter precipitated proteins and phospholipids from matrices with the goal of improved

signal-to-noise. Sample preparation for plasma, bile, and liver utilize the ISOLUTE PLD+ phospholipid depletion columns using procedures as described below.

#### *Cell culture sample preparation*

Cell culture medium was aspirated. 1 mL aliquots of culture medium were added to 4 mL ACN and 5 ng IS in glass culture tubes and vortexed quickly, then centrifuged at 2,000 rpm for 10 minutes. 4 mL of each supernatant was transferred to fresh glass culture tubes and dried down under N<sub>2</sub> flow. Extracts were resuspended in 100 µL 1:1 ACN:water with 0.01% FA, resulting in a final IS concentration of 50 ng/mL, and transferred to LC-MS vials, then stored at -20 °C until injection. For cells, 1 mL RIPA buffer with 5 ng each IS was added to each plate or well following PBS wash. Culture dishes were rocked at 4°C for 1 hour, then scraped. Total protein was estimated at this point using the Bradford assay. Lysates were added to 4 mL 100% ACN in glass culture tubes and vortexed quickly, then centrifuged at 2,000 rpm for 10 minutes. 4 mL of each supernatant was transferred to fresh glass culture tubes and dried down under N<sub>2</sub> flow. Extracts were resuspended in 100 µL 1:1 ACN:water with 0.01% FA, resulting in a final IS concentration of 50 ng/mL, and transferred to LC-MS vials, then stored at -20 °C until injection.

#### *Plasma and bile preparation*

ISOLUTE PLD+ phospholipid depletion columns were filled before use with 400 µL ACN with 1% FA as protein crash solvent. 5 µL of 1 ng/µL internal standard solution and 100 µL plasma aliquot were added to the column and vortexed. Flow-through was then collected into glass culture tubes by applying approximately 4 p.s.i. positive pressure by nitrogen gas. Eluates were further dried down by nitrogen flow, then resuspended in 100 µL 1:1 ACN:water with 0.01% FA for LC-MS/MS injection. If resuspensions were not

injected that day, samples were stored at  $-80^{\circ}\text{C}$ . For bile samples, the protocol was performed similarly, save that the aliquoted bile was diluted 1:9 or 1:1000 with water and  $5\ \mu\text{L}$  of  $1\ \text{ng}/\mu\text{L}$  IS or  $100\ \mu\text{L}$  of  $50\ \text{ng}/\mu\text{L}$  IS, respectively to each dilution, was added before being applied to the ISOLUTE PLD+ column. Additionally, the bile diluted pre-extraction 1:1000 with water was diluted 1:100 post-extraction by resuspending in  $100\ \mu\text{L}$  1:1 ACN:water with 0.01% FA, then diluting  $10\ \mu\text{L}$  into  $1000\ \mu\text{L}$  of 1:1 ACN:water with 0.01% FA (resulting in a final dilution factor of 1:100,000) for the analysis of highly abundant analyte species. For all dilutions, final injections contained  $50\ \text{ng}/\text{mL}$  of each IS.

#### *Liver sample preparation*

Approximately  $50\ \text{mg}$  sections of liver initially removed from the central right lobe of naïve rhesus macaques were preweighed and added to Fisherbrand™ pre-filled bead mill tubes ( $2\ \text{mL}$ ,  $1.4\ \text{mm}$  beads) with  $750\ \mu\text{L}$  50% methanol. Tissue sections were homogenized using a Precellys 24 tissue homogenizer run at  $6,500\ \text{rpm}$  for 10 seconds; tubes were then centrifuged at  $500\ x\ g$  for 1 minute.  $600\ \mu\text{L}$  of each homogenate was aspirated and spiked with IS ( $1\ \text{ng}$  each internal standard per  $10\ \text{mg}$  tissue section weight), then transferred to a new tube with  $3\ \text{mL}$  ice-cold alkaline acetonitrile (ACN with 5% *v/v*  $\text{NH}_4\text{OH}$ , equal to  $1.15\ \text{M}$   $\text{NH}_4\text{OH}$ ) and vortexed for 5 seconds. Homogenates were shaken at ambient room temperature ( $23 \pm 2^{\circ}\text{C}$ ) for 1 hour, then centrifuged at  $5,000\ x\ g$  for 10 minutes.  $3\ \text{mL}$  of each supernatant was applied to ISOLUTE PLD+ columns. Approximately 4 p.s.i. positive pressure was applied to collect flow-through into glass culture tubes. Flow-through fractions were dried under  $\text{N}_2$  flow and then resuspended in 1:1 ACN:water with 0.01% FA proportionally to starting tissue section weight and IS added. Final injections thus contained  $0.5\ \text{mg}$  of liver tissue per  $\mu\text{L}$  of resuspension. The

use of a basic crash solvent in this procedure has the disadvantage of dehydrating 7-hydroxy groups in 7-hydroxy-3-oxo-4-ene BA structures, causing loss of at least one analyte of interest during sample preparation (52).

### 3.2.6 Liquid chromatography-tandem mass spectrometry (LC-MS/MS)

#### Chromatography

The LC-MS/MS method used was adapted from Han, J. et al. 2015 (35). LC-MS/MS analysis was performed on a Waters I-Class UPLC coupled to a Waters Xevo TQ-XS triple quadrupole mass spectrometer (Waters Corporation, Milford, MA). Separation was effected by a Waters ACQUITY BEH (ethylene bridged hybrid) C<sub>18</sub> UPLC column (150 mm x 2.1 mm, 1.7 μm) using gradient elution with the following mobile phases: water with 0.01% FA (solvent A) and ACN with 0.01% FA (solvent B). The gradient was as follows: 25% to 40% solvent B in 12 minutes and then 40% to 75% solvent B in 14 minutes. Solvent B was increased to 100% over 30 seconds and held for 2 minutes to wash the column. Return to 25% B was accomplished over 30 seconds and allowed to re-equilibrate over 4 minutes. The column was maintained at 55°C with a flow rate of 350 μL/min. 2 μL of sample was injected per run.

#### Electrospray ionization tandem mass spectrometry

Detection was performed in negative ion mode using electrospray ionization (ESI). Source conditions were as follows: capillary voltage was 2.50 kV, and cone voltage was 10 V. The desolvation temperature was set to 500 °C and the source temperature to 150 °C. The desolvation gas flow operated at 800 L/hr, the cone gas flow at 150 L/hr, and the collision gas flow at 0.15 mL/min. The Q1 low mass (LM) resolution was set to 3.06 and

the (high mass) HM resolution to 14.84. The Q3 LM resolution was set to 2.73 and HM resolution to 15.11. Ion guides offset were set to 3 V and 0.3 V. Both the entrance and exit potentials were set to 1.0. Dwell time for each analyte was 7.0 milliseconds.

BA species were detected using scheduled multiple reaction monitoring (MRM) wherein each BA is detected with MRM according to a unique precursor to product ion  $m/z$  transition or selected ion monitoring (SIM) where a single ion is detected in both Q1 and Q3 with no fragmentation (Table 3.1). Each BA was further identified by their chromatographic retention time (Table 3.1).

Analyte	Mass transition	R <sub>t</sub> (min)	Collision (eV)
Lithocholic acid (LCA)	375.3 > 375.3	21.99	18
Chenodeoxycholic acid (CDCA)	391.3 > 391.3	17.22	18
Deoxycholic acid (DCA)	391.3 > 391.3	17.76	18
Ursodeoxycholic acid (UDCA)	391.3 > 391.3	13.06	18
Cholic acid (CA)	407.3 > 407.3	12.72	18
Allocholic acid (ACA)	407.3 > 407.3	12.42	18
Glycolithodeoxycholic acid (GLCA)	432.3 > 74.1	18.35	35
Glycodeoxycholic acid (GDCA)	448.3 > 74.1	14.29	35
Glycoursodeoxycholic acid (GUDCA)	448.3 > 73.9	8.69	35
Glycochenodeoxycholic acid (GCDCA)	448.3 > 73.8	13.48	35
Glycocholic acid (GCA)	464.3 > 73.9	9.00	35
Taurolithocholic acid (TLCA)	482.3 > 80.0	17.55	50
Taurodeoxycholic acid (TDCA)	498.3 > 123.8	13.05	40
Taurochenodeoxycholic acid (TCDCA)	498.3 > 80.0	11.91	50
Taurocholic acid (TCA)	514.3 > 123.9	7.89	40
Isoallothocholic acid (IALCA)	375.3 > 375.3	19.82	10
3-oxo- <i>chol</i> -4-enic acid	371.0 > 123.0	19.82	30
3-oxo-CA	405.0 > 289.0	11.88	30
7 $\alpha$ -hydroxy-3-oxo- <i>chol</i> -4-en-24-oic acid	387.0 > 263.0	13.79	28
<b>Internal standard</b>			
Cholic acid-d <sub>4</sub> (CA-d <sub>4</sub> )	411.3 > 347.3	12.72	35
Glycochenodeoxycholic acid-d <sub>4</sub> (GCDCA-d <sub>4</sub> )	452.3 > 73.8	13.48	35

**Table 3.1** Summary of  $m/z$  transitions, retention times, and collision energies used for analyte detection.

## Data processing

Data were processed using Waters MassLynx and TargetLynx software (version 4.1 SCN 901). Analyte responses were determined by the peak area of the BA, and an analyte

concentrations were determined by calibration curves constructed for each BA standard by plotting the ratio of the response for each BA to the IS response against the nominal concentration. Linearity of calibration curves was assessed through linear regression analysis using a weighting factor of  $1/x$ . Calculated concentrations of analytes were converted from ng/mL to ng/mg of starting liver tissue by dividing by a factor of 500 to reflect the theoretical 500 mg of liver tissue in every 1 mL of final prepared resuspension used for injection. Bile measurements were multiplied by their dilution factors (i.e. either x10 or x100,000) to reflect the initial dilution with water and post-extraction dilution in mobile phase.

### 3.2.7 Method validation

Method validation studies were designed by following the FDA's Guidance for Industry for Bioanalytical Method Validation for sensitivity, linear range, precision, accuracy, recovery, and bench-top stability. Because BAs are endogenous compounds and blank matrix is not feasible to obtain, the non-endogenous IS compounds were used as surrogates to validate the LC-MS/MS method. Intra- and inter-day precision was determined by injection of the same set of prepared plasma samples spiked with IS 4 and 24 hours apart, respectively. Similarly, plasma spiked with IS was left at room temperature ( $23 \pm 2^\circ\text{C}$ ) for 4 hours before performing sample preparation and compared to plasma spiked with IS prepared freshly in order to assess benchtop precision. Identical validation experiments were conducted for bile, liver tissue, and cultured cells (COS-1 cells used for validation experiments) and cell media.

### 3.2.8 Statistics

Student's T-test analyses were performed using GraphPad Prism software (version 8.3.0).

### 3.3 Results

#### 3.3.1 Method development

##### Sample preparation optimization

Initially, the protocol from Han and colleagues (35) was duplicated for use in plasma; however, this resulted in poor extraction efficiency (5-15%) with the HybridSPE-Phospholipid 96-well plates and continuously had issues with the wells becoming clogged with biological samples. However, a similar sample preparation method provided by another vendor, i.e. the ISOLUTE PLD+ protein and phospholipid removal plate, which provided better recovery but exhibited high variability between wells. Subsequently, it was determined that using the ISOLUTE PLD+ phospholipid depletion columns yielded the most robust extraction (i.e. highest and most consistent recovery and lowest coefficient of variation [CV] values) and utilized this method for the remainder of our experiments in biofluids and tissue. The protocol developed for use with these columns required less than half the time; it was also less labor- and resource-intensive than other methods (35). Biotage ISOLUTE PLD+ protein and phospholipid depletion columns were utilized for plasma, bile, and liver sample preparation. Cultured cells and media did not require solid phase extraction procedures.

##### LC-MS/MS

The LC-MS/MS assay includes 19 BA analytes and uses stable isotope-labeled internal standards (IS) (Table S3). CA-d<sub>4</sub> was used as an IS for the unconjugated BAs (LCA,

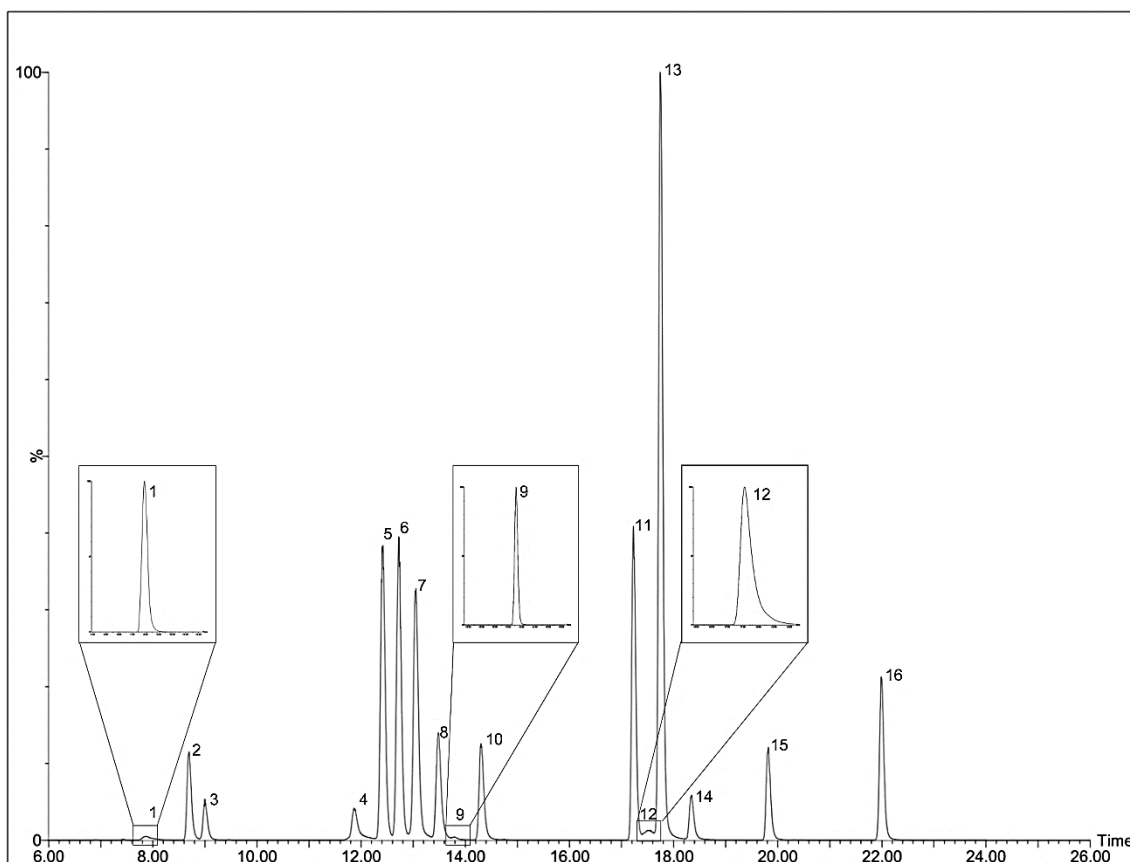


**Figure 3.1** Total ion chromatogram of included analytes inset with individual  $m/z$  transition channels for those analytes with less prominent peaks (1, 9, and 12). Authentic standards dissolved in mobile phase at 500 ng/ml each. 1: TCA; 2: GUDCA; 3: GCA; 4: TCDCA, UDCA, and 3-oxo-CA; 5: ACA; 6: CA and CA-d<sub>4</sub>; 7: TDCA; 8: GCDCA and GCDCA-d<sub>4</sub>; 9: 7 $\alpha$ -hydroxy-3-oxo-cholesterol-4-en-24-oic acid; 10: GDCA; 11: CDCA; 12: TLCA; 13: DCA; 14: GLCA; 15: IALCA and 3-oxo-cholesterol-4-enic acid; 16: LCA.

CDCA, DCA, UDCA, CA, ACA, 7 $\alpha$ -hydroxy-3-oxo-cholesterol-4-en-24-oic acid, IALCA, 3-oxo-cholesterol-4-enic acid, 3-oxo-CA), and GCDCA-d<sub>4</sub> was used as an IS for the conjugated BAs (GLCA, GDCA, GUDCA, GCA, TLCA, TDCA, TCDCA, TCA). BAs were resolved with a reverse-phase gradient UPLC separation using a 150 mm column with a sub-2  $\mu$ m particle size C<sub>18</sub> stationary phase with an ACN/water/FA-based mobile phase. Retention times ranged from 7.9 min (TCA) to 22.0 min (LCA) (Table 3.1). BAs that fragmented well were detected according to an  $m/z$  transition (Table 3.1). Some BAs exhibited poor fragmentation efficiency and were more suitably detected by monitoring the precursor ion in both Q1 and Q3 (LCA, CDCA, DCA, UDCA, CA, ACA, and IALCA). Those BAs that

share a similar nominal mass and utilize the same SRM transitions are chromatographically resolved (Fig. 3.1).

### 3.3.2 Method validation

BA sensitivity and linearity were evaluated using authentic standards for each BA. Because BAs are endogenous species, IS (CA-d<sub>4</sub> and GCDCA-d<sub>4</sub>) were used as non-endogenous BA surrogates to evaluate intra- and inter-day precision and accuracy, apparent recovery, and benchtop stability (Table 3.3).

#### Sensitivity and linearity

Sensitivity and linearity were determined by evaluating calibrants ranging in concentration from 0.05 ng/mL to 2500 ng/mL. The limit of detection (LOD) is defined as those points within the calibration curves with a signal-to-noise ratio (S/N) greater than 3. The lower limit of quantification (LLOQ) is defined as the lowest point on the calibration curve whose S/N is greater than 10 and whose calculated value is  $\leq 20\%$  of the nominal value. The LOD for BAs in this assay ranged from 0.05 ng/mL to 10 ng/mL with most BAs having LODs of 0.05-0.5 ng/mL (Table 3.2). LLOQs for the various BAs is represented by the lower limit of the calibration curves in Table 1 and were between 0.1-10 ng/mL with most BAs having LLOQs between  $\leq 0.5$  ng/mL. The most sensitive LLOQ was TLCA (0.1 ng/mL) whereas the least sensitive LLOQ was for 3-oxo-chol-4-enic acid (10 ng/mL). The upper limit of quantification (ULOQ) was 2500 ng/mL for all BAs included in this assay. Linearity was evaluated via regression coefficients ( $r^2$ ) for calibration curves, which exceeded 0.99, ranging from 0.990-0.999 (Table 3.2).

Analyte	LOD (ng/mL)	Linear range (ng/mL)	r <sup>2</sup>
Lithocholic acid (LCA)	0.5	0.5–2500	0.991
Chenodeoxycholic acid (CDCA)	0.5	0.5–2500	0.991
Deoxycholic acid (DCA)	0.1	0.5–2500	0.995
Ursodeoxycholic acid (UDCA)	0.5	0.5–2500	0.997
Cholic acid (CA)	0.1	0.5–2500	0.990
Allocholic acid (ACA)	0.5	1–2500	0.991
Glycolithocholic acid (GLCA)	0.05	0.5–2500	0.998
Glycodeoxycholic acid (GDCA)	0.05	0.5–2500	0.999
Glycoursodeoxycholic acid (GUDCA)	0.05	0.5–2500	0.999
Glychenodeoxycholic acid (GCDCA)	0.05	0.5–2500	0.997
Glycocholic acid (GCA)	0.1	0.5–2500	0.999
Tauroolithocholic acid (TLCA)	0.05	0.1–2500	0.997
Taurodeoxycholic acid (TDCA)	1	5–2500	0.995
Taurochenodeoxycholic acid (TCDCA)	0.1	1–2500	0.997
Taurocholic acid (TCA)	0.5	1–2500	0.999
Isoallothocholic acid (IALCA)	5	5–2500	0.992
3-oxo-chole-4-enic acid	10	10–2500	0.990
3-oxo-cholic acid (3-oxo-CA)	0.5	5–2500	0.990
7 $\alpha$ -hydroxy-3-oxo-chole-4-en-24-oic acid	0.5	1–2500	0.996

**Table 3.2** Summary of linear ranges and LODs and LLOQs for BAs in this assay. These values were determined using authentic standards dissolved in mobile phase. LOD is defined as analyte peak area having  $S/N > 3$ . LLOQ is represented as the lower end of the linear range and is defined as analyte peak area having  $S/N > 10$  and deviation from the nominal value less than  $\pm 20\%$ . The  $r^2$  value reflects fit to linear regression with  $1/x$  weighting.

### Precision and accuracy

Intra-day and inter-day instrument precision and accuracy were evaluated for plasma, bile, liver, cell lysate, and cell media. Intra-day precision for all matrices evaluated was less than 15%, ranging from 2.4% to 14.6% (Table 3.3). Inter-day precision was also less than 15%, ranging from 2.6 to 14.5%. (Table 3.3). Intra- and inter-day accuracy for all matrices ranged from 80.4% to 119.5% and from 88.2% to 113.3%, respectively.

Internal Standard	Recovery	Intra-day precision (4 hr)	Intra-day accuracy (4 hr)	Inter-day precision (24 hr)	Inter-day accuracy (24 hr)	Benchtop stability (4 hr)
<b>Plasma</b>						
CA-d <sub>4</sub>	45.5 (±13.2)%	8.2 (±10.8)%	95.6 (±11.9)%	8.1 (±10.8)%	88.2 (±19.7)%	11.2 (±9.0)%
GCDCA-d <sub>4</sub>	114.9 (±28.6)%	14.6 (±4.7)%	117.7 (±5.6)%	14.5 (±4.2)%	108.4 (±20.9)%	3.9 (±5.4)%
<b>Bile</b>						
CA-d <sub>4</sub>	100.0 (±28.9)%	12.7 (±5.0)%	119.5 (±26.8)%	12.4 (±1.7)%	113.3 (±2.0)%	10.5 (±8.4)%
GCDCA-d <sub>4</sub>	100.0 (±25.7)%	7.3 (±4.1)%	98.9 (±8.8)%	5.7 (±8.1)%	95.4 (±9.7)%	11.3 (±8.9)%
<b>Liver</b>						
CA-d <sub>4</sub>	73.1 (±4.2)%	8.0 (±5.6)%	80.4 (±25.8)%	9.8 (±5.8)%	108.4 (±9.9)%	13.2 (±0.2)%
GCDCA-d <sub>4</sub>	73.3 (±4.5)%	2.4 (±2.6)%	91.3 (±26.9)%	2.6 (±1.1)%	100.2 (±3.6)%	2.8 (±1.1)%
<b>Cell lysate</b>						
CA-d <sub>4</sub>	74.1 (±2.2)%	13.6 (±3.3)%	109.1 (±17.7)%	13.3 (±10.6)%	89.7 (±17.0)%	13.6 (±4.1)%
GCDCA-d <sub>4</sub>	66.0 (±8.4)%	7.8 (±7.3)%	97.1 (±10.3)%	12.6 (±13.5)%	90.0 (±13.3)%	8.0 (±7.4)%
<b>Cell medium</b>						
CA-d <sub>4</sub>	98.8 (±8.4)%	14.1 (±6.7)%	86.0 (±5.8)%	7.0 (±8.6)%	93.4 (±8.0)%	8.5 (±11.8)%
GCDCA-d <sub>4</sub>	85.5 (±4.7)%	8.0 (±8.7)%	120.0 (±24.5)%	13.6 (±11.8)%	109.8 (±21.0)%	8.5 (±9.3)%

**Table 3.3** Values are presented as mean ± standard deviation.  $n \geq 5$  for all validation experiments. Recovery was obtained from the ratio of response from samples spiked with IS pre-extraction to responses from samples spiked with IS post-extraction for each matrix. Intra-day studies were performed using 4 hour intervals for each matrix. Inter-day studies were performed using 24 hour intervals for each matrix. Benchtop stability was evaluated by leaving specified matrix with spiked IS at ambient room temperature ( $23 \pm 2^\circ\text{C}$ ) for 4 hours before performing extraction. COS-1 cells grown with DMEM were used for method validation.

### Recovery

Apparent recovery of CA-d<sub>4</sub> and GCDCA-d<sub>4</sub> in cell lysates was 74.1% and 66.0%, respectively, and in cell medium was 98.8% and 85.5%, respectively, with excellent reproducibility for each ( $< \pm 8.4\%$ ). Bile and liver had similar recovery for CA-d<sub>4</sub> and GCDCA-d<sub>4</sub>, 100% for both in bile and 73% for both in liver tissue. Variability in recovery was less for liver ( $< \pm 4.5\%$ ) than in bile ( $< \pm 28.9\%$ ). Plasma had different levels of recovery for CA-d<sub>4</sub> and GCDCA-d<sub>4</sub> with CA-d<sub>4</sub> having  $45.5 \pm 13\%$  recovery and GCDCA-d<sub>4</sub> having  $114.9 \pm 28.6\%$  recovery (Table 3.3).

### Bench-top stability

Bench-top stability was evaluated for plasma, bile, liver, cell lysate, and cell media at room temperature ( $23 \pm 2^\circ\text{C}$ ) for 4 hours. BA stability in each of the matrices was between 2.8 to 13.6% deviation of the nominal value, indicating acceptable stability (as

defined as  $\leq 15\%$ ) over this time period at these conditions in each of these matrices (Table 3.3).

### 3.3.3 Application

In order to demonstrate the utility of this method, several *in vitro* and *in vivo* model systems frequently used to study hepatic function were designated for investigation. The normal BA pools of two immortalized cell lines, as well as human primary hepatocytes, were determined. The BA levels in the liver tissue, plasma, and bile of healthy *M. mulatta*, a NHP laboratory model, were also established.

Bile acid composition of cultured cell systems.

Hepatic cell systems commonly used include two immortalized hepatoblastoma cell lines, HepG2 and HuH-7, as well as HPHs. HepG2 and HuH-7 cells are routinely grown in DMEM, whereas HPHs require a supplemented medium such as HCM. The basal levels of BAs in the immortalized cells grown in both types of media were determined for comparison to HPHs (Table 3.4, Table 3.5). Additionally, both types of medium with and without COS-1 growth were analyzed to ensure no exogenous BAs were present. For the most part, slightly more BAs were present in HCM than in unsupplemented DMEM, though this difference was only statistically significant when examining individual BAs, not total bile acids (TBA) as a whole. This was most obvious in the cases of CDCA and its taurine-conjugate, TCDCA, and was true in both the measured medium aliquots and cell lysates (Table 3.4, Table 3.5).

HuH-7 and HepG2 cells demonstrated highly similar BA compositions both intra- and extracellularly compared with one another; however, the BA pools within the cells and

in media were distinct (Table 3.4 and Table 3.5, respectively). That is, the medium removed from cultured cells exhibited primarily conjugated BAs with the highest proportions being, in descending order: TCDCA (24.8-36.3% of TBA), TCA (18.5-22.3%), GCA (9.1-16.6%), GDCA (8.2-10.7%), TDCA (7.7-9.8%), and GCDCA (6.6-10.9%) (Table 3.5, Fig. 3.2), whereas the intracellular BAs were mostly unamidated (Table 3.4, Fig. 3.2). Interestingly, the medium also revealed slightly higher concentrations of taurine-conjugated than glycine-conjugated BAs, which is contrary to the pattern found in healthy human liver (53, 54). The BA pool within the cell lysates of immortalized cells was made up nearly entirely of CA (91.7-94.5%) and ACA (4.8-7.0%) (Table 3.4, Fig. S1). This pattern was not reflected in HPHs, which exhibited high proportions of conjugated BAs (almost entirely GCA) both intra- and extracellularly (94.1% at an average of 9.1 ng/ $\mu$ g protein and 88.0% at an average of 6.3 ng/ $\mu$ g protein, respectively) (Fig. 3.2C). The remaining BA pool in HPH cell culture medium consisted of GCDCA, TCA, TCDCA,

TDCA, GDCA, TLCA, GLCA, and CA; in cells, the remaining BAs were GCDCA, TCA, CA, TCDCA, and ACA (Fig. 3.2C).

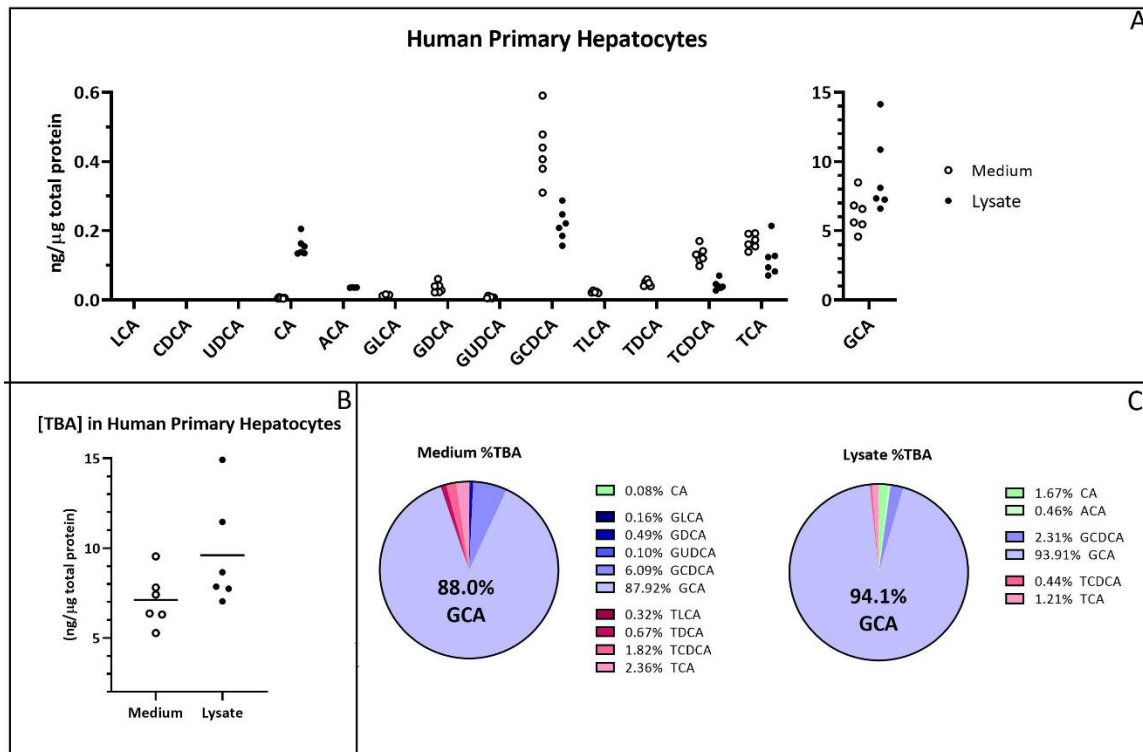


**Figure 3.2** Concentrations of BAs determined in human primary hepatocytes. A: BAs measured in HPH cell media and lysates, presented as ng/ $\mu$ g total protein. B: Concentrations of TBA measured in HPH cell media and lysates, presented as ng/ $\mu$ g total protein. C: Composition of BA pool in HPHs, presented as a average (n=6) percent of TBA. Unconjugated BAs are represented in shades of green, G-amidated BAs in shades of blue, and T-amidated BAs in shades of red. Constructed from data in Tables 2 and 3.

BA in cultured cell lysates	HuH-7 HCM <sup>a</sup>	HuH-7 DMEM <sup>a</sup>	HepG2 HCM <sup>a</sup>	HepG2 DMEM <sup>a</sup>	HPH HCM <sup>b</sup>
<i>Unconjugated</i>					
LCA	230 ± 32.3	162 ± 40.2	325 ± 101	339 ± 168	336 ± 248
CDCA	0.270	0.185 ± 0.088	0.353 ± 0.187	0.174 <sup>c</sup>	<LOD
DCA	3.40 ± 1.89 <sup>c</sup>	<LOD/LLOQ	1.09 ± 0.06	<LOD	<LOD
CA	<LOD	<LOD	<LOD	<LOD	<LOD
ACA	212 ± 25.2	150 ± 36.3	308 ± 97.3	315 ± 156	155 ± 27.2
UDCA	15.9 ± 6.3	11.5 ± 4.1	15.5 ± 3.2	23.4 ± 12.8	36.0 ± 0.6
	0.783 <sup>c</sup>	<LOD	<LLOQ	<LOD	<LOD
<i>Glycine-conjugated</i>					
GLCA	0.0007 ± 0.0006	0.053 ± 0.031 <sup>c</sup>	0.127 ± 0.097	0.081 ± 0.050	9,270 ± 2,950
GCDCA	<LOD	<LOD	<LOD	<LOD	<LOD
GDCA	0.0002 ± 0.0002	0.031 <sup>c</sup>	0.127 ± 0.097	0.081 ± 0.050	218 ± 45.9
GCA	0.0008 <sup>c</sup>	<LOD	<LOD/LLOQ	<LOD/LLOQ	<LOD
GUIDCA	<LOD/LLOQ	0.07 <sup>c</sup>	<LOD	<LLOQ	9,060 ± 2,910
	<LOD	<LOD	<LOD	<LOD/LLOQ	<LOD
<i>Taurine-conjugated</i>					
TLCA	<LOD	1.17 ± 0.90 <sup>c</sup>	<LOD	2.04 <sup>c</sup>	161 ± 65.9
TCDCa	<LOD	<LOD	<LOD	<LOD	<LOD
TDCA	<LOD	1.17 ± 0.890 <sup>c</sup>	<LOD	2.04 <sup>c</sup>	42.7 ± 14.9
TCA	<LOD	<LOD	<LOD	<LOD	<LOD
	<LOD	<LOD	<LOD	<LOD	119 ± 51.9
TBA	231 ± 32.3	162 ± 41.0	326 ± 100	340 ± 170	9,610 ± 3,020

**Table 3.4** Concentrations of BAs found in cultured cell lysates. Determined concentration is displayed as mean ± SD.

*a* Values are presented as picograms per microgram of total protein corresponding to cells grown to confluence in n = 3 10 cm dishes over 48 h containing 10 ml total medium per plate.

*b* Values are presented as picograms per microgram of total protein corresponding to cells grown to confluence in n = 6 wells of a 6-well plate over 48 h containing 2 ml total medium per well per 24 h.

*c* Indicates at least one value <LLOQ and, thus, not included (n < 3 for HepG2 and HuH-7 cells).

BA in culture medium	HuH-7 HCM <sup>a</sup>	HuH-7 DMEM <sup>a</sup>	HepG2 HCM <sup>a</sup>	HepG2 DMEM <sup>a</sup>	HPH HCM <sup>b</sup>
<i>Unconjugated</i>					
LCA	<LLOQ	31.5 ± 4.1	24.7 ± 10.9	14.3 ± 13.7	5.4 ± 1.6
CDCA	<LOD	0.61 ± 0.12 <sup>c</sup>	9.82 ± 2.21	1.91 <sup>c</sup>	<LOD
DCA	<LOD	31.1 ± 4.5	4.0 <sup>c</sup>	13.7 ± 14.3	<LOD
CA	<LOD	<LOD	<LOD	<LOD	<LOD
ACA	<LOD	<LOD	3.10 <sup>c</sup>	<LOD	5.40 ± 1.57
UDCA	<LOD	<LOD	<LOD/LLOQ	<LOD	<LOD
			16.3 ± 13.8	<LOD	<LOD
<i>Glycine-conjugated</i>					
GLCA	121 ± 37.2	81.0 ± 14.3	192 ± 68.4	200 ± 89.3	6,750 ± 1,460
GCDCA	8.03 ± 0.62	<LOD/LLOQ	12.20 ± 6.49	18.0 <sup>c</sup>	11.50 ± 3.44
GDCA	29.2 ± 7.1	23.3 ± 3.1	45.7 ± 18.3	54.1 ± 28.5	434 ± 95.6
GCA	41.8 ± 20.4	19.9 ± 6.02	66.7 ± 21.3	61.5 ± 14.4 <sup>c</sup>	35.7 ± 14.8
GUCCA	41.6 ± 9.1	34.5 ± 4.4	66.5 ± 24.6	80.3 ± 35.2	6,260 ± 1,360
	0.55 <sup>c</sup>	0.58 ± 0.15	1.31 <sup>c</sup>	2.34 ± 2.08 <sup>c</sup>	7.45 ± 2.73
<i>Taurine-conjugated</i>					
TLCA	264 ± 68.5	131 ± 21.5	450 ± 154	275 ± 134	365 ± 34.8
TCDCA	12.2 ± 4.04	4.36 ± 0.95	13.3 ± 5.69	6.86 ± 1.59 <sup>c</sup>	22.9 ± 2.80
TIDCA	129 ± 44.1	59.6 ± 6.3	244 ± 85.0	135 ± 68.7	130 ± 24.6
TCA	38.2 ± 12.4	22.1 ± 5.2	62.1 ± 32.3	39.4 ± 24.2	48.1 ± 7.6
	85.1 ± 16.1	45.0 ± 9.9	130 ± 38.2	96.7 ± 45.0	169 ± 21.1
TBA	386 ± 105	244 ± 36.5	666 ± 217	490 ± 236	7,120 ± 1,490

**Table 3.5** Concentrations of BAs found in medium removed from cultured cells. Determined concentration is displayed as mean ± SD.

*a* Values are presented as picograms per microgram of total protein corresponding to cells grown to confluence in n = 3 10 cm dishes over 48 h containing 10 ml total medium per plate.

*b* Values are presented as picograms per microgram of total protein corresponding to cells grown to confluence in n = 6 wells of a 6-well plate over 48 h containing 2 ml total medium per well per 24 h.

*c* Indicates at least one value <LLOQ and, thus, not included (n < 3 for HepG2 and HuH-7 cells).

Both the immortalized and the primary cells exhibited levels of secondary BAs (namely, UDCA, LCA, and DCA and their conjugates) to some extent, though this was much more pronounced in the HepG2 and HuH-7 cell lines and especially true for DCA and its amidated conjugates (Tables 3.4, Table 3.5, Fig. 3.3). In HPHs, these species were only detectable in conjugated forms (G- and T-amidated) in the culture medium (Fig. 3.2). Secondary BAs are often reported to be synthesized by bacterial species within the gut; however, it has become clear in recent years that this is not their exclusive origin (1, 3, 5, 55-57).

Additionally, there were similar intracellular and extracellular levels of TBA produced in both lines of immortalized cells, totaling 240-670 pg BAs/ $\mu$ g total protein in medium and 160-340 pg BAs/ $\mu$ g total protein in cell lysates (Table 3.4, Table 3.5). HPHs demonstrated much higher levels of basal BAs, approximately 30-60 times the amount of BAs/ $\mu$ g of protein in cell lysates and 10-30 times the amount of BAs/ $\mu$ g of protein in culture medium than immortalized cells. Specifically, HPHs had an average intracellular TBA of 9.6 ng/ $\mu$ g total protein and an average extracellular TBA of 7.1 ng/ $\mu$ g total protein (Tables 3.4, Table 3.5, Fig. 3.3B).

Bile acid composition in plasma, bile, and liver tissue from a NHP model.

Naïve NHP plasma, bile, and liver tissue were examined to determine detailed baseline information of the BA pool for later comparison to liver and gut injury models in these animals as well as to humans. In plasma, CDCA and its taurine and glycine conjugates predominated with the unconjugated BA as the most abundant. Hence, within plasma, unconjugated BAs were the most abundant species, totaling an estimated average of 73% of TBA with 69% of this being CDCA (Fig 3.4A). Glycine-conjugated and taurine-

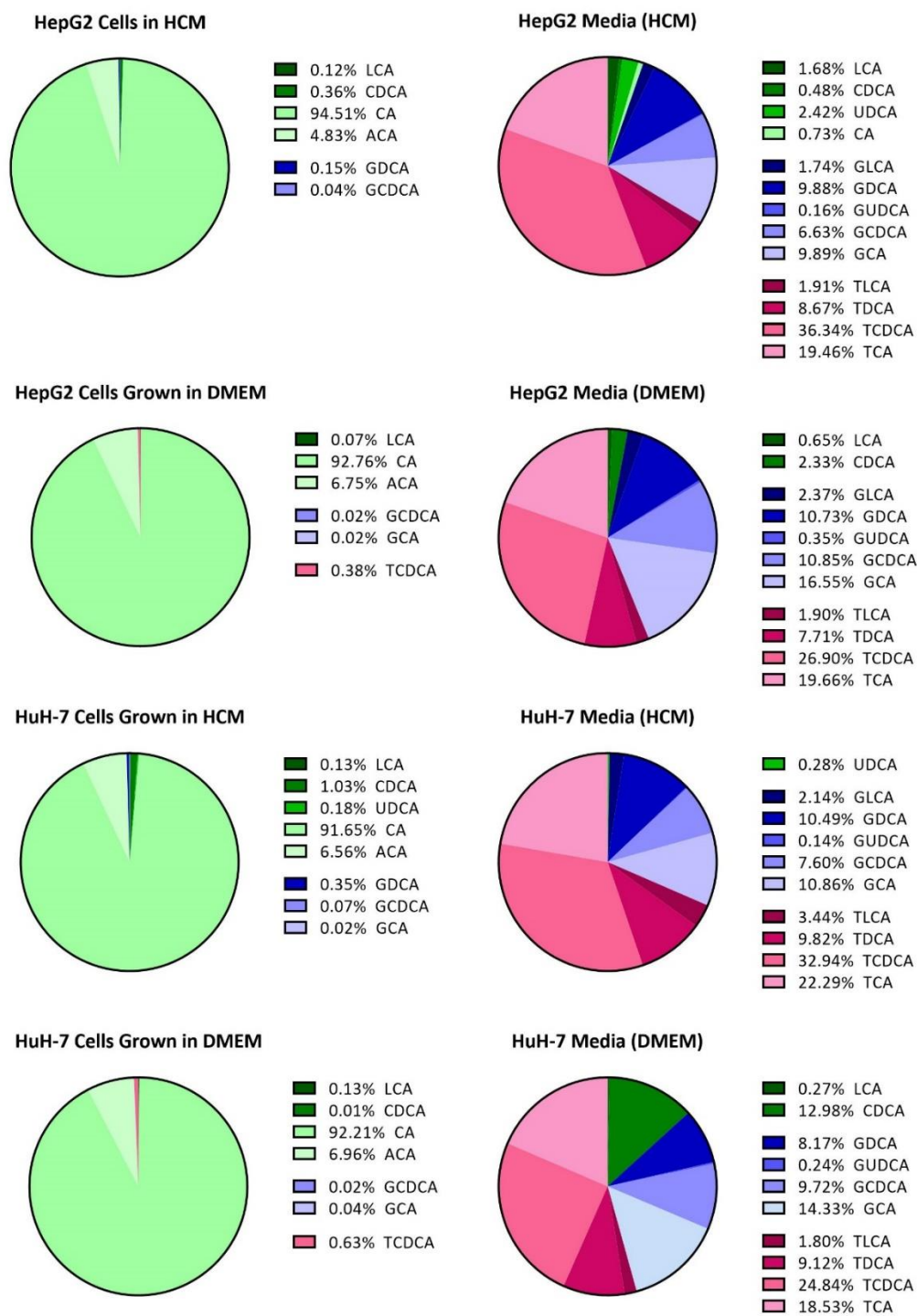


**Figure 3.3** BA pool in immortalized cells and media, presented as average (n=3) percent of TBA. Unconjugated BAs are represented in shades of green, G-amidated BAs in shades of blue, and T-amidated BAs in shades of red.

conjugated BAs made up averages of approximately 10% and 17% of the plasma BA pool, respectively, again being mostly conjugates of CDCA (Fig. 3.4A). Total circulating BAs ranged from 1.17-2.58  $\mu\text{g/mL}$  and averaged 1.82  $\mu\text{g/mL}$  (Table 3.6).

BA profiles within NHP bile and liver tissue were very similar to one another. In both, conjugated BAs – specifically TCDCA and TCA – dominated the BA pool. In bile, TCDCA occupied an average of nearly half of BA species (40.5% of TBA) at 180.7 mg/mL (Table 3.6, Fig. 3.4). TCDCA concurrently made up an average of approximately one-fourth of the BA pool in liver (26.5% of TBA) at 17.9 ng/mg tissue (Fig. 3.3C). On average, TCA comprised 21% (89 mg/mL) of the BA pool in bile and 29.1% in liver tissue (32 ng/mg tissue). The succeeding most abundant BA species were also very similar between liver and bile. In bile, the next most prominent BA species were, in descending order: GCA (13.8% of TBA), GDCA (9.8%), GCDCA (6.3%), and TDCA (5.4%) (Fig. S3B). In liver, the next most abundant BAs were GCA (18.7% of TBA), GCDCA (9.8%), GDCA (6.4%), and TDCA (5.7%) (Fig. 3.3C). In total, conjugated BAs made up most of both the bile and liver BA pools in similar ratios, with taurine-conjugated species comprising 68.6% (bile) and 62.3% (liver) and glycine-conjugated species making up 31.4% (bile) and 36.3% (liver) of TBA, on average. Thus, conversely to plasma, unconjugated BAs were minor constituents and totaled less than 1.5% TBA in liver and 0.004% TBA in bile, reflecting the high proficiency of the healthy hepatic conjugative enzyme systems. TBA in bile ranged between 378 mg/mL and 485 mg/mL (Table 3.6), an average of roughly 430 mg/mL. In liver, TBA was highly variable and ranged between 19.5 ng/mg tissue and 175.5 ng/mg tissue, averaging 97.5 ng/mg tissue. The high variability is a consequence of this study's small sample size and *ad libitum* feeding; additional samples and control of

fasting/feeding status would provide a better indication of TBA concentration, as well as individual BA concentration, in healthy *M. mulatta* liver and bile.

BA	Plasma (n=7)	Bile (n=2)	Liver tissue (n=2)
	<i>ng/mL</i>	<i>μg/mL</i>	<i>pg/mg tissue</i>
<i>Unconjugated</i>	1360 ± 592	16.8 ± 1.36	477 ± 70.0
LCA	45.6 ± 46.4	0.8 ± 0.8	7.40 ± 7.6
CDCA	1300 ± 601	1.5 ± 0.9	403 ± 110
DCA	<LOD	2.0 ± 1.4	<LOD
CA	13.0 ± 7.4	12.5 ± 0.1	57.9 ± 43.5
ACA	<LOD	0.0062 ± 0.0008	<LOD
UDCA	4.0 ± 2.6	0.024 ± 0.03	1.3 <sup>c</sup>
7α-hydroxy-3-oxo- chol-4-en-24-oic acid	<LOD	0.01 ± 0.006	<LOD
3-oxo-cholic acid	<LOD	<LLOQ	<LOD
	<i>ng/mL</i>	<i>mg/mL</i>	<i>ng/mg tissue</i>
<i>Glycine-conjugated</i>	164 ± 118	133 ± 7.0	37.8 ± 44.2
GLCA	11.8 ± 6.05	5.95 ± 3.5	1.6 ± 2.1
GCDCA	78.1 ± 77.9	27.7 ± 10.6	8.3 ± 8.6
GDCA	22.9 ± 12.7	40.6 ± 14.3	9.0 ± 11.9
GCA	50.5 ± 33.0	58.5 ± 0.08	18.7 ± 21.5
GUDCA	0.7 ± 0.4	211 ± 76.6	0.22 ± 0.25
	<i>ng/mL</i>	<i>mg/mL</i>	<i>ng/mg tissue</i>
<i>Taurine-conjugated</i>	296 ± 179	299 ± 82.8	59.2 ± 66.2
TLCA	15.9 ± 4.1	6.9 ± 4.8	1.21 ± 1.54
TCDCA	234 ± 166	181 ± 99.9	17.9 ± 15.3
TDCA	23.7 ± 5.1	21.6 ± 15.1	8.13 ± 10.9
TCA	32.5 ± 16.3	89.4 ± 2.8	32.0 ± 38.5
	<i>μg/mL</i>	<i>mg/mL</i>	<i>ng/mg tissue</i>
TBA	1.82 ± 0.59	431 ± 75.8	97.5 ± 110

**Table 3.6** Concentrations of BAs discovered in NHP tissues. Determined concentration is displayed as mean ± SD. Units are specified separately within the table due to the wide range of concentrations.

a Values are in nanograms per milliliter.

b Values are in micrograms per milliliter.

c Values are picograms per milligram of tissue.

d Indicates at least one value was <LLOQ and was not included.

e Values are in milligrams per milliliter.

f Values nanograms per milligram of tissue.

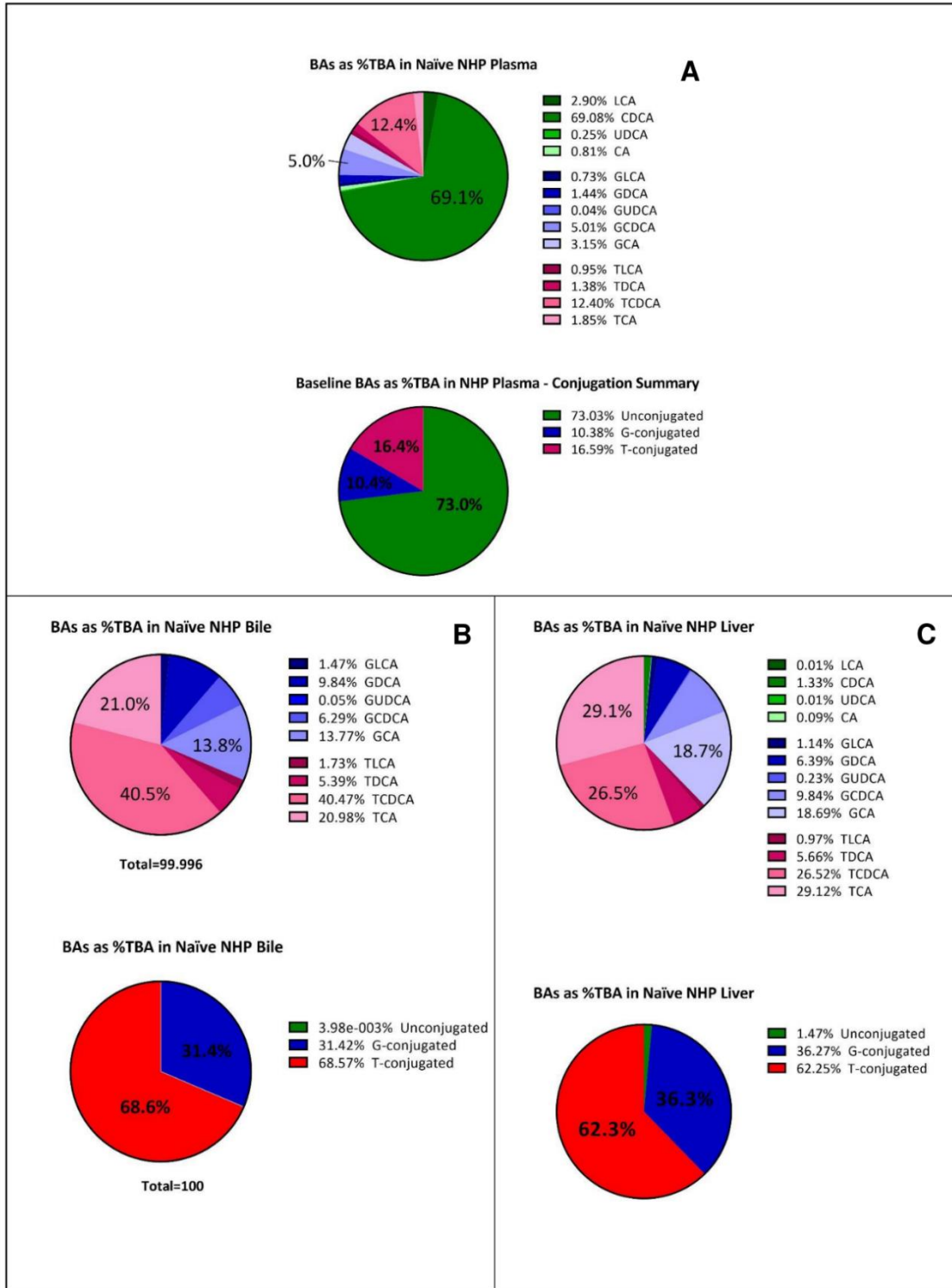


**Figure 3.4** BA pools and amidation summaries in *M. mullatta* tissue and biofluids, presented as a average percent TBA. A: BA pool in plasma. B: BA pool in bile. C: BA pool in liver. The amounts of three largest portions of the BA pool are explicitly stated within the pie charts. Unconjugated BAs are represented in shades of green, G-amidated in shades of blue, and T-amidated in shades of red.

## 3.4 Discussion

### 3.4.1 LC-MS/MS methodology

A LC-MS/MS assay was developed for quantification of BA concentrations in a variety of cell systems and relevant biomatrices. These studies illustrate the validation of a simplified, rapid sample preparation in comparison to recent methods. Using this method, BA isomers were reliably separated; however, additional specificity for these and similar molecules could be gained by using an instrument with higher resolution capabilities. Of note, the first baseline level assessment for planar BAs, including ACA, in cell lines, biofluids, and tissue under healthy conditions is included. This single assay and simple sample preparation methods are highly adaptable and could be easily applied to a variety of experimental conditions relevant to BA homeostasis and pathology. This methodology could also be applied to human clinical samples or other animal models with the addition of species-specific BAs. Furthermore, the sensitivity of this method allows for the quantification of even low abundance BA species. A significant limitation of this method, however, is that its application for measurement of C27, sulfated, and glucuronidated BA species has not yet been assessed.

### 3.4.2 Cell culture BA quantification

Unsupplemented DMEM proved to be sufficient for the cellular production of BAs to allow measurement of the BA pool and total viability in immortalized HepG2 and HuH-7 cell lines for the time period examined (48 hours); however, slightly more BAs were present per total protein in both cell lines when incubated in supplemented medium (i.e. HCM) (Table 3.4, Table 3.5). In both media and cell lines, taurine conjugation was slightly more prevalent than glycine conjugation (Fig. 3.3), which is directly contrary to the case

in the HPHs examined herein (Fig. 3.2) and in humans *in vivo*, in which glycine conjugation predominates greatly (53, 54). This is especially interesting because neither DMEM nor HCM include taurine in their formulations – whereas glycine is included at a concentration of 30 mg/L (in DMEM) to 50 mg/L (in HCM) – indicating that all three of these cell types are synthesizing taurine to some degree. Biosynthesis of taurine occurs *in vivo* in the liver and represents a sulfur excretion mechanism, so it is to be expected that hepatic and hepatocyte-derived cells are capable of this reaction; however, it is unexpected that the immortalized cells studied herein preferentially amidate BAs with the limited taurine instead of the more available glycine molecule that is favored *in vivo* (58). The altered amidation pattern in immortalized cells must be a result of modified cell metabolism, such as impedance in uptake in one or both of these amino acids or altered functionality and/or selectivity in the bile acid-CoA:amino acid N-acyltransferase (BAAT), the enzyme responsible for BA conjugation (1, 3, 5, 55). Indeed, qRT-PCR analysis has demonstrated that *BAAT* mRNA is undetectable in HepG2 and HuH-7 cell lines in comparison to HPHs (59). This is supported by this study, which demonstrated approximately equal amounts of conjugated and unconjugated BAs produced per total protein content in these immortalized cells (Fig. 3.3). Thus, BA levels in HepG2s and HuH-7s indicate that the cells are capable of BA production and conjugation but are deficient in comparison to HPHs and the healthy whole liver. Supporting this, HepG2 and HuH-7 cells presented impaired BA synthesis as a whole, producing only up to ~6% of TBA produced by HPHs (Table 3.4, Table 3.5). This is also in agreement with previous studies, which show very low or undetectable levels of mRNAs associated with BA synthetic enzymes CYP7A1, CYP7B1, and CYP8B1 in HepG2 and HuH-7 cells (59). Conversely, these cell lines express *CYP27A1* mRNA, the

rate-limiting enzyme of the acidic or alternative pathway of BA synthesis, at levels 130-155% of HPHs (1, 59). This, combined with the higher proportions of CDCA and its conjugates, adds evidence to the theory that the acidic or alternative pathway of BA synthesis is more active in immortalized cells relative to primary cells; however, BA synthesis as a whole is still very depressed, which is likely due to decreased expression of the succeeding enzymes in the BA synthesis pathway (60, 61).

Of the BAs produced in immortalized cells, the amidated BAs were found almost exclusively in the culture medium, whereas the unconjugated BAs CA and ACA made up nearly all of the BA species within cells (Fig. 3.3). These distinct extracellular and intracellular profiles indicate that BA transport mechanisms selective for amidated BAs, such as BSEP, MDR2/3, and MRP, are still active within HepG2 and HuH-7 cells (1). Earlier studies demonstrated that, while *BSEP* and *MDR2/3* mRNA levels are marginal or are undetectable in HepG2 and HuH-7 cells, *MRP1* and *MRP4* mRNA is nearly as abundant or many times more abundant than in HPHs (59). Hence, HepG2 and HuH-7 cells are more capable of exporting than they are at synthesizing amidated BAs, which is underpinned by both the high proportion of unconjugated BAs within the cell lysates and by the production of secondary BAs, LCA and DCA, which are presumed to be produced *in vivo* by intestinal bacteria (Table 3.4, Table 3.5, Fig. 3.3) (1, 3, 5, 55, 56). Earlier studies investigating the production of BAs by cultured cell systems did not probe for secondary BAs and enzymatically deconjugated BAs before analysis; thus, to the best of our knowledge, this study offers the most detailed characterization of BA production in HepG2 and HuH-7 cells to date (60, 62, 63). The production of secondary BAs is presumably due to the buildup of unconjugated CA and CDCA within the cells: when insufficiently conjugated

and exported, these molecules are subject to dehydroxylation, which is likely performed by the same enzymes that rehydroxylate LCA and DCA in the normal liver, as this enzymatic reaction is reversible (64). The presence of secondary BAs in immortalized and primary cells calls into question the assumption that LCA and DCA are generated exclusively from the activity of intestinal bacteria *in vivo*. Further studies are needed to determine if hepatic synthesis of “secondary” BAs contribute significantly to the BA pool and if this contribution is altered during disease.

As far as we are aware, this study is the first to observe the presence of planar BAs in human-derived cultured cells, though planar BAs have been discovered in both healthy and compromised individuals (30, 65-67). A significant portion of the unconjugated BAs present in HepG2 and HuH-7 cell lysates was ACA, the 5 $\alpha$ -epimer of CA. The planar BAs represent a subset of BAs that retain the “flat” 3D structure of cholesterol instead of the “bent” or “twisted” structure of typical mammalian BAs (1, 24, 25, 31). This conformation can either be due to an  $\alpha$ -positioning of the C5 hydrogen atom, as in ACA, or a double bond between C4 and C5, as in 7 $\alpha$ -hydroxy-3-oxo-*chol*-4-en-24-oic acid (1, 19, 25, 31). These molecules are abundant in pregnancy and during the first few months of life but gradually disappear after infancy and are not usually detectable in healthy adults (25, 31). In certain cases of liver or GI disease, however, these species reappear among circulating BAs (31). The mechanisms of the recurrence of planar BAs have yet to be fully elucidated, but it is thought that their synthesis is due to immature hepatic enzyme systems that can be found in the underdeveloped hepatocytes of the fetus and in the dysregulated cells of the injured liver (31). Alternatively, it is possible that these species are isomerized from their more typical counterparts, either by hepatic or microbial enzymes (31). The production of

planar BAs by immortalized cells, however, substantiate the theory that proliferating hepatocytes must de-differentiate in order to repopulate the injured liver and therefore express less specialized or incomplete metabolic enzymes, resulting in the production of “fetal” BA species (68). Moreover, previous studies in HepG2 cells detected high levels of additional BA precursors and intermediates for which we did not probe (62).

Though HPHs seem to produce fewer total BAs compared to the whole healthy human liver, these cells at least appear to produce similar ratios of each BA and amidate in similar patterns (Fig. 3.2) (69, 70). Glycine amidation predominated the BA pool greatly, but it should be noted that HCM does not provide any exogenous taurine, as stated above, which is presumably why HPHs produced such a low proportion of taurine-conjugated BAs. Also, this study examined BA production only in the 48 hours following perfusion, so it should also be considered that the amounts of BAs generated changes over time and does not reach maximal production until day 6 (i.e. 144 hours) (60, 63). Finally, only one donor was assayed in this study; further investigations would tell if these findings are true of all HPH cultures. Primary cells therefore offer a relatively good model of human liver BA synthesis and metabolism, as long as the above limitations are considered (60, 69, 70). Conversely, the HepG2 and HuH-7 cell lines make very poor models for the study of BA synthesis and metabolism, as they do not produce nearly as many or the same pattern of BAs as HPHs or whole human liver.

### 3.4.3 NHP BA quantification

NHP models are the most relevant and preferred model systems currently available in drug discovery and development due to the high degree of phylogeny and homogeneity to humans (71). Despite this, BA synthesis and metabolism in these animals remains poorly

characterized. Herein, the BA pools of several compartments were quantified in an accepted laboratory model, the NHP.

Naïve NHP plasma BAs were dominated by unconjugated CDCA, distantly followed by TCDCA and GCDCA and then by GCA and TCA (Table 3.6, Fig. 3.4A). These results conform with previous studies indicating the prevalence of unconjugated BAs in rhesus macaque plasma; however, they disagree with previous studies regarding individual BAs, finding a higher percentage of unconjugated CDCA instead of DCA (46, 47, 72). Circulating TBA concentration in NHP plasma proved comparable to that in human plasma as reported in scientific literature, i.e. an average of 1.82  $\mu\text{g/mL}$  in NHP compared to 1.01-2.13  $\mu\text{g/mL}$  in human (Table 3.6) (35, 53, 70). It is important to note, however, that the composition of the BA pool was altered in naïve NHP plasma, yielding a higher CDCA:CA ratio than is usual in human plasma. NHP plasma also presented a high proportion (~73%) of total unconjugated BAs, specifically CDCA, whereas human plasma BAs are mostly (~56-59%) glycine-amidated (Fig. 3.4A) (35, 46, 53). Yet, this has been shown to change with diet and fasting state: the glycine:taurine ratio in humans can change with diet and cooking habits, and the ratio of unconjugated to amidated BAs is increased in the fasting state compared to the nonfasting state (35, 53).

The preponderance of CDCA compared to CA that occurred in plasma was also reflected in naïve macaque bile and liver, which demonstrated similar profiles when compared to one another (Fig. 3.4B-C). In these tissues, the BA pools were dominated by a high proportion of taurine-conjugated primary BAs, CDCA and CA. As has been reported in human bile and liver, an overwhelming majority of BAs in naïve macaque liver and bile were amidated, with only a very small fraction escaping conjugation (Fig. 3.4B-C) (1, 3,

5, 19, 70, 73). Though interindividual variability in this study was relatively high due to small sample size and *ad libidum* feeding, it is apparent that naïve NHP liver produced comparable TBA to healthy human liver as reported in previous studies, i.e. an average of 97.5 ng/mg of tissue versus 7.7-29.5 ng/mg of tissue in humans (Table 3.6) (70, 73). Although, as in plasma, NHP liver shows a notable difference in regards to the glycine/taurine ratio, preferring taurine to glycine amidation, which is converse to that in humans (Fig. 3.4B-C) (3, 35, 70).

In terms of TBA, NHP offers high resemblance to humans in plasma, liver tissue, and bile (35, 46, 53, 54, 69, 70, 73). The individual members of the BA pool in these tissues, however, are distinct between NHP and humans. The greatest differences observed in this study include: increased CDCA/CA ratio in the NHP BA pool, greater proportion of unconjugated compared to conjugated BAs within plasma, and the preference for taurine versus glycine amidation. Additionally, though this study did not evaluate sulfated BAs, at least one previous study has reported marked differences between the extent of this BA elimination pathway in NHP versus humans (46, 47). Overall, however, this laboratory animal represents a highly relevant model for the study of BA synthesis, metabolism, and pharmacology with relatively minor disparities in comparison to other models.

### 3.5 Conclusions and future directions

The optimization, validation, and application of a sensitive and selective LC-MS/MS method for the simultaneous detection and quantification of numerous BAs in cultured cell systems and several biomatrices are described herein. The immortalized hepatoblastoma cell lines HepG2 and HuH-7 were studied for comparison with cultured human primary hepatocytes and previous research examining whole liver *in vivo* (69, 70).

Results from these studies demonstrate that these immortalized cell systems are poor indicators of healthy hepatic BA metabolism; however, HPHs are a promising alternative. Although, before using these cells as models, it should be established whether supplementing culture medium with exogenous taurine would present a similar BA profile to that produced *in vivo*. In addition, more HPH donors should be examined to ensure that these findings are universal.

These experiments also support the use of NHP models in favor of murine models when studying BA synthesis and metabolism, especially for comparison to human systems. Laboratory rats and mice offer the advantages of low costs, rapid growth, and straightforward handling and use, but their low homology to man makes correlation to human systems challenging and usually inaccurate (38-43, 45). In BA research, the use of murine models is additionally complicated by the utilization of a set of unique BA epimers, the muricholic acids (MCA) (38, 39, 41, 45). NHPs offer a more homologous, suitable system for the study of BA synthesis and metabolism, both in physiology and in illness, that much more closely approximates that in healthy adult humans. Further characterization in these species, however, to elucidate such processes as BA elimination (i.e. renal versus biliary), sulfonation and glucuronidation, and signaling for comparison to man, should be pursued to establish physiological parameters that may be altered in relevant pathologies. The continued study of NHP BA synthesis with regards to C-27 BAs precursors and intermediates should prove valuable in aligning this laboratory model with human conditions. Additionally, the study of conjugated planar BAs (such as TACA and GACA) both in laboratory models and in human studies would be of increased relevance

due to the propensity of BAs to be amidated or otherwise conjugated in most biological systems.

In summary, these studies have proven the utility of a validated method for the quantification of common and planar C24 BAs in a variety of systems. Detailed baselines have been established herein for multiple model systems for the study of BA production and metabolism, which have implications for the selection and use of cell and animal models for the study of BA metabolism and pathology.

### 3.6 References

1. Marin J, Macias R, Briz O, Banales J, Monte M. Bile Acids in Physiology, Pathology and Pharmacology. *Current drug metabolism*. 2015;17.
2. Kuipers F, Bloks VW, Groen AK. Beyond intestinal soap—bile acids in metabolic control. *Nature Reviews Endocrinology*. 2014;10:488.
3. Hofmann AF, Hagey LR. Bile Acids: Chemistry, Pathochemistry, Biology, Pathobiology, and Therapeutics. *Cellular and Molecular Life Sciences*. 2008;65(16):2461-83.
4. Ferrebee CB, Dawson PA. Metabolic effects of intestinal absorption and enterohepatic cycling of bile acids. *Acta Pharmaceutica Sinica B*. 2015;5(2):129-34.
5. de Aguiar Vallim Thomas Q, Tarling Elizabeth J, Edwards Peter A. Pleiotropic Roles of Bile Acids in Metabolism. *Cell Metabolism*. 2013;17(5):657-69.
6. Rees DO, Crick PJ, Jenkins GJ, Wang Y, Griffiths WJ, Brown TH, Al-Sarireh B. Comparison of the composition of bile acids in bile of patients with adenocarcinoma of the pancreas and benign disease. *The Journal of Steroid Biochemistry and Molecular Biology*. 2017;174:290-5.
7. Resson HW, Xiao JF, Tuli L, Varghese RS, Zhou B, Tsai T-H, Nezami Ranjbar MR, Zhao Y, Wang J, Di Poto C, Cheema AK, Tadesse MG, Goldman R, Shetty K. Utilization of metabolomics to identify serum biomarkers for hepatocellular carcinoma in patients with liver cirrhosis. *Analytica Chimica Acta*. 2012;743:90-100.
8. Tadano T, Kanoh M, Matsumoto M, Sakamoto K, Kamano T. Studies of serum and feces bile acids determination by gas chromatography-mass spectrometry. *Rinsho Byori The Japanese Journal Of Clinical Pathology*. 2006;54(2):103-10.
9. Puri P, Daita K, Joyce A, Mirshahi F, Santhekadur PK, Cazanave S, Luketic VA, Siddiqui MS, Boyett S, Min HK, Kumar DP, Kohli R, Zhou H, Hylemon PB, Contos MJ, Idowu M, Sanyal AJ. The presence and severity of nonalcoholic steatohepatitis is associated with specific changes in circulating bile acids. *Hepatology*. 2018;67(2):534-48.
10. Raselli T, Hearn T, Wyss A, Atrott K, Peter A, Frey-Wagner I, Spalinger MR, Maggio EM, Sailer AW, Schmitt J, Schreiner P, Moncsek A, Mertens J, Scharl M, Griffiths WJ, Bueter M, Geier A, Rogler G, Wang Y, Misselwitz B. Elevated oxysterol levels in human and mouse livers reflect nonalcoholic steatohepatitis. *Journal of Lipid Research*. 2019;60(7):1270-83.
11. Janssen AWF, Houben T, Katiraei S, Dijk W, Boutens L, van der Bolt N, Wang Z, Brown JM, Hazen SL, Mandard S, Shiri-Sverdlov R, Kuipers F, Willems van Dijk K, Vervoort J, Stienstra R, Hooiveld GJEJ, Kersten S. Modulation of the gut microbiota

impacts nonalcoholic fatty liver disease: a potential role for bile acids. *Journal of Lipid Research*. 2017;58(7):1399-416.

12. Jiao N, Baker SS, Chapa-Rodriguez A, Liu W, Nugent CA, Tsompana M, Mastrandrea L, Buck MJ, Baker RD, Genco RJ, Zhu R, Zhu L. Suppressed hepatic bile acid signalling despite elevated production of primary and secondary bile acids in NAFLD. *Gut*. 2018;67(10):1881-91.

13. Ferrell JM, Chiang JYL. Understanding Bile Acid Signaling in Diabetes: From Pathophysiology to Therapeutic Targets. *Diabetes Metab J*. 2019;43(3):257-72.

14. Maghsoodi N, Shaw N, Cross GF, Alagband-Zadeh J, Wierzbicki AS, Pinkney J, Millward A, Vincent RP. Bile acid metabolism is altered in those with insulin resistance after gestational diabetes mellitus. *Clinical Biochemistry*. 2019;64:12-7.

15. Schonewille M, de Boer J, Groen A. Bile salts in control of lipid metabolism. *Curr Opin Lipidol*. 2016;27(3):295-301.

16. Shapiro H, Kolodziejczyk AA, Halstuch D, Elinav E. Bile acids in glucose metabolism in health and disease. *The Journal of Experimental Medicine*. 2018;215(2):383.

17. Schadt HS, Wolf A, Pognan F, Chibout S-D, Merz M, Kullak-Ublick GA. Bile acids in drug induced liver injury: Key players and surrogate markers. *Clinics and Research in Hepatology and Gastroenterology*. 2016;40(3):257-66.

18. Griffiths WJ, Abdel-Khalik J, Yutuc E, Roman G, Warner M, Gustafsson J-Å, Wang Y. Concentrations of bile acid precursors in cerebrospinal fluid of Alzheimer's disease patients. *Free Radical Biology and Medicine*. 2019;134:42-52.

19. Alnouti Y. Bile Acid Sulfation: A Pathway of Bile Acid Elimination and Detoxification. *Toxicological Sciences*. 2009;108(2):225-46.

20. Gérard P. Metabolism of cholesterol and bile acids by the gut microbiota. *Pathogens*. 2013;3(1):14-24.

21. Ikegami T, Honda A. Reciprocal interactions between bile acids and gut microbiota in human liver diseases. *Hepatology Research*. 2018;48(1):15-27.

22. Luo L, Aubrecht J, Li D, Warner RL, Johnson KJ, Kenny J, Colangelo JL. Assessment of serum bile acid profiles as biomarkers of liver injury and liver disease in humans. *PLOS ONE*. 2018;13(3):e0193824.

23. Mendoza ME, Monte MJ, El-Mir MY, Badia MD, Marin JJG. Changes in the pattern of bile acids in the nuclei of rat liver cells during hepatocarcinogenesis. *Clinical Science*. 2002;102(2):143-50.

24. Monte MJ, Martinez-Diez MC, El-Mir MY, Mendoza ME, Bravo P, Bachs O, Marin JJG. Changes in the pool of bile acids in hepatocyte nuclei during rat liver regeneration. *Journal of Hepatology*. 2002;36(4):534-42.
25. Stärkel P, Shindano T, Horsmans Y, Gigot JF, Fernandez-Tagarro M, Marin JJG, Monte MJ. Foetal 'flat' bile acids reappear during human liver regeneration after surgery. *European Journal of Clinical Investigation*. 2009;39(1):58-64.
26. Miyazaki-Anzai S, Masuda M, Kohno S, Levi M, Shiozaki Y, Keenan AL, Miyazaki M. Simultaneous inhibition of FXR and TGR5 exacerbates atherosclerotic formation. *Journal of Lipid Research*. 2018;59(9):1709-13.
27. Liang H, Huang H, Tan P-z, Liu Y, Nie J-h, Zhang Y-t, Zhang K-l, Diao Y, He Q, Hou B-y, Zhao T-t, Li Y-z, Lv G-x, Lee K-Y, Gao X, Zhou L-y. Effect of iron on cholesterol 7 $\alpha$ -hydroxylase expression in alcohol-induced hepatic steatosis in mice. *Journal of Lipid Research*. 2017;58(8):1548-60.
28. Nagahashi M, Yuza K, Hirose Y, Nakajima M, Ramanathan R, Hait NC, Hylemon PB, Zhou H, Takabe K, Wakai T. The roles of bile acids and sphingosine-1-phosphate signaling in the hepatobiliary diseases. *Journal of Lipid Research*. 2016;57(9):1636-43.
29. Lan K, Su M, Xie G, Ferslew BC, Brouwer KLR, Rajani C, Liu C, Jia W. Key Role for the 12-Hydroxy Group in the Negative Ion Fragmentation of Unconjugated C24 Bile Acids. *Analytical Chemistry*. 2016;88(14):7041-8.
30. Griffiths WJ, Gilmore I, Yutuc E, Abdel-Khalik J, Crick PJ, Hearn T, Dickson A, Bigger BW, Wu TH-Y, Goenka A, Ghosh A, Jones SA, Wang Y. Identification of unusual oxysterols and bile acids with 7-oxo or 3 $\beta$ ,5 $\alpha$ ,6 $\beta$ -trihydroxy functions in human plasma by charge-tagging mass spectrometry with multistage fragmentation. *Journal of Lipid Research*. 2018;59(6):1058-70.
31. Shiffka SJ, Kane MA, Swaan PW. Planar bile acids in health and disease. *Biochimica et Biophysica Acta (BBA) - Biomembranes*. 2017;1859(11):2269-76.
32. Griffiths WJ, Sjövall J. Bile acids: analysis in biological fluids and tissues. *Journal of lipid research*. 2010;51(1):23-41.
33. Kakiyama G, Muto A, Takei H, Nittono H, Murai T, Kurosawa T, Hofmann AF, Pandak WM, Bajaj JS. A simple and accurate HPLC method for fecal bile acid profile in healthy and cirrhotic subjects: validation by GC-MS and LC-MS. *Journal of Lipid Research*. 2014;55(5):978-90.
34. Lee C-S, Kimura A, Wu J-F, Ni Y-H, Hsu H-Y, Chang M-H, Nittono H, Chen H-L. Prognostic roles of tetrahydroxy bile acids in infantile intrahepatic cholestasis. *Journal of Lipid Research*. 2017;58(3):607-14.

35. Han J, Liu Y, Wang R, Yang J, Ling V, Borchers CH. Metabolic Profiling of Bile Acids in Human and Mouse Blood by LC–MS/MS in Combination with Phospholipid-Depletion Solid-Phase Extraction. *Analytical Chemistry*. 2015;87(2):1127-36.
36. Fang N, Yu S, Adams SH, Ronis MJJ, Badger TM. Profiling of urinary bile acids in piglets by a combination of enzymatic deconjugation and targeted LC-MRM-MS. *Journal of Lipid Research*. 2016;57(10):1917-33.
37. Schmid A, Neumann H, Karrasch T, Liebisch G, Schäffler A. Bile Acid Metabolome after an Oral Lipid Tolerance Test by Liquid Chromatography-Tandem Mass Spectrometry (LC-MS/MS). *PLoS ONE*. 2016;11(2):1-13.
38. Rudling M. Understanding mouse bile acid formation: Is it time to unwind why mice and rats make unique bile acids? *Journal of Lipid Research*. 2016;57(12):2097-8.
39. Takahashi S, Fukami T, Masuo Y, Brocker CN, Xie C, Krausz KW, Wolf CR, Henderson CJ, Gonzalez FJ. Cyp2c70 is responsible for the species difference in bile acid metabolism between mice and humans. *Journal of Lipid Research*. 2016;57(12):2130-7.
40. Honda A, Miyazaki T, Iwamoto J, Hirayama T, Morishita Y, Monma T, Ueda H, Mizuno S, Sugiyama F, Takahashi S, Ikegami T. Regulations of bile acid metabolism in mouse models with hydrophobic bile acid composition. *Journal of Lipid Research*. 2019.
41. de Boer JF, Verkade E, Mulder NL, de Vries HD, Huijkman NCA, Koehorst M, Boer T, Wolters JC, Bloks VW, van de Sluis B, Kuipers F. A Human-like Bile Acid Pool Induced by Deletion of Cyp2c70 Modulates Effects of Farnesoid X Receptor Activation in Mice. *Journal of Lipid Research*. 2019.
42. Lee JM, Ong JR, Vergnes L, de Aguiar Vallim TQ, Nolan J, Cantor RM, Walters JRF, Reue K. Diet1, bile acid diarrhea, and FGF15/19: mouse model and human genetic variants. *Journal of Lipid Research*. 2018;59(3):429-38.
43. Wahlström A, Kovatcheva-Datchary P, Ståhlman M, Khan M-T, Bäckhed F, Marschall H-U. Induction of farnesoid X receptor signaling in germ-free mice colonized with a human microbiota. *Journal of Lipid Research*. 2017;58(2):412-9.
44. Song X, Chen Y, Valanejad L, Kaimal R, Yan B, Stoner M, Deng R. Mechanistic insights into isoform-dependent and species-specific regulation of bile salt export pump by farnesoid X receptor. *Journal of Lipid Research*. 2013;54(11):3030-44.
45. Li J, Dawson PA. Animal models to study bile acid metabolism. *Biochimica et Biophysica Acta (BBA) - Molecular Basis of Disease*. 2019;1865(5):895-911.
46. Thakare R, Alamoudi JA, Gautam N, Rodrigues AD, Alnouti Y. Species differences in bile acids I. Plasma and urine bile acid composition. *Journal of Applied Toxicology*. 2018;38(10):1323-35.

47. Thakare R, Alamoudi JA, Gautam N, Rodrigues AD, Alnouti Y. Species differences in bile acids II. Bile acid metabolism. *Journal of Applied Toxicology*. 2018;38(10):1336-52.
48. Cohen EP, Hankey KG, Farese AM, Parker GA, Jones JW, Kane MA, Bennett A, MacVittie TJ. Radiation Nephropathy in a Nonhuman Primate Model of Partial-body Irradiation with Minimal Bone Marrow Sparing—Part 1: Acute and Chronic Kidney Injury and the Influence of Neupogen. *Health Physics*. 2019;116(3):401-8.
49. Parker GA, Cohen EP, Li N, Takayama K, Farese AM, MacVittie TJ. Radiation Nephropathy in a Nonhuman Primate Model of Partial-Body Irradiation With Minimal Bone Marrow Sparing—Part 2: Histopathology, Mediators, and Mechanisms. *Health Physics*. 2019;116(3).
50. Parker GA, Li N, Takayama K, Booth C, Tudor GL, Farese AM, MacVittie TJ. Histopathological Features of the Development of Intestine and Mesenteric Lymph Node Injury in a Nonhuman Primate Model of Partial-body Irradiation with Minimal Bone Marrow Sparing. *Health Physics*. 2019;116(3):426-46.
51. Parker GA, Li N, Takayama K, Farese AM, MacVittie TJ. Lung and Heart Injury in a Nonhuman Primate Model of Partial-body Irradiation with Minimal Bone Marrow Sparing: Histopathological Evidence of Lung and Heart Injury. *Health Physics*. 2019;116(3):383.
52. Saeed A, Floris F, Andersson U, Pikuleva I, Lövgren-Sandblom A, Bjerke M, Paucar M, Wallin A, Svenningsson P, Björkhem I.  $7\alpha$ -hydroxy-3-oxo-4-cholestenoic acid in cerebrospinal fluid reflects the integrity of the blood-brain barrier. *Journal of Lipid Research*. 2014;55(2):313-8.
53. Bathena SPR, Mukherjee S, Olivera M, Alnouti Y. The profile of bile acids and their sulfate metabolites in human urine and serum. *Journal of Chromatography B*. 2013;942-943:53-62.
54. Xie G, Wang Y, Wang X, Zhao A, Chen T, Ni Y, Wong L, Zhang H, Zhang J, Liu C, Liu P, Jia W. Profiling of Serum Bile Acids in a Healthy Chinese Population Using UPLC–MS/MS. *Journal of Proteome Research*. 2015;14(2):850-9.
55. Hofmann AF, Hagey LR. Key discoveries in bile acid chemistry and biology and their clinical applications: history of the last eight decades. *Journal of Lipid Research*. 2014;55(8):1553-95.
56. Kriaa A, Bourgin M, Potiron A, Mkaouar H, Jablaoui A, Gérard P, Maguin E, Rhimi M. Microbial impact on cholesterol and bile acid metabolism: current status and future prospects. *Journal of Lipid Research*. 2019;60(2):323-32.
57. Shoda J, Toll A, Axelson M, Pieper F, Wikvall K, Sjövall J. Formation of  $7\alpha$ - and  $7\beta$ -hydroxylated bile acid precursors from 27-hydroxycholesterol in human liver microsomes and mitochondria. *Hepatology*. 1993;17(3):395-403.

58. Hansen SH. Taurine homeostasis and its importance for physiological functions. 2003. p. 739-47.
59. Guo L, Dial S, Shi L, Branham W, Liu J, Fang J-L, Green B, Deng H, Kaput J, Ning B. Similarities and Differences in the Expression of Drug Metabolizing Enzymes between Human Hepatic Cell Lines and Primary Human Hepatocytes. *Drug Metabolism and Disposition*. 2010;dmd.110.035873.
60. Einarsson C, Ellis E, Abrahamsson A, Ericzon B-G, Bjorkhem I, Axelson M. Bile acid formation in primary human hepatocytes. *World J Gastroenterol*. 2000;6(4):522-5.
61. Shi J, Wang X, Lyu L, Jiang H, Zhu H-J. Comparison of protein expression between human livers and the hepatic cell lines HepG2, Hep3B, and Huh7 using SWATH and MRM-HR proteomics: Focusing on drug-metabolizing enzymes. *Drug Metabolism and Pharmacokinetics*. 2018;33(2):133-40.
62. Axelson M, Mörk B, Everson GT. Bile acid synthesis in cultured human hepatoblastoma cells. *Journal of Biological Chemistry*. 1991;266(27):17770-7.
63. Axelson M, Ellis E, Mörk B, Garmark K, Abrahamsson A, Björkhem I, Ericzon BG, Einarsson C. Bile acid synthesis in cultured human hepatocytes: support for an alternative biosynthetic pathway to cholic acid. *Hepatology*. 2000;31(6):1305-12.
64. Penning TM. Molecular Endocrinology of Hydroxysteroid Dehydrogenases. *Endocrine Reviews*. 1997;18(3):281-305.
65. Mazzacuva F, Mills P, Mills K, Camuzeaux S, Gissen P, Nicoli E-R, Wassif C, te Vruchte D, Porter FD, Maekawa M, Mano N, Iida T, Platt F, Clayton PT. Identification of novel bile acids as biomarkers for the early diagnosis of Niemann-Pick C disease. *FEBS Letters*. 2016;590(11):1651-62.
66. Maekawa M, Misawa Y, Sotoura A, Yamaguchi H, Togawa M, Ohno K, Nittono H, Kakiyama G, Iida T, Hofmann AF, Goto J, Shimada M, Mano N. LC/ESI-MS/MS analysis of urinary 3 $\beta$ -sulfooxy-7 $\beta$ -N-acetylglucosaminyl-5-cholen-24-oic acid and its amides: New biomarkers for the detection of Niemann-Pick type C disease. *Steroids*. 2013;78(10):967-72.
67. Meng L-J, Reyes H, Palma J, Hernandez I, Ribalta J, Sjövall J. Profiles of bile acids and progesterone metabolites in the urine and serum of women with intrahepatic cholestasis of pregnancy. *Journal of Hepatology*. 1997;27(2):346-57.
68. Kholodenko IV, Yarygin KN. Cellular Mechanisms of Liver Regeneration and Cell-Based Therapies of Liver Diseases. *BioMed Research International*. 2017;2017:17.
69. Setchell KD, Rodrigues CM, Clerici C, Solinas A, Morelli A, Gartung C, Boyer J. Bile acid concentrations in human and rat liver tissue and in hepatocyte nuclei. *Gastroenterology*. 1997;112(1):226-35.

70. García-Cañaveras JC, Donato MT, Castell JV, Lahoz A. Targeted profiling of circulating and hepatic bile acids in human, mouse, and rat using a UPLC-MRM-MS-validated method. *Journal of lipid research*. 2012;53(10):2231-41.
71. Singh VK, Olabisi AO. Nonhuman primates as models for the discovery and development of radiation countermeasures. *Expert Opinion on Drug Discovery*. 2017;12(7):695-709.
72. Sturman J, Messing J, Rossi S, Hofmann A, Neuringer M, Gastroenterology Do. Growth, Development and Aging Tissue Taurine Content, Activity of Taurine Synthesis Enzymes and Conjugated Bile Acid Composition of Taurine-Deprived and Taurine-Supplemented Rhesus Monkey Infants at 6 and 12 mo of Age. 2019.
73. Greim H, Czygan P, Schaffner F, Popper H. Determination of bile acids in needle biopsies of human liver. *Biochemical Medicine*. 1973;8(2):280-6.

## Chapter 4 4. Investigating the Co-Evolution of SLC10A2 and Bile Salts

### 4.1 Introduction

While BAs have been studied for nearly a century, human BAs encompass nearly 50 species synthesized by the human body alone, and modifications made by intestinal bacteria result in almost 400 derivatives of the C<sub>24</sub> core structure (1). Most of these species are still poorly characterized (1). One of the least studied subspecies are the “flat” BAs, a group of C<sub>24</sub> cholanoic acids that retain the planar structure of their cholesterol predecessor instead of the “bent” or “twisted” structure of the typical mammalian BAs (2-10). These so-called “flat” or “planar” BAs comprise several subspecies, and the study thereof is the foundation for this project.

#### 4.1.1 Bile acids as phenotypes of evolution

BAs are produced by every class of vertebrate animals, with chemical variation within exceeding that of any other type of endogenous small molecule (11, 12). The generically termed “bile salts” are made up of several subgroups of cholesterol end products across species: the C<sub>27</sub> bile alcohols, C<sub>24</sub> bile acids, and C<sub>24</sub> bile acids, differing in the length of the carbon side chain and oxidation state (figure 4.1) (11, 12). The C<sub>27</sub> bile alcohols are considered the ancestral bile salts, as they are found as the bile salts of the earliest evolving extant species (jawless and lobe-finned fish such as the lamprey and hagfish), whereas the most recently evolved species utilize C<sub>24</sub> BAs (11, 12). The C<sub>27</sub> bile alcohols are also in the 5 $\alpha$  configuration, whereas the more evolutionarily furthered vertebrate species (nearly all mammals and humans, for example) have 5 $\beta$  C<sub>24</sub> BAs, demonstrating two evolutionary shifts: the C5 hydrogen atom from an *alpha* to a *beta* configuration and the decrease in side chain length from 8 to 5 carbon atoms (11, 12). The

latter represents the addition of several enzymatic steps taking place within multiple cellular compartments, but little is known about the biosynthetic pathways that produce either the  $5\alpha$   $C_{27}$  alcohols or  $5\alpha$   $C_{24}$  acids (11, 12). Moreover, there are several extant species, mostly lizards in the Iguanidae phylogenetic family, that utilize entirely  $5\alpha$  (allo) bile acids or bile alcohols (11, 12). Thus, one hypothesis behind the presence of flat BAs is that the immature hepatic state in humans during liver proliferation is responsible for the formation of  $5\alpha$  BAs and is enzymatically and metabolically reflective of a less evolved BA biosynthesis pathway.

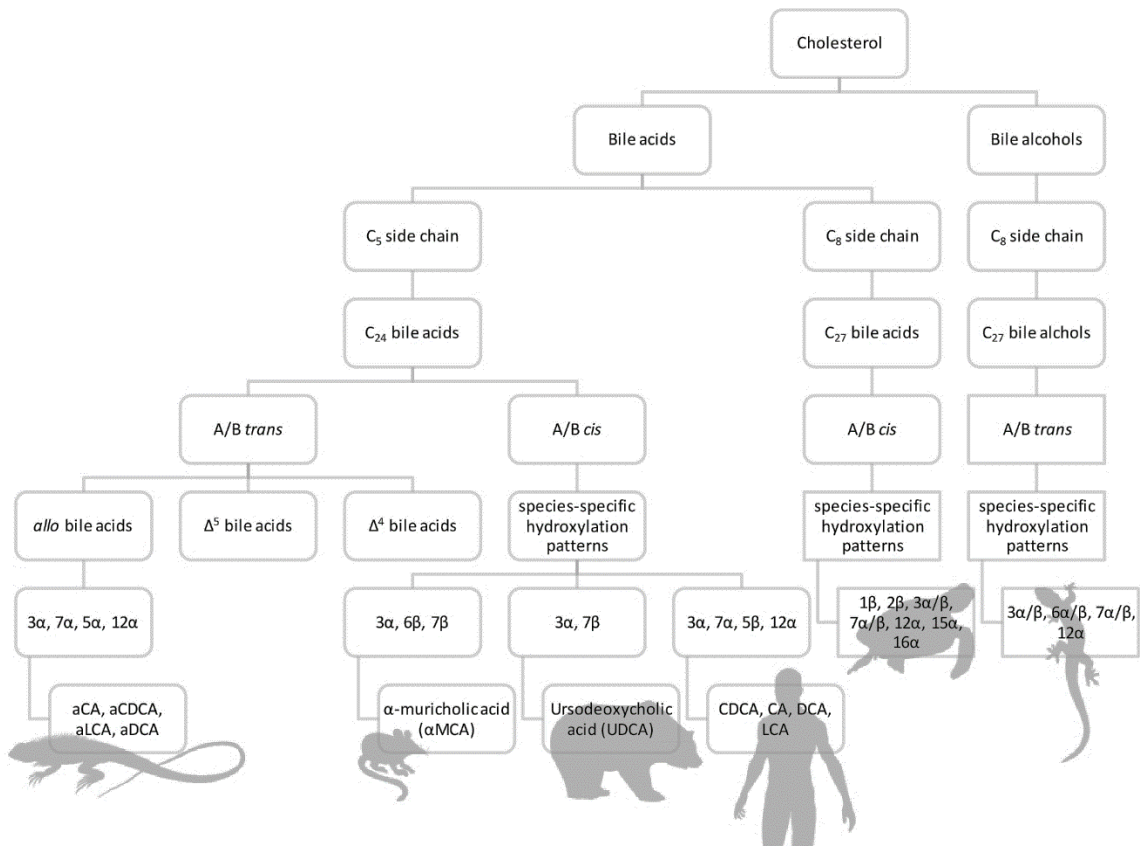


**Figure 4.1** A simplified flowchart of the different types of bile acids and alcohols used across many species. Bile acids are diversified by the length and oxidation state of the side chain, the configuration of various stereocenters, and the presence of hydroxy or oxo groups at multiple points of the steroid backbone. Additionally, different species' bile acid pools are modified by species-specific gut microbe metabolism and preferred mechanisms of detoxification, including amidation, sulfation, glucuronidation, and others.

#### 4.1.2 Planar bile acids in human health and disease

Planar BAs are mostly found as highly abundant BAs in the healthy human fetus, newborn, and pregnant woman; however, they are normally very lowly abundant or undetectable in the healthy adult (13-15). What makes these molecules relevant, however, is not necessarily their importance in early life, but instead their recurrence in adult patients suffering from various types of liver injury or disease, such as cancer (2, 10). As discussed in a recent review, these typically fetal flat BAs become abundant at various stages of hepatocellular carcinoma, following liver ablation, and in other malignancies and subsequently disappear upon recovery (16). Thus, there has been renewed interest in studying these fetal flat bile acid species in recent years since their original discovery by Ohta in 1939 (17). Common interests include using these molecules as biomarkers for liver proliferation and damage as well as discovering their role in disease states.

During synthesis from cholesterol, isomerization and saturation of the C5-C6 double bond results in a “bent” or “twisted” conformation of the steroid backbone (16). The so-called “flat” BAs are thus molecules that retain the A/B *trans* structure of cholesterol, wherein the steroid backbone exists within the same spatial plane, instead of the A/B *cis* structure of typical human BAs (Fig. 2.1A, 2.1B). The A/B *trans* structure is relatively abnormal among the C<sub>24</sub> BAs and is due to either the *alpha* arrangement of the C5 hydrogen atom – in contrast with the standard *beta* arrangement – or an unsaturation affecting the C5 bond (2). Both of these configurations result in molecules that occupy the category of flat BAs and, as mentioned, are found in healthy humans only during gestation and shortly after birth (16).

Human ASBT transport *in vitro* and *in vivo* has already been well-characterized by previous research in our and other laboratories (18-21). To examine how Asbt has evolved over time with bile acid biosynthesis, it would be prudent to also characterize orthologs, such as those mentioned herein, in more detail. These experiments sought to do this using representative bile acids as probes to investigate the binding and transport capacity of these proteins. Moreover, these studies offer an improvement over existing uptake experiments because they do not rely on a commercially available or custom synthesized radiolabeled compound. In most cases of bile acid transporter studies, researchers choose to use radiolabeled TCA, which, as demonstrated below, may be poorly transported by certain orthologs (22).

## 4.2 Materials and methods

### 4.2.1 Materials

All solvents used were of LC-MS grade or higher and purchased from Fischer Scientific (Pittsburgh, PA). Solid standards were purchased from either Sigma-Aldrich (St Louis, MO), Toronto Research Chemicals (North York, ON, Canada), Cambridge Isotope Laboratories (Tewksbury, MA), Isosciences (Ambler, PA), Bridge Organics (Vicksburg, MI), or Steraloids (Newport, RI). 3-oxo-cholic acid was generously provided by Dr. James E. Polli's lab (University of Maryland, Baltimore, MD). Orthologs of ASBT/Asbt were previously developed by members of our lab (hASBT, mAsbt, and dmSlc10) or generously shared by the Boyer laboratory (Yale University) (leAsbt [little skate Asbt, previously called skAsbt] and pmAsbt [sea lamprey Asbt, previously called lpAsbt]).

#### 4.2.2 Uptake assay and transporter kinetics

COS-1 cells were grown in Dulbecco's modified Eagle's medium (DMEM) containing 10% fetal bovine serum (FBS), 4.5 g/L glucose, 100 units/mL penicillin, and 100 µg/mL streptomycin (Life Technologies, Inc., Rockville, MD), then transiently transfected with one Asbt ortholog at a time using Turbofect transfection reagent (Thermo Fisher Scientific, Inc.) in a previously written protocol (18). Preliminary experiments examining total bile acid uptake were performed with and without sodium chloride (substituting choline chloride) to determine Na-dependent transport. For timecourse studies, cells were washed twice with warm Dulbecco's phosphate-buffered saline (DPBS), then incubated for up to 25 minutes with 10µM of bile acid in Modified Hank's balanced salt solution (MHBSS), pH 7.4 with 139.9 mM sodium chloride, in order to determine linearity of ortholog transport. Kinetic studies were performed similarly except at a single time point with variable (2.5-500 µM) concentrations of bile acids used. Uptake was quenched by aspiration and simultaneous flooding with DPBS. Cells were lysed via evaporation of 70% acetonitrile (ACN) in water containing internal standards (CA-d<sub>4</sub> and GCDCA-d<sub>4</sub>), then resuspended in 50% ACN in water for LC-MS/MS injection. Protein concentration was estimated using Pierce 660 nm protein assay and used to normalize uptake data.

#### 4.2.3 LC-MS/MS uptake analysis

The LC-MS/MS method used to quantify uptake was modified from that developed in Chapter 1. A shorter column (ACQUITY UPLC BEH C18 Column, 130Å, 1.7 µm, 2.1 mm X 50 mm; Waters) was used to expedite the 32-minute method to 10 minutes. As before, solvent A consisted of water with 0.01% formic acid (FA), and solvent B was ACN

with 0.01% FA. The chromatography was compressed to the specifications in table 4.1 with an increased flow rate of 0.5 mL/min. This method resulted in sufficient chromatographic resolution of independent analytes. Calibration curves were constructed and LLOQs and LLODs were determined as in Chapter 3.

#### 4.2.4 Data analysis

LC-MS/MS data were analyzed using Waters TargetLynx software and further processed within GraphPad Prism (version 8.4, San Diego, CA). Michaelis-Menten modeling was carried out within Prism.

Time (min)	% A	% B
0	75	25
4	60	40
8	25	75
9	0	100
9.5	75	25
10	75	25

**Table 4.1** Chromatographic run used for LC-MS/MS analysis of uptake studies.

### 4.3 Results

#### 4.3.1 Determining sodium-dependent uptake by multiple ASBT/Asbt orthologs

Preliminary uptake experiments were performed in order to assess which ortholog and bile acid combinations should be pursued in further studies. Results are illustrated in figure 4.2. Human ASBT demonstrated the highest overall sodium-dependent uptake for TCA, 3-oxo-cholic acid (3-oxo-CA), allocholic acid (ACA), and isoallothiocholic acid (IALCA). Conversely, sodium-dependent uptake of 3-oxo-chol-4-enic acid and 7 $\alpha$ -hydroxy-3-oxo-chol-4-en-24-oic acid did not significantly differ from sodium-independent diffusion.

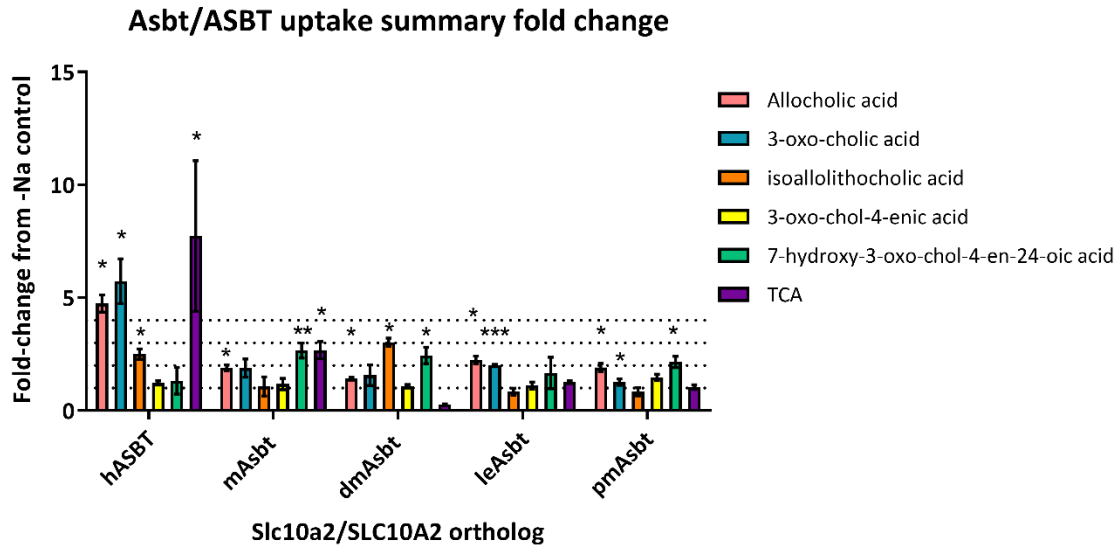


**Figure 4.2** Relative amount of bile acid or derivative transported into ASBT/Asbt-transfected COS-1 cells, normalized by sodium-independent diffusion. An asterisk (\*) indicates p-value < 0.05, \*\* indicates p < 0.01, and \*\*\* indicates p < 0.001.

Mouse Asbt was somewhat similar, preferentially transporting TCA, ACA, and 7 $\alpha$ -hydroxy-3-oxo-chol-4-en-24-oic acid with no significant transport of 3-oxo-CA, IALCA, or 3-oxo-chol-4-enic acid. An early evolving vertebrate animal, little skate (*Leucoraja erinacea*, ortholog denoted leAsbt), diverged from the evolutionary tree approximately 300 million years ago and uses 5 $\beta$ -C27 bile alcohols as its primary bile salts (22). This ortholog demonstrated sodium-dependent uptake of the planar bile acid ACA and the oxo bile acid 3-oxo-cholic acid; uptake of IALCA, 3-oxo-chol-4-enic acid, 7 $\alpha$ -hydroxy-3-oxo-chol-4-en-24-oic acid, and TCA showed transport not significantly different from sodium-independent uptake. The earliest extant vertebrate model used herein, sea lamprey (*Petromyzon marinus*, ortholog denoted pmAsbt), appeared approximately 500 million years ago and uses the 5 $\alpha$ -C27 bile alcohols in its bile. This ortholog presented a similar profile to skate, demonstrating sodium-dependent uptake of ACA, 3-oxo-CA, and 7 $\alpha$ -hydroxy-3-oxo-chol-4-en-24-oic acid but not IALCA, 3-oxo-chol-4-enic acid, or TCA. Finally, the insect model *Drosophila melanogaster*, or fruit fly (ortholog denoted as

dmAsbt), which does not utilize bile acids in its digestion, demonstrated preferential uptake of only ACA, IALCA, and 7 $\alpha$ -hydroxy-3-oxo-chol-4-en-24-oic acid.

### 4.3.2 Characterizing transport

#### kinetics of ASBT/Asbt orthologs

Bile acids that demonstrated sodium-dependent uptake in the above preliminary studies are subject to further investigation. These studies are ongoing but have already revealed insights into the transport preferences of these orthologs. Human ASBT exhibited saturable sodium-dependent transport of TCA and ACA, as expected, with TCA having an affinity of about 3-fold higher, as inferred from the calculated  $K_m$  value. While sodium-dependent transport of 7 $\alpha$ -hydroxy-3-oxo-chol-4-en-24-oic acid was demonstrated, maximum transport

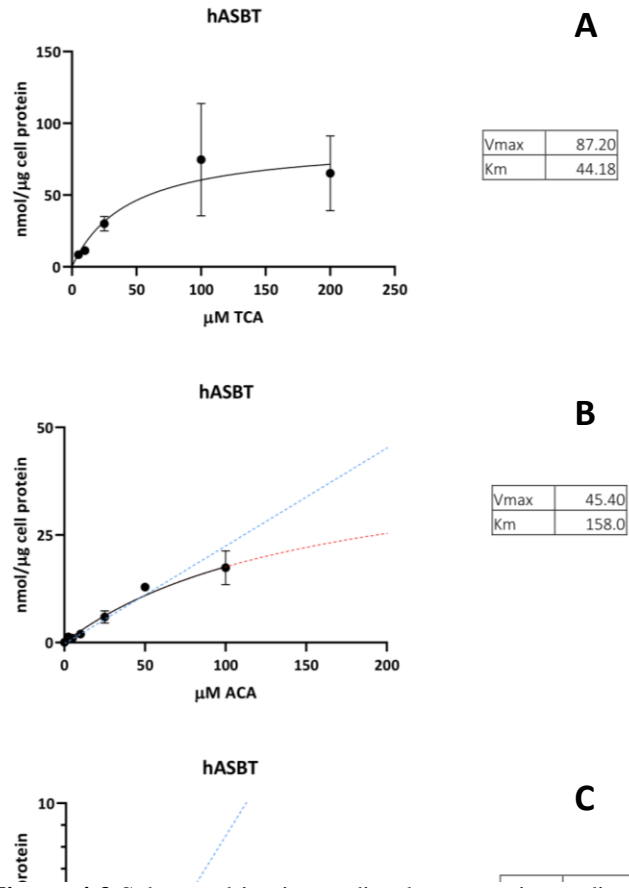


**Figure 4.3** Substrate kinetics studies demonstrating sodium-dependent uptake of bile acids in hASBT-transfected COS-1 cells. Michaelis-Menton models are given in black with red dashed lines representing continuation of the nonlinear function. Blue dashed lines represent the passive, linear component of transport as determined by higher concentrations of bile acid outside the saturable phase of uptake. All functions were calculated using GraphPad Prism, as in Materials and Methods. Panel A is TCA uptake, panel B is ACA uptake, and panel C is 7 $\alpha$ -hydroxy-3-oxo-chol-4-en-24-oic acid uptake. Data are given as nmol of bile acid/ $\mu$ g of total cell protein/12 minute of uptake.

was very low, indicating that passive diffusion of this compound is likely more physiologically relevant (figure 4.3).

The Asbt ortholog from sea lamprey (pmAsbt) demonstrated sodium-dependent uptake of ACA, 3-oxo-CA, and 7 $\alpha$ -hydroxy-3-oxo-chol-4-en-24-oic acid, as shown in figure 4.4. *P. marinus* Asbt seems to transport 7 $\alpha$ -hydroxy-3-oxo-chol-4-en-24-oic acid with higher affinity than ACA or 3-oxo-CA, as inferred from the Michaelis-Menton-like constant ( $K_m$ ). 3-oxo-CA showed sodium-dependent uptake but at a very low maximum rate. For comparison to hASBT, TCA was also assayed in kinetics experiments with pmAsbt and demonstrated saturable but low affinity transport.

While TCA seems to have demonstrated a saturable phase of

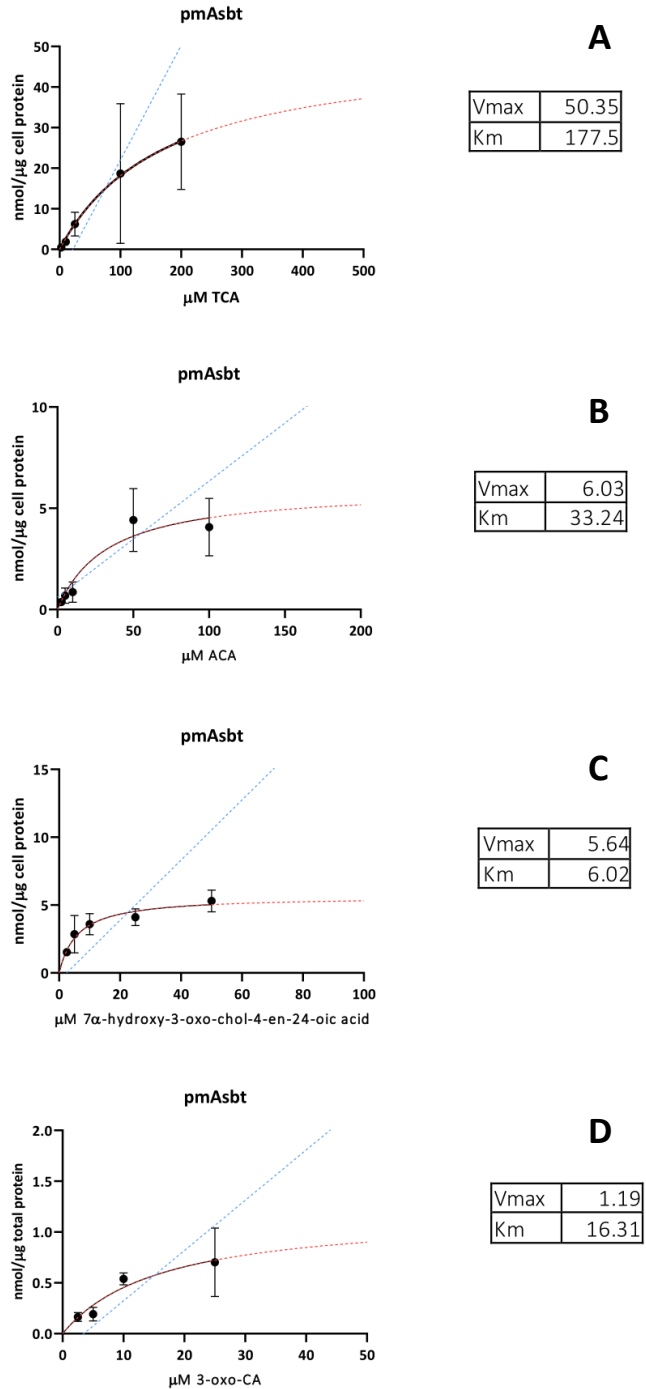


**Figure 4.4** Substrate kinetics studies demonstrating sodium-dependent uptake of bile acids in pmASBT-transfected COS-1 cells. Graphed functions are as in figure 4.3. Panel A is TCA uptake, panel B is ACA uptake, panel C is 7 $\alpha$ -hydroxy-3-oxo-chol-4-en-24-oic acid uptake, and panel D is 3-oxo-CA uptake. Data are given as nmol of bile acid/ $\mu$ g of total cell protein/12 minute of uptake.

sodium-dependent uptake, affinity was an order of magnitude lower than the planar bile acids.

Preliminary studies in the above section identified ACA and 3-oxo-CA as putative substrates for secondary active transport by the little skate ortholog of Asbt (leAsbt), so these compounds were further investigated in kinetics studies (figure 4.5). Again, TCA was assayed for comparison to hASBT; like with pmAsbt, leAsbt-mediated transport of TCA seemed to exhibit a saturable profile, but did so at a very low affinity, as indicated by the calculated  $K_m$  value.

Interestingly, the calculated  $K_m$  value for ACA was about one-third of that for TCA.

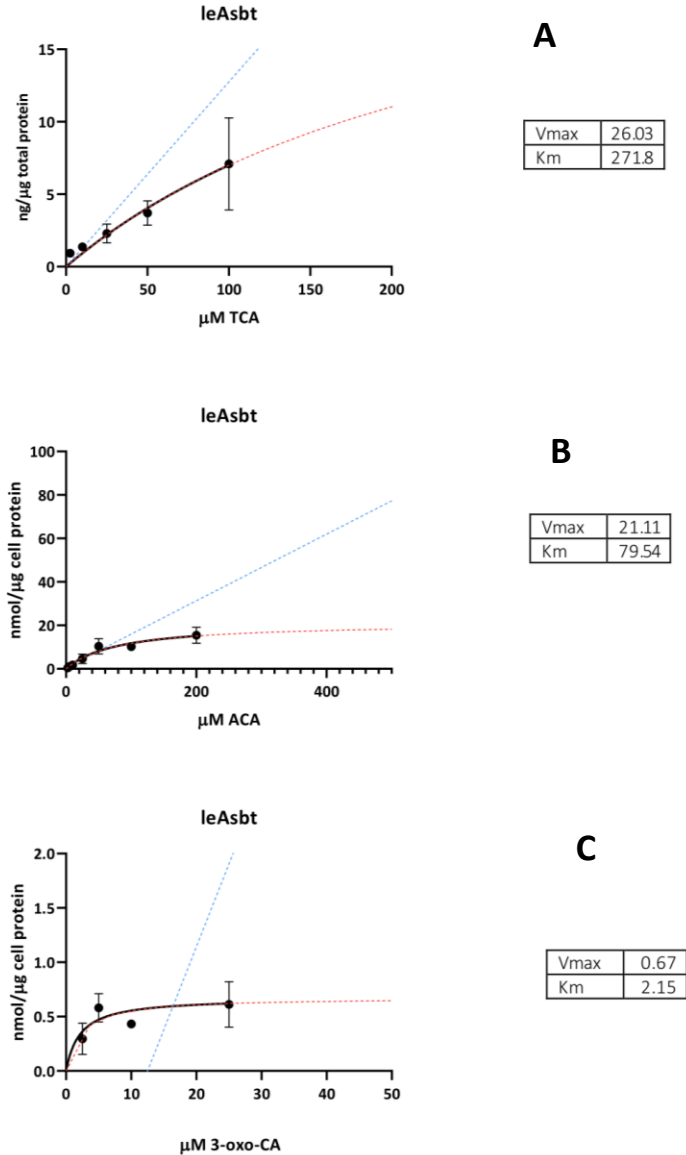


**Figure 4.5** Substrate kinetics studies demonstrating sodium-dependent uptake of bile acids in leASBT-transfected COS-1 cells. Graphed functions are as in figure 4.3. Panel A is TCA uptake, panel B is ACA uptake, and panel C is 3-oxo-CA uptake. Data are given as nmol of bile acid/ $\mu$ g of total cell protein/12 minute of uptake.

#### 4.4 Discussion

For the most part, the preliminary total uptake studies were able to predict the more detailed kinetic profiles of Asbt ortholog-mediated uptake of bile acids and derivatives. These earlier experiments reinforced our hypothesis that ASBT/Asbt has evolved alongside bile acid synthesis for the specific uptake of bile acids. Overall sodium-dependent uptake was manyfold higher for hASBT versus any of the orthologs, also indicating the increased efficiency of this transporter. However, it is also possible that transfection was simply more efficient in this case, since we did not examine the expression of ASBT/Asbt specifically, only total protein content. Similarly, it is important to note throughout the perusal of this discussion that, because data were normalized to total protein and not to the transporter protein in particular, transfection efficiency cannot be assumed, and  $V_{\max}$  cannot be compared between groups; however,  $K_m$  can be compared to determine differences in transporter affinity for specific bile acids (22).

As expected, hASBT demonstrated the most overall sodium-dependent uptake of TCA, the prototypical primary human bile salt (23). It also demonstrated sodium-dependent uptake of ACA, 3-oxo-CA, and isoallothiocholic acid (IALCA) to some extent (figure 4.2). This is consistent with previous studies demonstrating the ability of hASBT to take up earlier evolved bile salt forms in addition to modern bile salts (22). Additionally, pharmacophore modeling for hASBT indicates that the planar (*trans* conformation of the A ring) backbone of the allo bile acids should not be a hinderance to uptake (24, 25). As indicated by their names, ACA and 3-oxo-CA have only small changes to the typical CA and LCA that hASBT is known to readily transport (24). ACA is the  $5\alpha$ -epimer of CA; 3-oxo-CA swaps an oxo group for the normal  $3\alpha$ -hydroxy group in CA, and IALCA is the

3 $\beta$ /5 $\alpha$  epimer of LCA. As demonstrated in figure 4.3, hASBT had a higher affinity for TCA than ACA by about 3-fold.

Asbt from mouse demonstrated a similar profile to hASBT (figure 4.2), preferentially transporting TCA and ACA with the addition of 7 $\alpha$ -hydroxy-3-oxo-cholesterol-4-en-24-oic acid, a bile acid similar to CDCA that switches an oxo group for the C3 hydroxyl and has a double bond at the C4-C5 position, making it a planar BA. As with hASBT, these molecules closely resemble the normal substrates of mAsbt and may be metabolites of normal BA biosynthesis, so it is not surprising that they show active transport (16).

Little skate (leAsbt) represents the next latest evolving vertebrate model in this study. Total uptake profiles diverged from that of the mammalian ASBT/Asbt, showing no significant sodium-dependent transport of TCA. Instead, leAsbt demonstrated uptake of ACA and 3-oxo-cholic acid. When investigated further during kinetics experiments, leAsbt seemed to show some saturable transport of TCA but at very low affinity, consistent with previous studies (figure 4.4) (22).

Sea lamprey (pmAsbt) evolved approximately 200 million years before the little skate, and its existence as one of the earliest extant vertebrates is also thought to represent the earliest development of bile salts and the biliary tree (22). This ortholog exhibited significant sodium-dependent uptake of ACA, 3-oxo-CA, and 7 $\alpha$ -hydroxy-3-oxo-cholesterol-4-en-24-oic acid but not TCA (figure 4.3). As with leAsbt, further studies revealed low affinity but saturable transport for TCA via pmAsbt. Again, the highest affinity transport as inferred from the  $K_m$  value was for 7 $\alpha$ -hydroxy-3-oxo-cholesterol-4-en-24-oic acid.

#### 4.5 Conclusions and Future Directions

Preferential transport of compounds representative of ancestral bile salts by phylogenetically older species lends credence to our hypothesis that ASBT has evolved with bile acids for their specific uptake. As mentioned in an earlier section, this work is in progress, and we intend to continue characterizing the kinetic profiles of the bile acids and derivatives that showed sodium-dependent uptake in dmAsbt and mAsbt. However, multiple avenues of related research could also be pursued in tandem. Further characterization of Asbt orthologs would improve our understanding of their molecular structure and function, as well as assist in more rigorous comparison with human ASBT. This could include further kinetic uptake studies with additional bile acids and derivatives as well as other functional assays and expression studies. In addition, more investigation regarding the expression and function of Asbt orthologs *in vivo* would inform on the functional capacity of this transporter in these organisms, which would further elucidate its role at that point in the phylogenetic timeline.

#### 4.6 References

1. Lan K, Su M, Xie G, Ferslew BC, Brouwer KLR, Rajani C, Liu C, Jia W. Key Role for the 12-Hydroxy Group in the Negative Ion Fragmentation of Unconjugated C24 Bile Acids. *Anal Chem.* 2016;88(14):7041-8.
2. El-mir MY, Badia MD, Luengo N, Monte MJ, Marin JJG. Increased levels of typically fetal bile acid species in patients with hepatocellular carcinoma. *Clin Sci.* 2001;100:499-208.
3. Hofmann AF, Hagey LR. Bile Acids: Chemistry, Pathochemistry, Biology, Pathobiology, and Therapeutics. *Cell Mol Life Sci.* 2008;65:2461-83.
4. Mendoza ME, Monte MJ, El-mir MY, Badia MD, Marin JJG. Changes in the pattern of bile acids in the nuclei of rat liver cells during hepatocarcinogenesis. *Clin Sci.* 2002;102:143-50.
5. Mendoza ME, Monte MJ, Serrano MA, Pastor-Anglada M, Steiger B, Meier PJ, Medarde M, Marin JJG. Physiological characteristics of *allo*-cholic acid. *J Lipid Res.* 2003;44:84-92.
6. Monte MJ, El-mir MY, Sainz GR, Bravo P, Marin JJG. Bile acid secretion during synchronized rat liver regeneration. *Biochim Biophys Acta.* 1997;1362:56-66.
7. Monte MJ, Fernandez-Tagarro M, Macias RIR, Jimenez F, Gonzalez-San Martin F, Marin JJG. Changes in the expression of genes related to bile acid synthesis and transport by the rat liver during hepatocarcinogenesis. *Clin Sci.* 2005;109:199-207.
8. Monte MJ, Fernandez-Tagarro M, Marin JJG. Transient changes in the expression pattern of key enzymes for bile acid synthesis during rat liver regeneration. *Biochim Biophys Acta.* 2005;1734:127-35.
9. Sjovall J, Meurant G. Sterols and bile acids. Amsterdam: Elsevier Science; 1985. 255-61 p.
10. Stärkel P, Shindano T, Horsmans Y, Gigot JF, Fernandez-Tagarro M, Marin JJG, Monte MJ. Foetal 'flat' bile acids reappear during human liver regeneration after surgery. *Eur J Clin Invest.* 2009;39(1):58-64.
11. Hagey LR, Vidal N, Hofmann AF, Krasowski MD. Evolutionary diversity of bile salts in reptiles and mammals, including analysis of ancient human and extinct giant ground sloth coprolites. *BMC Evolutionary Biology.* 2010;10:133.
12. Hofmann AF, Hagey LR, Krasowski MD. Bile salts of vertebrates: structural variation and possible evolutionary significance. *Journal of Lipid Research.* 2010;51:226-46.
13. Kimura A, Mahara R, Inoue T, Nomura Y, Murai T, Kurosawa T, Tohma M, Noguchi K, Hoshima A, Fujisawa T, Kato H. Profile of Urinary Bile Acids in Infants and Children: Developmental Pattern of Excretion of Unsaturated Ketonic Bile Acids and 7 $\beta$ -Hydroxylated Bile Acids. *Ped Res.* 1999;45(4):603-9.

14. Kimura A, Suzuki M, Murai T, Inoue T, Kato H, Hori D, Nomura Y, Yoshimura T, Kurosawa T, Tohma M. Perinatal bile acid metabolism: analysis of urinary bile acids in pregnant women and newborns. *J Lipid Res.* 1997;38:1954-62.
15. Suzuki M, Murai T, Yoshimura T, Kimura A, Kurosawa T, Tohma M. Determination of 3-oxo- $\Delta^4$ - and 3-oxo- $\Delta^{4,6}$ -bile acids and related compounds in biological fluids of infants with cholestasis by gas chromatography-mass spectrometry. *J Chrom B.* 1997;693:11-21.
16. Shiffka SJ, Kane MA, Swaan PW. Planar bile acids in health and disease. *Biochimica et Biophysica Acta (BBA) - Biomembranes.* 2017;1859(11):2269-76.
17. Ohta K. Tetraoxy-norsterocholansäure aus der „Gigi“-Fischgalle (*Pelteobagrus nudiceps*). *Hoppe-Seyl Z* 1939;259(1-6):53-61.
18. Banerjee A, Ray A, Chang C, Swaan PW. Site-Directed Mutagenesis and Use of Bile Acid-MTS Conjugates to Probe the Role of Cysteines in the Human Apical Sodium-Dependent Bile Acid Transporter (SLC10A2). *Biochemistry.* 2005;44(24):8908-17.
19. Ayewoh EN, Czuba LC, Nguyen TT, Swaan PW. S-acylation status of bile acid transporter hASBT regulates its function, metabolic stability, membrane expression, and phosphorylation state. *BBA - Biomembranes.* 2021;1863(2).
20. Chothe PP, Czuba LC, Moore RH, Swaan PW. Human bile acid transporter ASBT (SLC10A2) forms functional non-covalent homodimers and higher order oligomers. *BBA - Biomembranes.* 2018;1860(3):645-53.
21. Czuba LC. Molecular Insight into the Structure, Function, and Regulation of Bile Acid Transport [dissertation]2017.
22. Lionarons DA, Boyer JL, Cai S-Y. Evolution of substrate specificity for the bile salt transporter ASBT (SLC10A2) [S]. *Journal of Lipid Research.* 2012;53(8):1535-42.
23. Marin J, Macias R, Briz O, Banales J, Monte M. Bile Acids in Physiology, Pathology and Pharmacology. *Current drug metabolism.* 2015;17.
24. Anwer M, Stieger B. Sodium-dependent bile salt transporters of the SLC10A transporter family: more than solute transporters. *Pflugers Archiv European Journal of Physiology.* 2014;466(1):77-89.
25. Zheng X, Ekins S, Raufman J-P, Polli JE. Computational Models for Drug Inhibition of the Human Apical Sodium-Dependent Bile Acid Transporter. *Molecular Pharmaceutics.* 2009;6(5):1591-603.

## Chapter 5 5. Disruption of Bile Acid Homeostasis in A Non-Human Primate Model of Radiation Injury

### 5.1 Introduction

Exposure to ionizing radiation causes the development of gastrointestinal acute radiation syndrome (GI-ARS). GI-ARS is characterized by nausea, vomiting, and/or diarrhea, which contribute to and can be exacerbated by electrolyte and fluid loss, nutritional deficits, weight loss, and injury of other organs (1, 2). The effects of GI-ARS are primarily due to immune system dysfunction, inflammation, and disruption of the intestinal barrier (3). Acute GI-ARS is a leading cause of morbidity and mortality following radiation exposure due to the threat of bacterial translocation across the disrupted gastrointestinal (GI) membrane and subsequent sepsis (1, 3). Long-term effects of GI-ARS include alterations in the structure and absorptive capacity of the gut membrane, which can further predispose the GI tract to maladies such as luminal narrowing, infection, and perforation (1). Treatment for GI-ARS is currently limited to supportive care, including the administration of anti-diarrheal agents and replacement fluids (2).

Treatment of malignant patients with radio- and chemotherapy also causes significant GI dysfunction and clinical GI symptoms (4, 5). Despite advances in cancer therapies, these symptoms are the most common problem as a result of treatment in cancer patients and have the greatest effect on quality of life (4, 6).

The malabsorption and/or dysregulation of bile acids (BAs), the regulatory and digestive end-products of cholesterol metabolism, are well-established contributors to GI dysfunction (7-10). Among the most prevalent of these issues in patients is bile acid diarrhea (BAD), a condition caused by the increased emptying of BAs into the colon and

feces (11). Increased luminal concentration of BAs in the small and large intestines causes diarrhea by a number of mechanisms, including increased water and electrolyte secretion, modified intestinal permeability, and stimulation of colonic propulsive contractions (11-13). The composition of the BA pool is also important, as some BAs (i.e. the di-hydroxy BAs) are stronger instigators of diarrhea, whereas others are more potent activators of cell membrane and nuclear receptors (8, 10, 12, 13).

Bile acid malabsorption (BAM) and subsequent BAD are recognized as important contributors to GI symptoms in cancer patients receiving chemotherapeutics (6). While most of these symptoms resolve once treatment is completed, a large portion of patients continue to have chronic GI upset (4). Previous studies have reported that administration of BA sequestrants such as cholestyramine can ameliorate GI symptoms in patients suffering from BAM and BAD; however, BAM is rarely diagnosed and thus usually left untreated in irradiated patients (6, 12, 13). In the population of patients that do receive BA sequestrant treatment, results are complicated by poor patient compliance due to the palatability of BA binders (12, 13). Alternative therapeutics for BAM and BAD are for the most part still in preclinical stages (13). Thus, dysregulation of bile acid homeostasis may be an important factor in the development and treatment of GI symptoms following irradiation. A more complete understanding of these mechanisms can help the development of medical countermeasures (MCM) to ameliorate acute symptoms and prevent the development of chronic GI issues.

This study was designed to examine the natural history of acute GI-ARS mechanisms following radiation injury. A single-dose partial-body irradiation (PBI) model with 2.5% bone marrow sparing (BM2.5) was applied to non-human primates (NHP),

which were then observed without medical intervention and sacrificed at various time points in the acute period. This model was developed to mirror exposure to ionizing radiation and has been extensively described by ourselves and collaborators (14, 15). This model offers the advantages of increased resemblance to human physiology in comparison to, for example, rodent models, as well as the interrogation of GI-ARS in the context of multi-organ injury (MOI) that is more relevant to intentional or accidental radiation exposure (14, 15). Bile acids were examined as a proportion of the total bile acid pool and as individual concentrations within liver tissue, plasma, and bile in order to observe the effect of radiation injury on the bile acid pool's composition and overall BA homeostasis. Additionally, several genes involved in the enterohepatic cycling of bile acids were examined using qRT-PCR to further investigate molecular mechanisms of GI-ARS as related to bile acid dysregulation.

## 5.2 Materials and Methods

### 5.2.1 Radiation Animal Model

All animal procedures were conducted in accordance with the NIH guidelines for the care and use of laboratory animals and experiments were performed with prior approval from the University of Maryland Institutional Animal Care and Use Committee (IACUC) (table 5.1). Plasma was obtained from EDTA-anticoagulated peripheral blood of male rhesus macaques (*Macaca mulatta*); tissue was collected from the ileum and right central lobe of the liver and were snap frozen in liquid nitrogen. Plasma and tissues were stored at -80 °C until assay. Samples were provided by the laboratory of Thomas J. MacVittie, University of Maryland School of Medicine, Department of Radiation Oncology (Baltimore, MD). Description of the animal models, including radiation exposure and

day	#N		Group	Euthanization type	Day	Animal #
day 0	2		Baseline/naïve	Baseline	0	RA0876
day 4	4			Baseline	0	RA0879
day 5	1		Days 4-5	Scheduled	4	RA0191
day 8	7			Scheduled	4	RA0261
day 9	4			Scheduled	4	RA0809
day 10	1			Scheduled	4	RA0827
day 11	5			Cause	5	RA0260
day 12	3		Days 8-10	Scheduled	8	RA0231
day 13	1			Scheduled	8	RA0398
day 14	1			Scheduled	8	RA0841
day 15	5			Scheduled	8	RA0878
day 16	2			Cause	8	RA0806
day 17	1			Cause	8	RA0849
day 18	1			Cause	8	RA0870
day 21	2			Cause	9	RA0805
day 22	1			Cause	9	RA0832
				Cause	9	RA0839
			Cause	9	RA0848	
			Cause	10	RA0812	
			Days 11-14	Scheduled	11	RA0432
				Scheduled	11	RA0829
				Scheduled	11	RA0869
				Scheduled	11	RA0871
				Cause	11	RA0433
				Cause	12	RA0403
				Cause	12	RA0817
				Cause	12	RA0823
				Cause	13	RA0256
				Cause	14	RA0804
			Days 15-22	Scheduled	15	RA0414
				Scheduled	15	RA0838
				Scheduled	15	RA0868
				Scheduled	15	RA0873
				Scheduled	21	RA0863
				Scheduled	21	RQ9724
				Scheduled	22	RA0847
				Cause	15	RA0248
				Cause	16	RA0229
				Cause	16	RA0803
			Cause	17	RA0822	
			Cause	18	RA0272	

**Table 5.1** Animal identifiers, euthanasia day and type, and groupings used during analysis.

dosimetry, medical management (supportive care and health monitoring), as well as collection of tissue have been previously described (14). Briefly, NHP [5.5 – 11.3 kg body

weight] were exposed to 12 Gy partial body irradiation with 2.5% bone marrow sparing (PBI/BM 2.5) with 6 MV LINAC-derived photons at 0.80 Gy min<sup>-1</sup>. Bone marrow sparing was accomplished with tibiae outside the beam field. Timed euthanasia was planned at day 4, 8, 11, 15, and 21 after radiation. Early euthanasia due to cause for some animals resulted in a final count of n=4 animals at day 4, n=7 animals at day 8, n=4 animals at day 9, n=1 animal at day 10, n=4 animals at day 11, n=3 animals at day 12, n=1 animal at day 13, n=1 animal at day 14, n=5 animals at day 15, n=2 animals at day 16, n=1 animals for days 17 and 18, n=2 animals at day 21, and n=1 animal at day 22 (table 5.1). Samples were arranged into 5 groups as follows: day 0 (baseline/naïve; n=7 for plasma, n=2 for tissue and bile); day 4 (n=4); days 8-10 (n=12); days 11-14 (n=9); and days 15-22 (n=12). Plasma (n=7) and tissue (n=2) from non-irradiated animals were used as baseline controls.

### 5.2.2 Quantification of Bile Acids

Quantification of bile acids in plasma, bile, and liver tissue was carried out as described previously in detail (16). In brief, 100µL of plasma was added to an ISOLUTE PLD+ phospholipid deletion column (Biotage, Uppsala, Sweden) containing ACN with 1% FA as crash solvent and CA-d<sub>4</sub> and GCDCA-d<sub>4</sub> as internal standards (IS). Columns were vortexed before collecting flow-through by positive pressure. Flow-through fractions were dried down and then resuspended for injection. Bile samples were processed similarly but diluted 1:9 and 1:1,000 with water pre-extraction; before resuspension, the bile samples that were diluted 1:1,000 were additionally diluted 1:100 during resuspension for a final dilution of 1:100,000 for the analysis of BAs at high abundance.

Liver tissue dissected from the central right lobe of NHPs were sectioned and weighed, then approximately 50 mg were added to Fisherbrand prefilled bead mill tubes

(Pittsburgh, PA) with 50% methanol. Tissue sections were homogenized using a Precellys 24 tissue homogenizer (Bertin Technologies, Paris, France), then centrifuged at 2,000 rpm for 10 minutes. Homogenates were aspirated, spiked with IS, mixed with ACN with 1% FA and vortexed, shaken at ambient room temperature ( $23\pm 2$  C°) for 1 hour, and finally centrifuged. Supernatants were applied to ISOLUTE PLD+ columns; flow-through was collected and dried under N<sub>2</sub> gas flow, then resuspended proportionally to starting weight to make a 50 mg/mL solution for final injection.

A Waters ACQUITY BEH C<sub>18</sub> UPLC column (150 x 2.1 mm, 1.7 $\mu$ m) was used with a Waters I-Class UPLC coupled to a Waters Xevo TQ-XS triple quadrupole mass spectrometer (Waters Corporation, Milford, MA) using ESI in negative ion mode. The chromatographic gradient was a linear gradient over 32 min with a mobile phase consisting of water with 0.01% FA and ACN with 0.01% FA with a flow rate of 0.35 mL/min. Detection was performed using scheduled MRM or SIM. Data were processed using Waters MassLynx and TargetLynx software (version 4.1 SCN 901).

### 5.2.3 qRT-PCR

Representative samples (those with the most drastic changes from naïve in the bile acid analysis) were used for each grouping of NHP tissue. These and primer sequences can be found in tables 5.2 and 5.3, respectively. Approximately 50mg of tissue from liver and ileum were sectioned and weighed before homogenization using a Precellys 24 tissue homogenizer in 50% methanol, as above. Total mRNA was isolated from liver and ileum sections using TRIzol reagent and reverse transcribed using High-Capacity cDNA Reverse Transcription Kit (Thermo Fisher Scientific, Waltham, MA) following manufacturer recommendations. Gene expression was normalized to *Gapdh*. Assays were performed in

96-well optical plates with SYBR Green PCR Master Mix using a StepOne Real-Time PCR System and software (version 2.3). Relative expression was calculated using the  $2^{-\Delta\Delta C_t}$  method (17).

Group	Animal identifier
Naive/baseline	RA0876
	RA0879
Days 4-5	RA0191
	RA0261
	RA0827
Days 8-10	RA0848
	RA0841
	RA0870
Days 11-14	RA0869
	RA0817
	RA0403
Days 15-22	RQ9724
	RA0847
	RA0868
	RA0838

**Table 5.2** Experimental NHP groupings used for qRT-PCR

Gene	F primer	R primer	Reference
			<a href="https://biodb.swu.edu.cn/qprimerdb/primer">https://biodb.swu.edu.cn/qprimerdb/primer</a>
Abcb11 (Bsep)	TTGCAGAAAATATTCGCTACGG	TCCATGATGAAGTTGTAGGCAT	<i>M.mulatta.006180v1</i>
Cyp7a1	TTTGGTTATGAAACATGCGGAG	TTCATCTGCAAGTCATTTAGCG	<i>M.mulatta.002936v1</i>
Cyp7b1	GACATGAATGATGAGCTTACC	GTAGCTGGGATTCAAACACTTG	<i>M.mulatta.001992v1</i>
Cyp27a1	GTGTAGGACTTCCCGTTTC	GCCTCTCAAATAACTTTTCGCT	<i>M.mulatta.003035v1</i>
Nr1h4 (Fxr)	GGCAACCAATCATGTACAAGTT	GAAAATCTCAGCTGAACGAAGG	<i>M.mulatta.001627v1</i>
Slc10a1 (Ntcp)	GCAAGATCAAGGCTCACTTATG	GGTCATCACAATGCTGAGATT	<i>M.mulatta.010063v1</i>
Slc10b1 (Oat1b1)	AGAAGTGATGCTTGTCTAACGA	CTAGAATCCTCCTAGTGCTCG	<i>M.mulatta.003838v1</i>
Gapdh (housekeeping)	ACATCAAGAAGGTAGTGAAGCA	AAATGAGCTTGACAAAGTGGTC	<i>M.mulatta.003802v1</i>
Slc10a2 (Asbt)	TTGATCCAGATAGGTGAACGAG	TATTTTTCTCCCACTAGCACG	<i>M.mulatta.003406v1</i>
MRP2	ATGTCACGTGGAATACCAGC	ACCATTACCTTGCTACTGTCCATGA	<a href="https://doi.org/10.1016/j.ejphar.2019.172883">https://doi.org/10.1016/j.ejphar.2019.172883</a> (human MRP2)
Shp	CAAGATGCTGTGACCTTTGAAG	CTTTCAGGCAGGCATATTCCTT	<i>M.mulatta.004621v1</i>
Tgr5 (M-bar)	TGACTTCTGCCCTATCATATCG	GACAAAAGTGGGAAGACGAAA	<i>M.mulatta.010236v1</i>
MDR2/3 (ABC4)	GCAGACGGTGGCCCTGGTTGG	TGGAAAACAGCACCGGCTCCTG	DOI: 10.1038/srep06899 (human MDR2/3)
Cyp8b1	CATGGCTTCCGGAAGAATATG	GCACTGAACGGTATCCAAATAC	<i>M.mulatta.012188v1</i>
Oatp1b1 (Oatp2, Slc21a6)	AGAAGTGATGCTTGTCTAACGA	CTAGAATCCTCCTAGTGCTCG	<i>M.mulatta.003838v1</i>
Mrp3	CCTATCTACTCCCACTTTTCGG	GTTGGAGATGATGTAGGGGTAG	<i>M.mulatta.001550v1</i>
Mrp4	GGAAAGTGCCAAAGTAATCCAG	ACATGGCTATTCGTAACCTCAT	<i>M.mulatta.009796v1</i>
FGF19	ATGGCTACAATGTGTACCGATC	AGAAAGCCTCTGTTCTGTACA	<i>H.sapiens.003277v1</i>
Osta (Slc51a)	CCAATACGCCTTCTGAAGATA	CTGTGCTTGTCTCAGAAATGTC	<i>M.mulatta.010183v1</i>
Ibabp (Fabp6)	ATGACCAACAAGTTCACCTGTTG	TGGTGATAGTTGGGAAATCA	<i>M.mulatta.010352v1</i>

**Table 5.3** Primer sequences used in qRT-PCR

#### 5.2.4 Statistics

Welch's and Dunnett's tests were performed to determine statistical significance using GraphPad Prism software (version 8.2.1 [441]).

#### 5.3 Results

In order to investigate perturbation of the enterohepatic circulation following 12 Gy PBI/BM 2.5, bile acids were quantified in multiple compartments (i.e. liver tissue, bile, and plasma) and compared as concentration and percent of total bile acids. Several genes were also assayed by qRT-PCR to further probe mechanisms involved in EHC dysregulation.

##### 5.3.1 Plasma

Total BAs (TBA) in plasma decreased following 12 Gy PBI/BM 2.5, dropping to approximately 15% of naïve levels at days 8-10 (figure 5.1A, table 5.3). Amidated BAs increased as the proportion of TBA by over 6.5-fold (figure 5.1B). Specifically, conjugation to glycine increased by over 4-fold and taurine by approximately 2.4-fold. At the same time, the proportion of unconjugated BAs dropped to about 24% of baseline.

Individual BAs were examined both as concentration and as percentage of TBA within plasma, which sometimes revealed opposing trends (table 5.4). For example, the concentration of LCA decreased within circulation by a maximum factor of approximately 40; however, there was no statistically significant change of LCA as a percentage of TBA in plasma. Conversely, while the amount of DCA showed no appreciable difference in concentration following PBI, it demonstrated a significant increase as ratio of TBA in plasma, growing by over 7-fold. CA demonstrated a slight 1.1-fold increase in plasma concentration at days 8-10 but a concurrent increase of nearly 5-fold in the proportion of

TBA.

Meanwhile, some BAs showed contrary trends between concentration and % of TBA. The concentration of glycine-conjugated CA (GCA) decreased by nearly 5-fold, yet

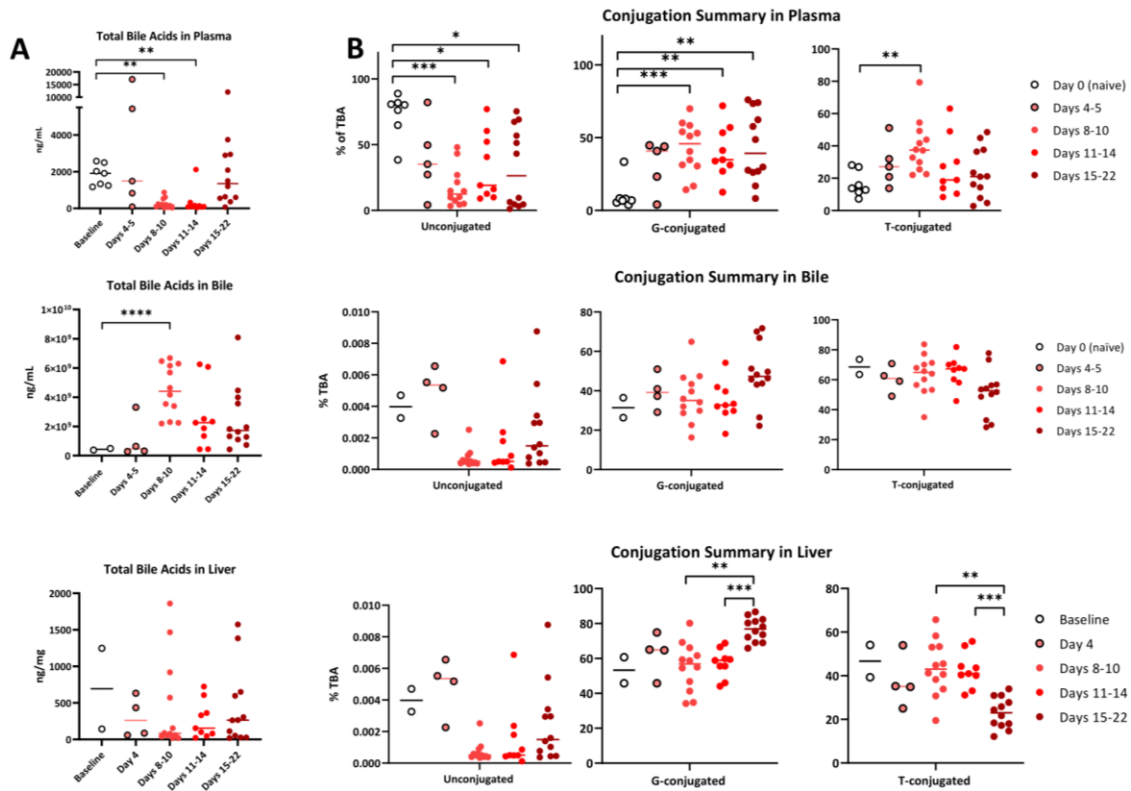


**Figure 5.1** Summary of total bile acids (A) and conjugation profiles (B) in each tissue compartment.

its proportion of TBA increased by over 3-fold. This phenomenon was also observed in taurine-conjugated deoxycholic acid (TDCA), whose concentration decreased by about half while its fraction of TBA increased by nearly 3-fold at days 8-10.

As a proportion of TBA, increases were seen in GCDCA, TCDCA, DCA, and TDCA, in addition to those mentioned above and to ACA, which demonstrated over 100-fold increase at days 15-22 relative to naïve plasma. These accompanied decreases in TCA, CDCA, and TLCA. When measured as concentration in plasma, GCDCA was the only BA

to increase, overtaken by decreases in CA and its conjugates, CDCA, TDCA, and LCA and its conjugates.

	Plasma (µg/mL)					Liver (ng/mg tissue)					Bile (mg/mL)				
	Baseline	Days 4-5	Days 8-10	Days 11-15	Days 15-22	Baseline	Days 4-5	Days 8-10	Days 11-15	Days 15-22	Baseline	Days 4-5	Days 8-10	Days 11-15	Days 15-22
TBA	1.82 ± 0.59	4.98 ± 7.07	0.26 ± 0.36	0.35 ± 0.67	2.39 ± 3.27	695.7 ± 782.0	303.2 ± 278.0	443.9 ± 637.1	269.7 ± 255.5	439.9 ± 531.1	0.43 ± 0.06	1.14 ± 1.46	4.48 ± 1.75	2.62 ± 2.15	2.53 ± 2.18
Unconjugated BAs	0.20 ± 0.20	1.90 ± 2.42	0.06 ± 0.12	0.06 ± 0.08	1.03 ± 2.35	0.3 ± 0.3	0.2 ± 0.2	0.6 ± 1.0	0.7 ± 1.8	0.6 ± 0.7	0.02 ± 0.001	0.04 ± 0.03	0.03 ± 0.02	0.04 ± 0.06	0.03 ± 0.02
G-conjugated BAs	0.05 ± 0.05	1.65 ± 3.0	0.11 ± 0.12	0.17 ± 0.39	0.93 ± 1.05	328.9 ± 343.6	196.1 ± 181.8	176.4 ± 237.9	157.2 ± 145.5	320.2 ± 361.7	0.13 ± 0.01	0.42 ± 0.54	1.73 ± 1.12	0.90 ± 0.80	1.08 ± 0.70
T-conjugated BAs	0.44 ± 0.34	1.43 ± 2.27	0.10 ± 0.09	0.11 ± 0.21	0.42 ± 0.41	365.5 ± 438.2	106.9 ± 96.5	199.2 ± 336.5	109.0 ± 111.0	121.6 ± 172.5	0.30 ± 0.08	0.71 ± 0.92	2.76 ± 1.14	1.72 ± 1.43	1.45 ± 1.60

	Plasma (% TBA)					Liver (% TBA)					Bile (% TBA)				
	Baseline	Days 4-5	Days 8-10	Days 11-15	Days 15-22	Baseline	Days 4-5	Days 8-10	Days 11-15	Days 15-22	Baseline	Days 4-5	Days 8-10	Days 11-15	Days 15-22
Unconjugated BAs	73.0 ± 6.4	40.0 ± 13.0	17.4 ± 4.3	33.0 ± 8.4	37.7 ± 8.7	0.05 ± 0.01	0.12 ± 0.06	0.10 ± 0.13	0.19 ± 0.24	0.34 ± 0.45	0.004 ± 0.001	0.005 ± 0.002	0.001 ± 0.001	0.002 ± 0.002	0.002 ± 0.003
G-conjugated BAs	10.4 ± 3.9	31.4 ± 7.9	42.9 ± 5.1	40.3 ± 6.0	44.0 ± 7.0	53.3 ± 10.5	62.6 ± 12.1	55.2 ± 13.9	57.2 ± 8.19	76.6 ± 6.78	31.4 ± 7.1	39.6 ± 9.0	36.8 ± 12.9	34.6 ± 10.0	48.8 ± 15.3
T-conjugated BAs	16.6 ± 3.0	29.0 ± 6.3	40.0 ± 4.7	26.6 ± 6.2	23.2 ± 4.5	46.7 ± 10.5	37.3 ± 12.1	43.8 ± 12.7	42.6 ± 8.20	23.0 ± 7.06	68.6 ± 7.1	60.4 ± 9.0	63.2 ± 12.9	65.4 ± 10.0	51.2 ± 15.3

**Table 5.4** Summary of total bile acids (TBI) and conjugation in each tissue compartment.

### 5.3.2 Bile

Following PBI, the concentration of biliary TBA increased over 10-fold (figure 1A, table 5.6A). Converse to what was seen in plasma, there was no significant change in percentage of conjugated versus unconjugated BAs in biliary TBA from naïve (figure 5.1B, table 5.3). The concentration of most individual BAs included in this study increased significantly within bile following radiation; however, as in plasma, the largest differences were not always replicated in the changes in ratio of TBA. Interestingly, only two BAs showed significant changes in their ratios of TBA: GCDCA increased by 2.4-fold, while TCA decreased by 1.7-fold (figure 5.2, table 5.6B).

BA as % TBA	Plasma	Bile	Liver
CA (1°)	↑	↔	↔
GCA	↑	↔	↔
TCA	↓	↓	↓
CDCA (1°)	↓	↔	↔
GCDCA	↑	↑	↑
TCDCa	↑	↔	↔
DCA (2°)	↑	↔	↔
GDCA	↑	↔	↑
TDCA	↑	↔	↔
LCA (2°)	↔	↔	↔
GLCA	↔	↔	↑
TLCA	↓	↔	↑
UDCA (2°)	n.d.	↔	↔
GUDCA	n.d.	↔	↔
ACA (planar)	↑	↔	n.d.
IALCA (planar)	n.d.	↔	↔
7αOH3ochol4enic acid (planar)	n.d.	↔	↔

[BA]	Plasma	Bile	Liver
CA (1°)	↓	↔	↔
GCA	↓	↑	↔
TCA	↓	↑	↔
CDCA (1°)	↓	↔	↔
GCDCA	↑	↑	↔
TCDCa	↔	↑	↔
DCA (2°)	↔	↔	↔
GDCA	↔	↑	↔
TDCA	↓	↑	↔
LCA (2°)	↓	↔	↔
GLCA	↓	↔	↔
TLCA	↓	↑	↔
UDCA (2°)	n.d.	↔	↔
GUDCA	n.d.	↑	↔
ACA (planar)	↔	↑	n.d.
IALCA (planar)	n.d.	↔	↔
7αOH3ochol4enic acid (planar)	n.d.	↔	↔

	Plasma	Bile	Liver
TBA	↓	↑	↔
% Unconjugated	↓	↔	↔
% G-conjugated	↑	↔	↑
% T-conjugated	↑	↔	↓

**Figure 5.2** Summary of statistically significant changes in bile acid concentration (left) and proportion of total bile acids (right) demonstrated following PBI.

### 5.3.3 Liver Tissue

TBA concentration within liver tissue did not significantly change during the course of this study (figure 5.1A, table 5.5A). The proportions of unconjugated BAs between the groups showed no appreciable differences, while glycine conjugation increased slightly (1.4-fold), and taurine conjugation decreased slightly (1.9-fold) (figure 5.1B, 5.2). As was the case in plasma, significant differences in individual BA concentration were not often in agreement with significant differences in the proportion of the TBA pool. In fact, no individual BA demonstrated a statistically significant change in liver tissue when measured as concentration normalized by tissue weight (figure 5.2). This effect is likely due to the high variability within each group. Examining the BAs by proportion of TBA revealed maximal increases in GCDCA (5-fold), GDCA (7-fold), GLCA (24-fold), and TLCA (nearly 4-fold) with a simultaneous decrease in the proportion of TCA (5.7-fold) (figure 5.2, table 5.5B). The most pronounced differences within liver tissue following PBI occurred at the latest time point in this study (days 15-22); this is in contrast to what was seen in plasma and bile, which usually demonstrated maximal changes earlier (days 8-10).

### 5.3.4 Planar Bile Acids

The planar bile acids ACA, IALCA, and  $7\alpha$ -hydroxy-3-oxo- $\text{chol-4-en-24-oic acid}$  were quantified in this study in order to better interrogate the roles of these molecules in their reappearance during disease and injury. In plasma, IALCA and  $7\alpha$ -hydroxy-3-oxo- $\text{chol-4-en-24-oic acid}$  were below the LLOD, but ACA demonstrated an approximate 124-fold increase in proportion of TBA between baseline and days 15-22 while showing no statistically significant change as concentration. In bile, all three species of planar BAs were quantifiable, but again only ACA changed, increasing by over 11-fold in

concentration between baseline and days 8-10 but exhibiting no statistically significant change as percent of TBA. In liver tissue, ACA was below the LLOD, and IALCA and 7 $\alpha$ -hydroxy-3-oxo-chol-4-en-24-oic acid presented no change as either percent of TBA or concentration.

### 5.3.5 mRNA

Several target genes in liver and ileum were assayed using qRT-PCR. Only three of the genes assayed demonstrated statistically significant differences in relative expression: *Cyp7a1* in liver and *Fxr* and *Fgf19* in ileum (figure 5.3). *Cyp7a1* was increased by approximately 5-fold at days 8-10 and at days 11-14, whereas other BA synthetic genes (*Cyp27a1* and *Cyp8b1*) showed no change. Ileal *Fxr* was downregulated by about 50% at days 4-5; conversely, *Fgf19* demonstrated an approximate 15-fold induction in ileum at days 8-10 (group 3) and then decreased nearly to basal levels by days 11-14 and 15-22. Other regulatory and signaling elements (hepatic *Fxr*, *Shp*, *Tgr5*, and ileal *Ibabp*) were examined but showed no statistically significant change. Likewise, no statistically significant differences were observed in any of the transporter genes assayed (*Bsep*, *Ntcp*, *Oatp1b1*, *Asbt*, *Osta*, *Mrp2*, *Mrp3*, *Mrp4*, or *Mdr2/3*).

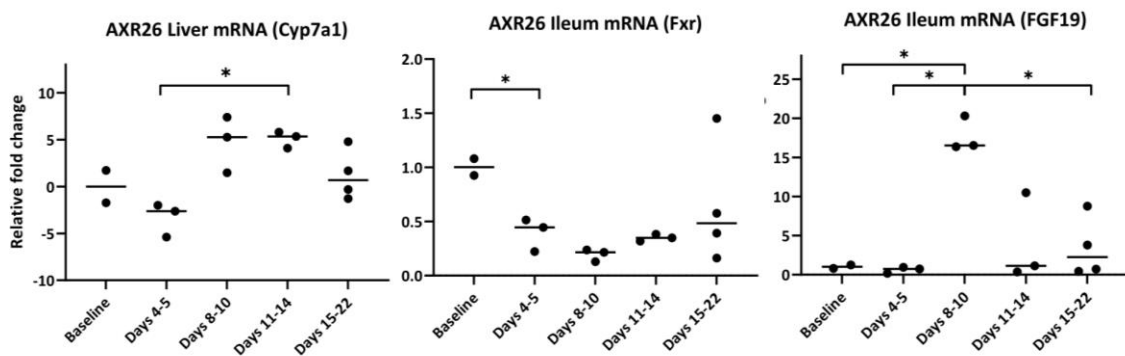


**Figure 5.3** Relative changes in mRNA determined by qRT-PCR.

A

ng/mL	Baseline										Days 4-5										Days 8-10									
	9050081	9052341	8051751	9030501	8052041	RA0876	RA0879	RA0191	RA0261	RA0809	RA0827	RA0260	RA0398	RA0841	RA0878	RA0231	RA0806	RA0849	RA0870	RA0805	RA0832	RA0839	RA0848	RA0812						
LCA	24.6538	33.2974	123.0645	99.947	20.7249	6.448	10.9748	54.8082	13.2843	12.4191	5.2955	3.0825	0.5543	3.5616	2.3037	1.8502	1.5478	<LLOQ	0.0694	<LLOQ	0.0463	<LLOQ	<LLOQ							
CDCA	2249.229	1585.928	1390.955	788.2089	425.7292	1602.083	1063.829	109.0584	352.7029	4.1946	387.3929	12.153	5.7195	7.846	0.6829	57.2969	76.6177	6.3031	1.0066	5.0152	4.825	18.5358	2.3714							
DCA	<LLOQ	<LLOQ	<LLOQ	<LLOQ	<LLOQ	0.566	2.9297	67.1551	44.2234	35.6564	19.6725	11.0087	0.5021	2.7642	1.8662	1.8662	8.472	6.206	1.2857	0.6056	0.4997	8.3013	0.2702							
CA	14.5785	12.7791	11.8829	3.5968	27.0476	7.2287	14.0005	61.6793	423.1896	7.8637	400.921	17.8554	5.0106	24.1362	1.2393	22.7659	4.8352	2.7562	1.149	0.8193	14.3651	0.5027								
ACA	0.253076	0.799931	0.588809	0.684688	0.058477	<LLOQ	0.393578	<LLOQ	4.4704	1.1972	5.5808	<LLOQ	0.4388	0.333	0.5628	0.3202	0.0743	<LLOQ	<LLOQ	0.4093	<LLOQ	0.4303								
GLCA	19.3503	11.8561	11.51	18.7822	11.4982	2.1962	7.2006	104.8088	21.7083	1.9346	<LLOQ	0.8298	0.0603	<LLOQ	<LLOQ	0.4402	4.3589	1.7559	0.4009	0.1791	<LLOQ	6.6841								
GDCA	17.5757	18.1685	28.5095	15.6549	49.6278	16.3696	14.1986	64.4641	774.0808	266.9658	4.055	5.1728	2.8545	66.7959	0.546	51.2011	9.7373	18.6985	3.4304	1.7921	17.6287	11.5844								
GDCCA	42.5654	49.9963	52.5959	27.5658	245.7808	100.1217	27.7262	120.928	1496.266	219.3431	26.4748	7.0178	18.3077	84.7192	8.621	212.0211	50.9226	101.9352	21.0409	6.9951	43.7083	27.9704								
GCA	20.2321	30.6155	37.93	30.6095	108.1756	62.1378	11.3218	75.1685	<LLOQ	177.0226	190.6887	7.782	4.2596	81.4791	24.5062	212.0211	50.9226	101.9352	21.0409	6.9951	43.7083	27.9704								
TLCA	19.2666	18.544	18.5942	20.0593	11.9603	11.0364	13.8561	9.9891	10.8934	1.6047	0.2714	2.1191	0.2752	1.0474	1.0884	1.7825	1.875	1.4333	0.4721	0.3248	0.1337	0.3646								
TDCA	20.3124	26.0063	27.8492	14.0938	25.8007	28.4076	23.2722	21.4758	607.9515	131.6481	111.1177	3.5122	2.1195	16.5554	11.8475	31.9894	7.3106	12.998	9.9384	0.8992	<LLOQ	8.2366								
TDCCA	128.9846	195.2658	178.5071	128.2957	287.5758	568.0388	79.6924	131.6619	3643.34	594.2287	581.7462	15.443	41.1113	99.8235	146.6136	155.2069	35.7246	73.5423	15.0849	7.532	57.3651	55.6872								
TCA	19.3425	39.2116	20.295	22.9474	24.0358	64.9451	36.6374	10.5255	>UOQ	31.344	53.9765	3.2032	2.16	1.5236	0.932	1.0691	0.5566	2.0081	1.1514	0.3449	1.7126	0.3489								
TBA	2577.842	2024.62	1911.054	1172.894	1244.005	2493.203	1334.576	831.7227	17074.9	1485.423	5427.193	89.5286	83.3734	524.5951	200.8096	611.2052	206.4565	241.7741	872.2957	58.7888	32.2362	154.3122								

ng/mL	Days 11-14										Days 15-22										
	RA0829	RA0869	RA0871	RA0433	RA0403	RA0817	RA0823	RA0256	RA0804	RA0414	RA0838	RA0873	RA0248	RA0229	RA0803	RA0822	RA0272	RA0863	RCQ724	RA0847	
LCA	2.8491	31.4555	2.7143	<LLOQ	<LLOQ	1.3998	0.5251	<LLOQ	5.0766	18.7854	125.4961	11.6937	4.6496	2.3046	1.8716	4.3315	1.1527	98.7731	3.5861	1.7966	5.655
CDCA	14.4098	140.1481	4.4372	6.7676	13.9995	3.1534	29.6692	89.6331	48.3643	19.0377	125.7431	21.7914	12.0043	57.1452	6.6146	0.4148	152.4701	2763.022	110.9488	980.0588	118.8208
DCA	7.1739	84.2988	21.8788	0.4657	1.0616	2.2704	3.3384	1.4118	2.6859	67.5293	701.9342	5.6414	4.8317	14.049	3.6145	0.769	9.363	1028.647	18.3765	252.9338	71.0483
CA	7.9939	9.1806	1.1925	5.3035	4.4581	1.0092	5.0953	15.7321	2.8732	10.3144	59.0061	14.696	3.0927	112.1598	4.5203	1.0579	74.7813	4375.746	191.0334	395.6645	256.1188
ACA	0.0263	2.5429	<LLOQ	<LLOQ	<LLOQ	<LLOQ	0.0736	0.7625	0.1097	2.1733	0.2134	0.9741	0.0267	0.4768	0.1381	0.3131	0.581	22.0982	0.1858	3.6692	1.0716
GLCA	0.1957	40.7659	0.843	0.0132	<LLOQ	0.4116	0.0288	<LLOQ	4.1392	5.4226	88.2428	18.2682	60.7201	2.0107	0.2779	5.5353	4.1388	76.5056	0.7714	0.0106	3.4686
GDCA	16.6762	437.2221	51.2726	<LLOQ	0.5599	19.8416	2.0694	0.7508	1.2439	1623.038	243.8699	90.976	206.8686	216.1572	51.9342	1.367	2.1311	532.6064	24.6987	139.6696	38.0474
GDCCA	61.164	680.2358	28.4297	19.7342	8.726	32.2827	32.5426	15.3416	23.5041	928.2859	92.6055	440.3176	913.0904	968.0619	176.8395	41.22	27.5398	1947.572	105.9352	611.5323	42.4575
GCA	10.0454	50.0436	4.25	7.636	3.6529	9.8295	4.5537	1.4158	1.6627	190.6591	23.1916	141.5046	247.0904	40.8472	6.4972	12.0056	598.8469	43.3718	28.2576	17.4339	
TLCA	0.7075	21.3405	0.7765	0.5128	0.1891	<LLOQ	0.3082	0.2312	0.3934	1.3031	17.3179	4.0289	30.4218	0.7438	0.2864	0.2956	3.7935	5.7631	<LLOQ	<LLOQ	0.5311
TDCA	24.9623	88.9339	3.4331	0.9999	<LLOQ	1.973	1.5228	1.121	<LLOQ	154.6195	3.3745	67.0515	134.9039	231.187	9.7428	1.1606	39.2793	103.4741	20.7702	83.2669	2.7197
TDCCA	177.9154	529.3166	38.931	37.5547	4.9363	13.3929	14.7895	13.3243	7.165	713.3308	21.4573	351.3953	582.4241	1038.384	65.0469	7.7363	205.5698	432.3207	109.461	384.0326	42.7765
TCA	2.6515	1.8753	0.4252	<LLOQ	0.1537	1.0957	0.6009	<LLOQ	0.6039	7.5082	0.4153	27.3634	11.0928	50.8367	2.0912	1.157	19.2748	26.275	1.9295	0.2861	0.7778
TBA	326.721	2117.36	158.5464	79.7108	38.15	86.6598	95.1075	139.9954	97.8219	3742.403	1502.868	1195.65	2083.211	2940.606	363.8242	71.8553	552.0808	1206.165	631.0684	2891.179	600.937

Table 5.5 Summary of total bile acids (A) and conjugation profiles (B) in NHP plasma.







A

Table 5.7 Summary of total bile acids (A) and conjugation profiles (B) in NHP bile.

Baseline		Days 3-10																							
ng/mL	RA078	RA079	RA080	RA081	RA082	RA083	RA084	RA085	RA086	RA087	RA088	RA089	RA090	RA091	RA092	RA093	RA094	RA095	RA096	RA097	RA098	RA099	RA100		
LCA	133.996	132.839	1474.68	11326.022	161.092	1336.91	3815.67	796.464	1468.91	2614.44	8891.79	2391.866	254.956	7611.056	394.409	1029.416	1057.413	1057.413	1057.413	1057.413	1057.413	1057.413	1057.413	1057.413	1057.413
CDCA	2151.75	824.617	679.681	6969.668	3910.077	4917.616	1784.788	8621.046	2918.44	8891.79	8891.79	8891.79	8891.79	8891.79	8891.79	8891.79	8891.79	8891.79	8891.79	8891.79	8891.79	8891.79	8891.79	8891.79	8891.79
DCA	1044.56	3003.2	2857.61	938.159	17519.869	6755.885	3102.768	4739.927	11178.822	3861.517	1286.032	2948.908	724.806	3985.531	251.407	91.977	91.977	91.977	91.977	91.977	91.977	91.977	91.977	91.977	91.977
CA	618.2	627.1	618.2	618.2	618.2	618.2	618.2	618.2	618.2	618.2	618.2	618.2	618.2	618.2	618.2	618.2	618.2	618.2	618.2	618.2	618.2	618.2	618.2	618.2	618.2
UCA	<LOQ	<LOQ	7.98	<LOQ	609.237	460.67	691.809	1514.519	271.289	105.939	553.922	30.173	146.464	594.413	400.216	178.92	178.92	178.92	178.92	178.92	178.92	178.92	178.92	178.92	178.92
GLCA	951.6010	83935.70	57884.70	7852.70	1133964.0	1133964.0	1133964.0	1133964.0	1133964.0	1133964.0	1133964.0	1133964.0	1133964.0	1133964.0	1133964.0	1133964.0	1133964.0	1133964.0	1133964.0	1133964.0	1133964.0	1133964.0	1133964.0	1133964.0	1133964.0
GDCA	30431360	50673810	27987700	51302070	119797400	202671830	368586150	295389950	137407720	92634880	687404390	37596990	70003340	16858030	231102500	16765920	24762050	24762050	24762050	24762050	24762050	24762050	24762050	24762050	24762050
GDCA	35134690	20185510	9981790	25483730	23429440	90769410	32993180	28691970	13302730	47395820	800529570	44351510	718577430	251998380	160054600	148955570	39342810	39342810	39342810	39342810	39342810	39342810	39342810	39342810	39342810
GDCA	582520	3845580	5477230	3088460	220820	7178350	8744620	44931430	10694780	5939560	76683280	20257280	60883280	6380380	16380380	29918400	29918400	29918400	29918400	29918400	29918400	29918400	29918400	29918400	29918400
GDCA	342240	103720	284580	493660	2379440	1184540	2333740	6488470	9476510	6705650	11437810	7883130	6442720	1129240	7029510	1848660	4376480	4376480	4376480	4376480	4376480	4376480	4376480	4376480	4376480
TDCA	10924050	32215410	7387420	1378860	7053900	12657500	14699150	17914770	19179870	10911400	1814000	18658630	35438150	13023780	41666210	17416820	8189570	8189570	8189570	8189570	8189570	8189570	8189570	8189570	8189570
TDCA	251336490	110635380	132300800	80730470	252916120	1288662970	1445460290	1524069590	1743770440	4338329710	2121402000	293952610	2121464840	950862240	2165532650	142852650	1063652910	1063652910	1063652910	1063652910	1063652910	1063652910	1063652910	1063652910	1063652910
MACA	91372510	87429150	41330640	38271610	97099640	651162950	41774450	45099360	31048350	79238540	58309560	461146650	1012577920	379327160	514850040	319062340	199819840	199819840	199819840	199819840	199819840	199819840	199819840	199819840	199819840
7 $\alpha$ -hydroxy 3-one-chole-4-en-24-oxoic acid	8.849	<LOQ	9.989	<LOQ	20.839	33.386	3.31	39.397	8.174	51.38	33.867	<LOQ	45.549	21.041	<LOQ	99.374	17.653	17.653	17.653	17.653	17.653	17.653	17.653	17.653	17.653
TEA	4826062282.2	377911515	1116043117	280658671.8	635450333.4	33134099536	3539504108	33986809519	6675132197	6293530720	5688967233	4173999573	6170914028	4037452199	2342807071	6137700453	2194381334	2296789442	2296789442	2296789442	2296789442	2296789442	2296789442	2296789442	2296789442

Baseline		Days 11-14										Days 15-22													
ng/mL	RA078	RA079	RA080	RA081	RA082	RA083	RA084	RA085	RA086	RA087	RA088	RA089	RA090	RA091	RA092	RA093	RA094	RA095	RA096	RA097	RA098	RA099	RA100		
LCA	8011.9	968.844	2703.135	15.293	46900.962	4237.925	2180.048	3839.157	10594.167	3012.399	551.196	2801.181	4078.658	1502.128	1557.658	5007.164	2484.677	21587.261	187.79	810.401	810.401	810.401	810.401	810.401	810.401
CDCA	10372.555	3772.542	2276.529	2915.606	4.964	56645.434	1413.22	3209.282	1232.314	23904.886	14602.134	4183.753	7647.862	6389.985	6594.159	2865.517	923.871	2784.431	1923.841	3092.719	3092.719	3092.719	3092.719	3092.719	3092.719
CA	64088.348	9552.924	1188.59	3.639	177.317	8051.715	5003.395	8567.244	553.763	1530.039	3119.911	2362.876	20211.864	3892.67	1548.113	3562.506	43261.51	11940.222	9584.861	2735.761	2735.761	2735.761	2735.761	2735.761	
UCA	9783.914	2590.007	69.418	<LOQ	66.976	112.168	58.206	27.92	824.018	127.457	22.648	25.604	131.184	15.686	61.171	29.398	117.796	28.45	80.809	529.445	529.445	529.445	529.445	529.445	
GLCA	612000	9333250	20235140	5423050	1095670	4787590	9079210	13311240	17396510	7338660	6400970	2032420	403376	2330.634	953.47	6857.766	2790.022	1659.08	2784.22	4901.648	4901.648	4901.648	4901.648	4901.648	
GDCA	21864480	62716030	17098470	3860270	34788390	42157920	24546410	29040120	11544480	9107960	1362900	70191960	51372480	5332480	3187200	9357600	46418780	62620730	62620730	62620730	62620730	62620730	62620730	62620730	
GDCA	32208870	88024730	9006100	1062090	1062090	29779070	34570330	34150460	11638480	14971840	10563360	15452300	12583070	12583070	4521900	3277200	11694180	11694180	11694180	11694180	11694180	11694180	11694180	11694180	
TDCA	1322950	7605110	20152210	1629900	20961520	3371480	1778430	14110590	1287470	5511280	2576640	12001080	8239360	15092630	4480860	1424020	10322500	15030790	111260	111260	111260	111260	111260	111260	
TDCA	27786580	234437680	6350700	5895970	29202630	108484970	25491650	4778910	39245740	6880770	21189180	2623470	7816040	117117680	37616340	5488160	164451570	10519610	645450	11629060	11629060	11629060	11629060	11629060	
TDCA	6507480	37423490	147114760	905440	644721300	15231650	78600340	23111820	13919520	13660990	8675730	4001640	25005530	22469930	2338890	13313270	53447570	78049520	1872280	2307620	2307620	2307620	2307620	2307620	
TDCA	25331860	63564010	105141980	181620	5716510	2629020	40388250	6082920	8008460	3381690	1941320	6844640	27418420	14731320	1854020	1854020	1854020	1854020	1854020	1854020	1854020	1854020	1854020	1854020	
MACA	482407	5349	20324	5.831	159349	6.821	11013	60.167	24.189	9.907	<LOQ	0.411	<LOQ	26.215	144.665	67.606	11.167	<LOQ	6.652	6.652	6.652	6.652	6.652	6.652	
7 $\alpha$ -hydroxy 3-one-chole-4-en-24-oxoic acid	56.198	<LOQ	<LOQ	<LOQ	63.722	<LOQ	8.71	<LOQ	<LOQ	<LOQ	<LOQ	<LOQ	<LOQ	<LOQ	<LOQ	<LOQ	<LOQ	<LOQ	9.866	3.758	<LOQ	<LOQ	<LOQ	<LOQ	
TEA	216203300	6980637167	186500594	448631564	4397786916	616441185	252884208	2250410754	134904992	1820982355	1520964973	1626107373	105856624	3986864079	363866995	182383355	446130074	1946594058	8083785347	7297278274	455689846	455689846	455689846	455689846	

Table 5.7 continued

B

% BA	Baseline										Days 4-5										Days 8-10										Days 11-14										Days 15-21																																																																																																																																																																																																																																																																																																																																																																																																																																																																																																																																																																																																																																																											
	BA0676	BA0679	BA0681	BA0682	BA0683	BA0684	BA0685	BA0686	BA0687	BA0688	BA0689	BA0690	BA0691	BA0692	BA0693	BA0694	BA0695	BA0696	BA0697	BA0698	BA0699	BA0700	BA0701	BA0702	BA0703	BA0704	BA0705	BA0706	BA0707	BA0708	BA0709	BA0710	BA0711	BA0712	BA0713	BA0714	BA0715	BA0716	BA0717	BA0718	BA0719	BA0720	BA0721	BA0722	BA0723	BA0724	BA0725	BA0726	BA0727	BA0728	BA0729	BA0730	BA0731	BA0732	BA0733	BA0734	BA0735	BA0736	BA0737	BA0738	BA0739	BA0740	BA0741	BA0742	BA0743	BA0744	BA0745	BA0746	BA0747	BA0748	BA0749	BA0750	BA0751	BA0752	BA0753	BA0754	BA0755	BA0756	BA0757	BA0758	BA0759	BA0760	BA0761	BA0762	BA0763	BA0764	BA0765	BA0766	BA0767	BA0768	BA0769	BA0770	BA0771	BA0772	BA0773	BA0774	BA0775	BA0776	BA0777	BA0778	BA0779	BA0780	BA0781	BA0782	BA0783	BA0784	BA0785	BA0786	BA0787	BA0788	BA0789	BA0790	BA0791	BA0792	BA0793	BA0794	BA0795	BA0796	BA0797	BA0798	BA0799	BA0800																																																																																																																																																																																																																																																																																																																																																																																																																																																																																																																																																																										
% BA	0.00012726	0.00013741	0.00015756	0.00016771	0.00017786	0.00018801	0.00019816	0.00020831	0.00021846	0.00022861	0.00023876	0.00024891	0.00025906	0.00026921	0.00027936	0.00028951	0.00029966	0.00030981	0.00031996	0.00033011	0.00034026	0.00035041	0.00036056	0.00037071	0.00038086	0.00039101	0.00040116	0.00041131	0.00042146	0.00043161	0.00044176	0.00045191	0.00046206	0.00047221	0.00048236	0.00049251	0.00050266	0.00051281	0.00052296	0.00053311	0.00054326	0.00055341	0.00056356	0.00057371	0.00058386	0.00059401	0.00060416	0.00061431	0.00062446	0.00063461	0.00064476	0.00065491	0.00066506	0.00067521	0.00068536	0.00069551	0.00070566	0.00071581	0.00072596	0.00073611	0.00074626	0.00075641	0.00076656	0.00077671	0.00078686	0.00079701	0.00080716	0.00081731	0.00082746	0.00083761	0.00084776	0.00085791	0.00086806	0.00087821	0.00088836	0.00089851	0.00090866	0.00091881	0.00092896	0.00093911	0.00094926	0.00095941	0.00096956	0.00097971	0.00098986	0.00099996	0.00101011	0.00102026	0.00103041	0.00104056	0.00105071	0.00106086	0.00107101	0.00108116	0.00109131	0.00110146	0.00111161	0.00112176	0.00113191	0.00114206	0.00115221	0.00116236	0.00117251	0.00118266	0.00119281	0.00120296	0.00121311	0.00122326	0.00123341	0.00124356	0.00125371	0.00126386	0.00127401	0.00128416	0.00129431	0.00130446	0.00131461	0.00132476	0.00133491	0.00134506	0.00135521	0.00136536	0.00137551	0.00138566	0.00139581	0.00140596	0.00141611	0.00142626	0.00143641	0.00144656	0.00145671	0.00146686	0.00147701	0.00148716	0.00149731	0.00150746	0.00151761	0.00152776	0.00153791	0.00154806	0.00155821	0.00156836	0.00157851	0.00158866	0.00159881	0.00160896	0.00161911	0.00162926	0.00163941	0.00164956	0.00165971	0.00166986	0.00168001	0.00169016	0.00170031	0.00171046	0.00172061	0.00173076	0.00174091	0.00175106	0.00176121	0.00177136	0.00178151	0.00179166	0.00180181	0.00181196	0.00182211	0.00183226	0.00184241	0.00185256	0.00186271	0.00187286	0.00188301	0.00189316	0.00190331	0.00191346	0.00192361	0.00193376	0.00194391	0.00195406	0.00196421	0.00197436	0.00198451	0.00199466	0.00200481	0.00201496	0.00202511	0.00203526	0.00204541	0.00205556	0.00206571	0.00207586	0.00208601	0.00209616	0.00210631	0.00211646	0.00212661	0.00213676	0.00214691	0.00215706	0.00216721	0.00217736	0.00218751	0.00219766	0.00220781	0.00221796	0.00222811	0.00223826	0.00224841	0.00225856	0.00226871	0.00227886	0.00228901	0.00229916	0.00230931	0.00231946	0.00232961	0.00233976	0.00234991	0.00236006	0.00237021	0.00238036	0.00239051	0.00240066	0.00241081	0.00242096	0.00243111	0.00244126	0.00245141	0.00246156	0.00247171	0.00248186	0.00249201	0.00250216	0.00251231	0.00252246	0.00253261	0.00254276	0.00255291	0.00256306	0.00257321	0.00258336	0.00259351	0.00260366	0.00261381	0.00262396	0.00263411	0.00264426	0.00265441	0.00266456	0.00267471	0.00268486	0.00269501	0.00270516	0.00271531	0.00272546	0.00273561	0.00274576	0.00275591	0.00276606	0.00277621	0.00278636	0.00279651	0.00280666	0.00281681	0.00282696	0.00283711	0.00284726	0.00285741	0.00286756	0.00287771	0.00288786	0.00289801	0.00290816	0.00291831	0.00292846	0.00293861	0.00294876	0.00295891	0.00296906	0.00297921	0.00298936	0.00299951	0.00300966	0.00301981	0.00302996	0.00304011	0.00305026	0.00306041	0.00307056	0.00308071	0.00309086	0.00310101	0.00311116	0.00312131	0.00313146	0.00314161	0.00315176	0.00316191	0.00317206	0.00318221	0.00319236	0.00320251	0.00321266	0.00322281	0.00323296	0.00324311	0.00325326	0.00326341	0.00327356	0.00328371	0.00329386	0.00330401	0.00331416	0.00332431	0.00333446	0.00334461	0.00335476	0.00336491	0.00337506	0.00338521	0.00339536	0.00340551	0.00341566	0.00342581	0.00343596	0.00344611	0.00345626	0.00346641	0.00347656	0.00348671	0.00349686	0.00350701	0.00351716	0.00352731	0.00353746	0.00354761	0.00355776	0.00356791	0.00357806	0.00358821	0.00359836	0.00360851	0.00361866	0.00362881	0.00363896	0.00364911	0.00365926	0.00366941	0.00367956	0.00368971	0.00369986	0.00371001	0.00372016	0.00373031	0.00374046	0.00375061	0.00376076	0.00377091	0.00378106	0.00379121	0.00380136	0.00381151	0.00382166	0.00383181	0.00384196	0.00385211	0.00386226	0.00387241	0.00388256	0.00389271	0.00390286	0.00391301	0.00392316	0.00393331	0.00394346	0.00395361	0.00396376	0.00397391	0.00398406	0.00399421	0.00400436	0.00401451	0.00402466	0.00403481	0.00404496	0.00405511	0.00406526	0.00407541	0.00408556	0.00409571	0.00410586	0.00411601	0.00412616	0.00413631	0.00414646	0.00415661	0.00416676	0.00417691	0.00418706	0.00419721	0.00420736	0.00421751	0.00422766	0.00423781	0.00424796	0.00425811	0.00426826	0.00427841	0.00428856	0.00429871	0.00430886	0.00431901	0.00432916	0.00433931	0.00434946	0.00435961	0.00436976	0.00437991	0.00439006	0.00440021	0.00441036	0.00442051	0.00443066	0.00444081	0.00445096	0.00446111	0.00447126	0.00448141	0.00449156	0.00450171	0.00451186	0.00452201	0.00453216	0.00454231	0.00455246	0.00456261	0.00457276	0.00458291	0.00459306	0.00460321	0.00461336	0.00462351	0.00463366	0.00464381	0.00465396	0.00466411	0.00467426	0.00468441	0.00469456	0.00470471	0.00471486	0.00472501	0.00473516	0.00474531	0.00475546	0.00476561	0.00477576	0.00478591	0.00479606	0.00480621	0.00481636	0.00482651	0.00483666	0.00484681	0.00485696	0.00486711	0.00487726	0.00488741	0.00489756	0.00490771	0.00491786	0.00492801	0.00493816	0.00494831	0.00495846	0.00496861	0.00497876	0.00498891	0.00499906	0.00500921	0.00501936	0.00502951	0.00503966	0.00504981	0.00505996	0.00507011	0.00508026	0.00509041	0.00510056	0.00511071	0.00512086	0.00513101	0.00514116	0.00515131	0.00516146	0.00517161	0.00518176	0.00519191	0.00520206	0.00521221	0.00522236	0.00523251	0.00524266	0.00525281	0.00526296	0.00527311	0.00528326	0.00529341	0.00530356	0.00531371	0.00532386	0.00533401	0.00534416	0.00535431	0.00536446	0.00537461	0.00538476	0.00539491	0.00540506	0.00541521	0.00542536	0.00543551	0.00544566	0.00545581	0.00546596	0.00547611	0.00548626	0.00549641	0.00550656	0.00551671	0.00552686	0.00553701	0.00554716	0.00555731	0.00556746	0.00557761	0.00558776	0.00559791	0.00560806	0.00561821	0.00562836	0.00563851	0.00564866	0.00565881	0.00566896	0.00567911	0.00568926	0.00569941	0.00570956	0.00571971	0.00572986	0.00574001	0.00575016	0.00576031	0.00577046	0.00578061	0.00579076	0.00580091	0.00581106	0.00582121	0.00583136	0.00584151	0.00585166	0.00586181	0.00587196	0.00588211	0.00589226	0.00590241	0.00591256	0.00592271	0.00593286	0.00594301	0.00595316	0.00596331	0.00597346	0.00598361	0.00599376	0.00600391	0.00601406	0.00602421	0.00603436	0.00604451	0.00605466	0.00606481	0.00607496	0.00608511	0.00609526	0.00610541	0.00611556	0.00612571	0.00613586	0.00614601	0.00615616	0.00616631	0.00617646	0.00618661	0.00619676	0.00620691	0.00621706	0.00622721	0.00623736	0.00624751	0.00625766	0.00626781	0.00627796	0.00628811	0.00629826	0.00630841	0.00631856	0.00632871	0.00633886	0.00634901	0.00635916	0.00636931	0.00637946	0.00638961	0.00639976	0.00640991	0.00642006	0.00643021	0.00644036	0.00645051	0.00646066	0.00647081	0.00648096	0.00649111	0.00650126	0.00651141	0.00652156	0.00653171	0.00654186	0.00655201	0.00656216	0.00657231	0.00658246	0.00659261	0.00660276	0.00661291	0.00662306	0.00663321	0.00664336	0.00665351	0.00666366	0.00667381	0.00668396	0.00669411	0.00670426	0.00671441	0.00672456	0.00673471	0.00674486	0.00675501	0.00676516	0.00677531	0.00678546	0.00679561	0.00680576	0.00681591	0.00682606	0.00683621	0.00684636	0.00685651	0.00686666	0.00687681	0.00688696	0.00689711	0.00690726	0.00691741	0.00692756	0.00693771	0.00694786	0.00695801	0.00696816	0.00697831	0.00

## 5.4 Discussion

In health, BAs are efficiently recycled via intestinal reabsorption through a number of active and passive mechanisms in a process termed enterohepatic circulation (EHC) (8, 18). In this way, less than 5% of BAs are lost to the feces per day. When the intestinal mucosa is dysregulated due to radiation insult, however, absorption is similarly disrupted, resulting in the loss of luminal contents – including water, nutrients, and bile acids (2, 3, 12). This effect was observed in the current study as a dramatic decrease in the concentration of TBA in plasma at days 8-10 and days 11-14 to nearly 10% of naïve levels (figure 1A). Simultaneously, biliary TBA was significantly increased over 10-fold, demonstrating the hepatic effort to replenish the BA pool. Though statistical significance was not reached due to high individual variability, it also appears that average TBA within liver tissue was trending toward an increase at the same time points. This is also supported by the increased expression of *Cyp7a1* mRNA (figure 5.3). Cytochrome P450 7A1 (CYP7A1/*Cyp7a1*) is the rate-limiting step of the classic BA biosynthetic pathway (8, 9, 18, 19). The increased expression of hepatic *Cyp7a1* mRNA in this study supports the increased *de novo* production of BAs by the liver in order to replenish the BA pool lost to malabsorption and subsequent diarrhea. Plasma TBA appeared to be returning to baseline by days 15-22, which agrees with the partial recovery of intestinal mucosa that occurs at that same time point as demonstrated in previous studies (2, 20). However, our results disagree partially with previous studies of ionizing radiation in the rat, in which hepatic *Cyp7a1* mRNA was unchanged, while hepatic *Cyp27a1* and *Cyp7b1* were decreased and *Cyp8b1* expression was increased (21, 22). We observed no significant changes in expression of these genes, save *Cyp7a1*, following 12 Gy PBI/BM2.5. This disagreement

may be due to a number of differences between the two studies, including species used and dose and administration of radiation.

Though *Cyp7a1* mRNA expression was increased by about 5-fold at days 11-14, this was confounded by decreased expression of ileal *Fxr* (approximately 50% of naïve) and increased expression of ileal *Fgf19* (>15-fold increase at days 8-10) (figure 5.3). Bile acids activate ileal FXR/Fxr while being shuttled from the intestinal lumen to the portal blood for delivery back to the liver (8, 19). Activation of ileal FXR causes the release of FGF19/Fgf19 from the enterocyte, which acts on the hepatic receptor FGFR4 in order to suppress expression of hepatic CYP7A1 (8, 19). Thus, decreased expression of ileal *Fxr* would be expected to lead to decreased expression of *Fgf19*. Likewise, the increased expression of the peptide hormone *Fgf19* would be expected to cause a decrease in hepatic *Cyp7a1*, while an increase was observed instead. This effect can potentially be attributed to the times at which these changes occurred: the increased expression of ileal *Fgf19* was not seen until days 8-10, while the increase in *Cyp7a1* mRNA had already occurred at that same time point and then appeared to decrease. Moreover, the loss of functional enterocytes as demonstrated in jejunum by this and other groups is likely to occur throughout the length of the small intestine (23, 24). This complicates the qRT-PCR analysis, as cell types were not isolated or identified before mRNA extraction. Additionally, because only mRNA was examined, it is possible that additional changes at the protein expression and functional level could be taking place.

The di-hydroxy BA, DCA, and its conjugates (i.e. GDCA and TDCA) were observed to increase as percent of TBA in plasma following PBI. Similarly, the taurine and glycine conjugates of CDCA (i.e. GCDCA and TCDCA) were also increased as

proportions of plasma TBA. The increased proportions of these di-hydroxy BAs may have contributed to or exacerbated diarrhea in this model, as these BAs are known to enhance colonic mucosal permeability as well as water and electrolyte secretion (12). In previous studies using this model, diarrhea reached maximal frequency at day 8 post-irradiation (15), which is the same time point with maximal increases as percent of TBA of TCDCA and GCDCA in plasma and as concentration of TCDCA and GCDCA in bile. This is supported by earlier studies. For example, a mouse model of pelvic irradiation demonstrated BAM and radiation-induced diarrhea (RID) concurrent with increased levels of DCA and CDCA in the colon and feces (25).

Among the BAs whose production were increased following radiation injury was one of the planar BAs - allocholic acid (ACA). This species, which like the other planar BAs is normally undetectable or of low abundance in the healthy adult mammal, has recently been discovered to increase following certain cases of liver injury (26). ACA demonstrated a substantial increase (124-fold) following PBI when measured as a proportion of plasma TBA, which was interestingly not accompanied by a significant increase in its concentration. ACA also increased when measured as concentration in bile. Though we did observe increased incidence of this planar BA, the other planar BAs assayed in this study – IALCA and 7 $\alpha$ -hydroxy-3-oxo-chol-4-en-24-oic acid – did not demonstrate significant difference between naïve and PBI groups; still, these BAs were detectable and quantifiable in most bile and liver tissue samples. Additionally, though ACA demonstrated a significant increase in its concentration within bile, the proportion of this species as a part of TBA did not. As far as the authors know, this is the first study to examine these planar BAs both as their concentration and as a percentage of the whole, so it would be interesting

to know if previous studies that reported increased production of these molecules also resulted in an increased proportion of TBA in that biomatrix (27-29). Furthermore, because most BAs assayed in this study increased in concentration within bile, it is possible that the increase in planar BAs is a reflection of all BAs increasing and not, as we first hypothesized, due to activation of a specific mechanism of liver injury, at least in this model. The increased ACA as a proportion of TBA in plasma could be due to a number of mechanisms due to radiation injury, including increased hepatic BA synthesis, skewing of the microbiome resulting in production of ACA as a secondary BA, and/or decreased proportions of the other BAs that make up the total bile acid pool.

## 5.5 Conclusion

Bile acids have long been recognized as having regulatory activities in addition to their digestive roles due to their activation of cell membrane and nuclear receptors (7, 8, 10). Thus, changes in the composition of the hepatic and/or intestinal bile acid pools can lead to changes in downstream signaling. In this and similar studies of GI-ARS, it is possible that increased proportions of LCA and DCA and their conjugates are partially responsible for the increased colonic motility that causes radiation-induced diarrhea (RID) and BAM via M-BAR activation, which is thought to be an important instigator of intestinal motility (7, 30). Additionally, because M-BAR activation by LCA and other hydrophobic BAs promotes anti-inflammatory processes (7), BA signaling may be important to the liver's resistance to radiation damage (21). Similarly, VDR signaling via LCA promotes pathways related to xenobiotic and bile acid detoxification (7); ergo, this may be another mechanism for hepatic resistance to radiation damage from increased BA levels. Though some of these signaling pathways are thought to play small parts in health, it is likely that they become more important in injury states when the BA pool is modulated

and/or elevated. This may be especially true herein, since the less active TCA decreased as a proportion of TBA in all biomatrices examined and was replaced by the more potent cell membrane and nuclear receptor activators, CDCA, LCA and DCA and/or their conjugates. Even so, additional studies would be required to determine the quantitative effects of bile acid signaling in the response to and recovery from radiation damage.

## 5.6 References

1. Singh VK, Olabisi AO. Nonhuman primates as models for the discovery and development of radiation countermeasures. *Expert Opinion on Drug Discovery*. 2017;12(7):695-709.
2. Macvittie T, Farese A, Parker G, Jackson W, Booth C, Tudor G, Hankey K, Potten C. The Gastrointestinal Subsyndrome of the Acute Radiation Syndrome in Rhesus Macaques: A Systematic Review of the Lethal Dose-Response Relationship With and Without Medical Management. *Health Physics*. 2019;116:1.
3. Garg S, Zheng J, Wang J, Authier S, Pouliot M, Hauer-Jensen M. Segmental Differences in Radiation-Induced Alterations of Tight Junction-Related Proteins in Non-Human Primate Jejunum, Ileum and Colon. *Radiation Research*. 2015;185(1):50-9.
4. Phillips F, Muls ACG, Lalji A, Andreyev HJN. Are bile acid malabsorption and bile acid diarrhoea important causes of loose stool complicating cancer therapy? *Colorectal Disease*. 2015;17(8):730-4.
5. Kumagai T, Rahman F, Smith AM. The Microbiome and Radiation Induced-Bowel Injury: Evidence for Potential Mechanistic Role in Disease Pathogenesis. *Nutrients*. 2018;10(10).
6. Andreyev HJN, Davidson SE, Gillespie C, Allum WH, Swarbrick E. Practice guidance on the management of acute and chronic gastrointestinal problems arising as a result of treatment for cancer. *Gut*. 2012;61(2):179.
7. de Aguiar Vallim Thomas Q, Tarling Elizabeth J, Edwards Peter A. Pleiotropic Roles of Bile Acids in Metabolism. *Cell Metabolism*. 2013;17(5):657-69.
8. Hofmann AF, Hagey LR. Bile Acids: Chemistry, Pathochemistry, Biology, Pathobiology, and Therapeutics. *Cellular and Molecular Life Sciences*. 2008;65(16):2461-83.
9. Hofmann AF, Hagey LR. Key discoveries in bile acid chemistry and biology and their clinical applications: history of the last eight decades. *Journal of Lipid Research*. 2014;55(8):1553-95.
10. Kuipers F, Bloks VW, Groen AK. Beyond intestinal soap—bile acids in metabolic control. *Nature Reviews Endocrinology*. 2014;10:488.
11. Sagar NM, Duboc H, Kay GL, Alam MT, Wicaksono AN, Covington JA, Quince C, Kokkorou M, Svolos V, Palmieri LJ, Gerasimidis K, Walters JRF, Arasaradnam RP. The pathophysiology of bile acid diarrhoea: differences in the colonic microbiome, metabolome and bile acids. *Scientific Reports*. 2020;10(1):20436.
12. Camilleri M. Bile Acid Diarrhea: Prevalence, Pathogenesis, and Therapy. *Gut & Liver*. 2015;9(3):332-9.

13. Camilleri M, Md, Vijayvargiya P. The Role of Bile Acids in Chronic Diarrhea. *Am J Gastroenterol.* 2020;115(10):1596-603.
14. MacVittie TJ, Bennett A, Booth C, Garofalo M, Tudor G, Ward A, Shea-Donohue T, Gelfond D, McFarland E, Jackson W, 3rd, Lu W, Farese AM. The prolonged gastrointestinal syndrome in rhesus macaques: the relationship between gastrointestinal, hematopoietic, and delayed multi-organ sequelae following acute, potentially lethal, partial-body irradiation. *Health Phys.* 2012;103(4):427-53.
15. MacVittie TJ, Farese AM, Bennett A, Gelfond D, Shea-Donohue T, Tudor G, Booth C, McFarland E, Jackson W, 3rd. The acute gastrointestinal subsyndrome of the acute radiation syndrome: a rhesus macaque model. *Health physics.* 2012;103(4):411-26.
16. Shiffka SJ, Jones JW, Li L, Farese AM, MacVittie TJ, Wang H, Swaan PW, Kane MA. Quantification of common and planar bile acids in tissues and cultured cells. *Journal of Lipid Research.* 2020;61(11):1524-35.
17. Lynch C, Pan Y, Li L, Heyward S, Moeller T, Swaan PW, Wang H. Activation of the constitutive androstane receptor inhibits gluconeogenesis without affecting lipogenesis or fatty acid synthesis in human hepatocytes. *Toxicology and Applied Pharmacology.* 2014;279(1):33-42.
18. Marin J, Macias R, Briz O, Banales J, Monte M. Bile Acids in Physiology, Pathology and Pharmacology. *Current drug metabolism.* 2015;17.
19. Alnouti Y. Bile Acid Sulfation: A Pathway of Bile Acid Elimination and Detoxification. *Toxicological Sciences.* 2009;108(2):225-46.
20. Parker GA, Li N, Takayama K, Booth C, Tudor GL, Farese AM, MacVittie TJ. Histopathological Features of the Development of Intestine and Mesenteric Lymph Node Injury in a Nonhuman Primate Model of Partial-body Irradiation with Minimal Bone Marrow Sparing. *Health Physics.* 2019;116(3):426-46.
21. Scanff P, Souidi M, Grison S, Griffiths NM, Gourmelon P. Alteration of the enterohepatic recirculation of bile acids in rats after exposure to ionizing radiation. *Canadian journal of physiology and pharmacology.* 2004;82(2):114-24.
22. Souidi M, Scanff P, Grison S, Gourmelon P, Aigueperse J. Effects of ionizing radiation on the activity of the major hepatic enzymes implicated in bile acid biosynthesis in the rat. *Comptes rendus biologiques.* 2007;330(12):861-70.
23. Jones JW, Bennett A, Carter CL, Tudor G, Hankey KG, Farese AM, Booth C, MacVittie TJ, Kane MA. Citrulline as a Biomarker in the Non-human Primate Total- and Partial-body Irradiation Models: Correlation of Circulating Citrulline to Acute and Prolonged Gastrointestinal Injury. *Health physics.* 2015;109(5):440-51.
24. Kumar P, Wang P, Tudor G, Booth C, Farese AM, MacVittie TJ, Kane MA. Evaluation of Plasma Biomarker Utility for the Gastrointestinal Acute Radiation Syndrome

in Non-human Primates after Partial Body Irradiation with Minimal Bone Marrow Sparing through Correlation with Tissue and Histological Analyses. *Health physics*. 2020;119(5):594-603.

25. Wang L, Zhou Y, Wang X, Zhang G, Guo B, Hou X, Ran J, Zhang Q, Li C, Zhao X, Geng Y, Feng S. Mechanism of Asbt (Slc10a2)-related bile acid malabsorption in diarrhea after pelvic radiation. *International Journal of Radiation Biology*. 2020;96(4):510-9.

26. Shiffka SJ, Kane MA, Swaan PW. Planar bile acids in health and disease. *Biochimica et Biophysica Acta (BBA) - Biomembranes*. 2017;1859(11):2269-76.

27. Mendoza ME, Monte MJ, El-Mir MY, Badia MD, Marin JJG. Changes in the pattern of bile acids in the nuclei of rat liver cells during hepatocarcinogenesis. *Clinical Science*. 2002;102(2):143-50.

28. Monte MJ, Martinez-Diez MC, El-Mir MY, Mendoza ME, Bravo P, Bachs O, Marin JJG. Changes in the pool of bile acids in hepatocyte nuclei during rat liver regeneration. *Journal of Hepatology*. 2002;36(4):534-42.

29. El-Mir MY, Badia MD, Luengo N, Monte MJ, Marin JJ. Increased levels of typically fetal bile acid species in patients with hepatocellular carcinoma. *Clinical science (London, England : 1979)*. 2001;100(5):499-508.

30. Alemi F, Poole DP, Chiu J, Schoonjans K, Cattaruzza F, Grider JR, Bunnett NW, Corvera CU. The Receptor TGR5 Mediates the Prokinetic Actions of Intestinal Bile Acids and Is Required for Normal Defecation in Mice. *Gastroenterology*. 2013;144(1):145-54.

## 6. Conclusions and Future Directions

The studies presented herein accomplished many of the original goals for which they were designed, as well as presented unexpected developments in the study of bile acid homeostasis. Of note, the work herein has resulted in the advancement of bile acid detection and quantification methods; improved characterization of cell culture and animal models; insights into the co-evolution of BA transport and BA synthesis; and establishment of BA dysregulation in acute radiation syndrome.

We have demonstrated the optimization, validation, and applications of a sensitive and selective LC-MS/MS method that has allowed us to simultaneously quantify numerous bile acids in cell culture systems and several biomatrices. Thereby, we have also reported the most detailed profile of the bile acid pool to date in immortalized liver cells, human primary hepatocytes, and *M. mulatta*. These studies have revealed important disparities between bile acid metabolism in immortalized cell lines and healthy hepatocytes. These data demonstrate the strong correlation of bile acid metabolism in human primary hepatocytes with that in hepatocytes in the whole organism; however, future work could expand on this by examining more primary hepatocyte donors and including additional media formulations in order to examine more aspects of BA metabolism.

A detailed baseline profile of the bile acid pool in *M. mulatta* – a popular laboratory non-human primate model – has also been established. Rodent models are often utilized when studying BA synthesis and metabolism; however, rodents' use of murine-specific bile acids and their low homology to humans make correlation to human systems challenging and often inaccurate. Ergo, the characterization of a more homologous model, such as NHP, is an important step in their widespread use in this field. While we have made

significant advancements over the data that had been available, additional processes involved in BA metabolism and elimination in these species should also be studied to establish physiological parameters that may be altered in relevant pathologies. These include renal elimination, sulfonation, glucuronidation, and BA-mediated signaling.

The quantitative assay developed herein also proved invaluable in the study of sodium-dependent bile acid uptake by ASBT and Asbt orthologs. These experiments have demonstrated that orthologs from earlier evolving vertebrate animals, such as sea lamprey and little skate, and invertebrates, such as the fruit fly, are poorly suited to transport modern bile salts. Meanwhile, human ASBT is specialized for highly efficient uptake of modern bile salts, but its efficiency deteriorates markedly in the transport of ancestral bile salts or bile alcohols. These findings lend credence to the hypothesis that ASBT/Asbt has evolved alongside bile acids for their specific uptake, but more studies are needed to fully characterize this adaptation. For example, further molecular characterization of Asbt orthologs using oxysterols and bile alcohols and other functional assays would help elucidate the exact substrate specificities of these transporters.

Finally, the detailed baseline profile that was established in *M. mulatta* in an earlier part of this dissertation was used to compare the changes in BA homeostasis in a natural history study of gastrointestinal acute radiation injury. The NHP model of radiation injury represents an important tool for the development of medical countermeasures in case of radiation exposure due to its high homology to humans; however, there are few studies examining detailed changes in the bile acid pool in this model. These changes are especially relevant because GI-ARS is a leading cause of morbidity and mortality following radiation exposure, and BA dysregulation is thought to be a significant factor in GI upset due to their

detergent and signaling capabilities. Thus, a more complete understanding of these mechanisms can further the development of medical countermeasures to ameliorate acute symptoms and prevent the development of chronic GI issues. With this goal, we have demonstrated the detailed changes to the BA profile that occur in an NHP model of GI-ARS in multiple enterohepatic tissues; additionally, we have probed for disturbances that occur at the transcriptional level. This work has revealed significant dysregulation to nearly all aspects of the BA profile following partial-body irradiation; however, surprisingly, few changes took place at the transcriptional level, indicating that these perturbations may be due to overall destruction of cells as opposed to metabolic changes taking place.

These studies have advanced multiple facets of bile acid research and highlight the importance of choosing an appropriate model, experimental design, and analytical method.

## 7. References

- Agus, A., et al. (2020). "Gut microbiota-derived metabolites as central regulators in metabolic disorders." Gut: gutjnl-2020-323071.
- Ahmed, M., et al. (2019). "Lung Bile Acid as Biomarker of Microaspiration and Its Relationship to Lung Inflammation." Journal of Heart & Lung Transplantation **38**: S255-S256.
- Alemi, F., et al. (2013). "The Receptor TGR5 Mediates the Prokinetic Actions of Intestinal Bile Acids and Is Required for Normal Defecation in Mice." Gastroenterology **144**(1): 145-154.
- Alnouti, Y. (2009). "Bile Acid Sulfation: A Pathway of Bile Acid Elimination and Detoxification." Toxicological Sciences **108**(2): 225-246.
- Anderson, I. G. and G. A. D. Haslewood (1962). "Comparative studies of `bile salts'. 15. The natural occurrence and preparation of allocholic acid." Biochemical Journal **85**(1): 236-242.
- Andreyev, H. J. N., et al. (2012). "Practice guidance on the management of acute and chronic gastrointestinal problems arising as a result of treatment for cancer." Gut **61**(2): 179.
- Anwer, M. and B. Stieger (2014). "Sodium-dependent bile salt transporters of the SLC10A transporter family: more than solute transporters." Pflugers Archiv European Journal of Physiology **466**(1): 77-89.
- Axelsson, M., et al. (2000). "Bile acid synthesis in cultured human hepatocytes: support for an alternative biosynthetic pathway to cholic acid." Hepatology **31**(6): 1305-1312.
- Axelsson, M., et al. (1991). "Bile acid synthesis in cultured human hepatoblastoma cells." Journal of Biological Chemistry **266**(27): 17770-17777.
- Ayewoh, E. N., et al. (2021). "S-acylation status of bile acid transporter hASBT regulates its function, metabolic stability, membrane expression, and phosphorylation state." BBA - Biomembranes **1863**(2).
- Banerjee, A., et al. (2005). "Site-Directed Mutagenesis and Use of Bile Acid-MTS Conjugates to Probe the Role of Cysteines in the Human Apical Sodium-Dependent Bile Acid Transporter (SLC10A2)." Biochemistry **44**(24): 8908-8917.

- Bathena, S. P. R., et al. (2013). "The profile of bile acids and their sulfate metabolites in human urine and serum." Journal of Chromatography B **942-943**: 53-62.
- Bernstein, H., et al. (2005). "Bile acids as carcinogens in human gastrointestinal cancers." Mutation Research/Reviews in Mutation Research **589**(1): 47-65.
- Camilleri, M. (2015). "Bile Acid Diarrhea: Prevalence, Pathogenesis, and Therapy." Gut & Liver **9**(3): 332-339.
- Camilleri, M., et al. (2020). "The Role of Bile Acids in Chronic Diarrhea." Am J Gastroenterol **115**(10): 1596-1603.
- Chiang, J. Y. L. and J. M. Ferrell (2018). "Bile Acid Metabolism in Liver Pathobiology." Gene expression **18**(2): 71-87.
- Chothe, P. P., et al. (2018). "Human bile acid transporter ASBT (SLC10A2) forms functional non-covalent homodimers and higher order oligomers." BBA - Biomembranes **1860**(3): 645-653.
- Cohen, E. P., et al. (2019). "Radiation Nephropathy in a Nonhuman Primate Model of Partial-body Irradiation with Minimal Bone Marrow Sparing—Part 1: Acute and Chronic Kidney Injury and the Influence of Neupogen." Health Physics **116**(3): 401-408.
- Czuba, L. C. (2017). Molecular Insight into the Structure, Function, and Regulation of Bile Acid Transport.
- Dawson, P. A. (2016). Chapter 12 - Bile Acid Metabolism. Biochemistry of Lipids, Lipoproteins and Membranes (Sixth Edition). N. D. Ridgway and R. S. McLeod. Boston, Elsevier: 359-389.
- de Boer, J. F., et al. (2019). "A Human-like Bile Acid Pool Induced by Deletion of Cyp2c70 Modulates Effects of Farnesoid X Receptor Activation in Mice." Journal of Lipid Research.
- de Aguiar Vallim, Thomas Q., et al. (2013). "Pleiotropic Roles of Bile Acids in Metabolism." Cell Metabolism **17**(5): 657-669.
- Einarsson, C., et al. (2000). "Bile acid formation in primary human hepatocytes." World journal of gastroenterology **6**(4): 522-525.
- Elliott, W. H. (1976). "The allo bile acids." NATO Adv. Study Inst. Ser., Ser. A **A7**(Hepatobiliary Syst.: Fundam. Pathol. Mech.): 469-483.

- El-Mir, M. Y., et al. (2001). "Increased levels of typically fetal bile acid species in patients with hepatocellular carcinoma." Clinical science (London, England : 1979) **100**(5): 499-508.
- El-mir, M. Y., et al. (2001). "Increased levels of typically fetal bile acid species in patients with hepatocellular carcinoma." Clin. Sci. **100**: 499-208.
- Fang, N., et al. (2016). "Profiling of urinary bile acids in piglets by a combination of enzymatic deconjugation and targeted LC-MRM-MS." Journal of Lipid Research **57**(10): 1917-1933.
- Ferrebee, C. B. and P. A. Dawson (2015). "Metabolic effects of intestinal absorption and enterohepatic cycling of bile acids." Acta Pharmaceutica Sinica B **5**(2): 129-134.
- Ferrell, J. M. and J. Y. L. Chiang (2019). "Understanding Bile Acid Signaling in Diabetes: From Pathophysiology to Therapeutic Targets." Diabetes Metab J **43**(3): 257-272.
- García-Cañaveras, J. C., et al. (2012). "Targeted profiling of circulating and hepatic bile acids in human, mouse, and rat using a UPLC-MRM-MS-validated method." Journal of Lipid Research **53**(10): 2231-2241.
- Garg, S., et al. (2015). "Segmental Differences in Radiation-Induced Alterations of Tight Junction-Related Proteins in Non-Human Primate Jejunum, Ileum and Colon." Radiation Research **185**(1): 50-59.
- Gérard, P. (2013). "Metabolism of cholesterol and bile acids by the gut microbiota." Pathogens (Basel, Switzerland) **3**(1): 14-24.
- Grant, S. M. and S. DeMorrow (2020). "Bile Acid Signaling in Neurodegenerative and Neurological Disorders." International Journal of Molecular Sciences **21**(17): 5982-5982.
- Greim, H., et al. (1973). "Determination of bile acids in needle biopsies of human liver." Biochemical Medicine **8**(2): 280-286.
- Griffiths, W. J., et al. (2019). "Concentrations of bile acid precursors in cerebrospinal fluid of Alzheimer's disease patients." Free Radical Biology and Medicine **134**: 42-52.
- Griffiths, W. J., et al. (2018). "Identification of unusual oxysterols and bile acids with 7-oxo or 3 $\beta$ ,5 $\alpha$ ,6 $\beta$ -trihydroxy functions in human plasma by charge-tagging mass spectrometry with multistage fragmentation." Journal of Lipid Research **59**(6): 1058-1070.

- Griffiths, W. J. and J. Sjövall (2010). "Bile acids: analysis in biological fluids and tissues." Journal of Lipid Research **51**(1): 23-41.
- Guo, L., et al. (2010). "Similarities and Differences in the Expression of Drug Metabolizing Enzymes between Human Hepatic Cell Lines and Primary Human Hepatocytes." Drug Metabolism and Disposition: dmd.110.035873.
- Hagey, L. R., et al. (2010). "Evolutionary diversity of bile salts in reptiles and mammals, including analysis of ancient human and extinct giant ground sloth coprolites." BMC Evolutionary Biology **10**: 133.
- Han, J., et al. (2015). "Metabolic Profiling of Bile Acids in Human and Mouse Blood by LC-MS/MS in Combination with Phospholipid-Depletion Solid-Phase Extraction." Analytical Chemistry **87**(2): 1127-1136.
- Hansen, S. H. (2003). Taurine homeostasis and its importance for physiological functions: 739-747.
- Hofmann, A. F. and L. R. Hagey (2008). "Bile Acids: Chemistry, Pathochemistry, Biology, Pathobiology, and Therapeutics." Cellular and Molecular Life Sciences **65**(16): 2461-2483.
- Hofmann, A. F. and L. R. Hagey (2014). "Key discoveries in bile acid chemistry and biology and their clinical applications: history of the last eight decades." Journal of Lipid Research **55**(8): 1553-1595.
- Hofmann, A. F., et al. (2010). "Bile salts of vertebrates: structural variation and possible evolutionary significance." Journal of Lipid Research **51**: 226-246.
- Honda, A., et al. (2019). "Regulations of bile acid metabolism in mouse models with hydrophobic bile acid composition." Journal of Lipid Research.
- Ikegami, T. and A. Honda (2018). "Reciprocal interactions between bile acids and gut microbiota in human liver diseases." Hepatology Research **48**(1): 15-27.
- Janssen, A. W. F., et al. (2017). "Modulation of the gut microbiota impacts nonalcoholic fatty liver disease: a potential role for bile acids." Journal of Lipid Research **58**(7): 1399-1416.
- Jiao, N., et al. (2018). "Suppressed hepatic bile acid signalling despite elevated production of primary and secondary bile acids in NAFLD." Gut **67**(10): 1881-1891.

- Jones, J. W., et al. (2015). "Citrulline as a Biomarker in the Non-human Primate Total- and Partial-body Irradiation Models: Correlation of Circulating Citrulline to Acute and Prolonged Gastrointestinal Injury." Health Physics **109**(5): 440-451.
- Kakiyama, G., et al. (2014). "A simple and accurate HPLC method for fecal bile acid profile in healthy and cirrhotic subjects: validation by GC-MS and LC-MS." Journal of Lipid Research **55**(5): 978-990.
- Kholodenko, I. V. and K. N. Yarygin (2017). "Cellular Mechanisms of Liver Regeneration and Cell-Based Therapies of Liver Diseases." BioMed Research International **2017**: 17.
- Kimura, A., et al. (1999). "Profile of Urinary Bile Acids in Infants and Children: Developmental Pattern of Excretion of Unsaturated Ketonic Bile Acids and 7 $\beta$ -Hydroxylated Bile Acids." Ped. Res. **45**(4): 603-609.
- Kimura, A., et al. (1997). "Perinatal bile acid metabolism: analysis of urinary bile acids in pregnant women and newborns." J. Lipid Res. **38**: 1954-1962.
- Kriaa, A., et al. (2019). "Microbial impact on cholesterol and bile acid metabolism: current status and future prospects." Journal of Lipid Research **60**(2): 323-332.
- Kuipers, F., et al. (2014). "Beyond intestinal soap—bile acids in metabolic control." Nature Reviews Endocrinology **10**: 488.
- Kumagai, T., et al. (2018). "The Microbiome and Radiation Induced-Bowel Injury: Evidence for Potential Mechanistic Role in Disease Pathogenesis." Nutrients **10**(10).
- Kumar, P., et al. (2020). "Evaluation of Plasma Biomarker Utility for the Gastrointestinal Acute Radiation Syndrome in Non-human Primates after Partial Body Irradiation with Minimal Bone Marrow Sparing through Correlation with Tissue and Histological Analyses." Health Physics **119**(5): 594-603.
- Lan, K., et al. (2016). "Key Role for the 12-Hydroxy Group in the Negative Ion Fragmentation of Unconjugated C24 Bile Acids." Analytical Chemistry **88**(14): 7041-7048.
- Lee, C.-S., et al. (2017). "Prognostic roles of tetrahydroxy bile acids in infantile intrahepatic cholestasis." Journal of Lipid Research **58**(3): 607-614.
- Lee, J. M., et al. (2018). "Diet1, bile acid diarrhea, and FGF15/19: mouse model and human genetic variants." Journal of Lipid Research **59**(3): 429-438.

- Lefort, C., et al. (2021). "The Liver under the Spotlight: Bile Acids and Oxysterols as Pivotal Actors Controlling Metabolism." Cells (2073-4409) **10**(2): 400.
- Li, J. and P. A. Dawson (2019). "Animal models to study bile acid metabolism." Biochimica et Biophysica Acta (BBA) - Molecular Basis of Disease **1865**(5): 895-911.
- Li, W., et al. (2020). "Fasting serum total bile acid level is associated with coronary artery disease, myocardial infarction and severity of coronary lesions." Atherosclerosis (00219150) **292**: 193-200.
- Liang, H., et al. (2017). "Effect of iron on cholesterol 7 $\alpha$ -hydroxylase expression in alcohol-induced hepatic steatosis in mice." Journal of Lipid Research **58**(8): 1548-1560.
- Lionarons, D. A., et al. (2012). "Evolution of substrate specificity for the bile salt transporter ASBT (SLC10A2) [S]." Journal of Lipid Research **53**(8): 1535-1542.
- Luo, L., et al. (2018). "Assessment of serum bile acid profiles as biomarkers of liver injury and liver disease in humans." PLOS ONE **13**(3): e0193824.
- Lynch, C., et al. (2014). "Activation of the constitutive androstane receptor inhibits gluconeogenesis without affecting lipogenesis or fatty acid synthesis in human hepatocytes." Toxicology and Applied Pharmacology **279**(1): 33-42.
- Macvittie, T., et al. (2019). "The Gastrointestinal Subsyndrome of the Acute Radiation Syndrome in Rhesus Macaques: A Systematic Review of the Lethal Dose-Response Relationship With and Without Medical Management." Health Physics **116**: 1.
- MacVittie, T. J., et al. (2012). "The prolonged gastrointestinal syndrome in rhesus macaques: the relationship between gastrointestinal, hematopoietic, and delayed multi-organ sequelae following acute, potentially lethal, partial-body irradiation." Health Phys **103**(4): 427-453.
- MacVittie, T. J., et al. (2012). "The acute gastrointestinal subsyndrome of the acute radiation syndrome: a rhesus macaque model." Health Physics **103**(4): 411-426.
- Maekawa, M., et al. (2013). "LC/ESI-MS/MS analysis of urinary 3 $\beta$ -sulfooxy-7 $\beta$ -N-acetylglucosaminyl-5-cholen-24-oic acid and its amides: New biomarkers for the detection of Niemann–Pick type C disease." Steroids **78**(10): 967-972.
- Maghsoodi, N., et al. (2019). "Bile acid metabolism is altered in those with insulin resistance after gestational diabetes mellitus." Clinical Biochemistry **64**: 12-17.

- Marin, J., et al. (2015). "Bile Acids in Physiology, Pathology and Pharmacology." Current drug metabolism **17**.
- Mazzacuva, F., et al. (2016). "Identification of novel bile acids as biomarkers for the early diagnosis of Niemann-Pick C disease." FEBS Letters **590**(11): 1651-1662.
- Mendoza, M. E., et al. (2002). "Changes in the pattern of bile acids in the nuclei of rat liver cells during hepatocarcinogenesis." Clinical Science **102**(2): 143-150.
- Mendoza, M. E., et al. (2003). "Physiological characteristics of *allo*-cholic acid." J. Lipid Res. **44**: 84-92.
- Meng, L.-J., et al. (1997). "Profiles of bile acids and progesterone metabolites in the urine and serum of women with intrahepatic cholestasis of pregnancy." Journal of Hepatology **27**(2): 346-357.
- Miyazaki-Anzai, S., et al. (2018). "Simultaneous inhibition of FXR and TGR5 exacerbates atherosclerotic formation." Journal of Lipid Research **59**(9): 1709-1713.
- Monte, M. J., et al. (1997). "Bile acid secretion during synchronized rat liver regeneration." Biochim. Biophys. Acta **1362**: 56-66.
- Monte, M. J., et al. (2005). "Changes in the expression of genes related to bile acid synthesis and transport by the rat liver during hepatocarcinogenesis." Clin. Sci. **109**: 199-207.
- Monte, M. J., et al. (2005). "Transient changes in the expression pattern of key enzymes for bile acid synthesis during rat liver regeneration." Biochim. Biophys. Acta **1734**: 127-135.
- Monte, M. J., et al. (2009). "Bile acids: chemistry, physiology, and pathophysiology." World journal of gastroenterology **15**(7): 804-816.
- Monte, M. J., et al. (2002). "Changes in the pool of bile acids in hepatocyte nuclei during rat liver regeneration." Journal of Hepatology **36**(4): 534-542.
- Nagahashi, M., et al. (2016). "The roles of bile acids and sphingosine-1-phosphate signaling in the hepatobiliary diseases." Journal of Lipid Research **57**(9): 1636-1643.
- Neujahr, D. C., et al. (2014). "Bile acid aspiration associated with lung chemical profile linked to other biomarkers of injury after lung transplantation." American journal

of transplantation : official journal of the American Society of Transplantation and the American Society of Transplant Surgeons **14**(4): 841-848.

- Ohta, K. (1939). "Tetraoxy-norsterocholansäure aus der „Gigi“-Fischgalle (Pelteobagrus nudiceps)." Hoppe-Seyl. Z. **259**(1-6): 53-61.
- Parker, G. A., et al. (2019). "Radiation Nephropathy in a Nonhuman Primate Model of Partial-Body Irradiation With Minimal Bone Marrow Sparing—Part 2: Histopathology, Mediators, and Mechanisms." Health Physics **116**(3).
- Parker, G. A., et al. (2019). "Histopathological Features of the Development of Intestine and Mesenteric Lymph Node Injury in a Nonhuman Primate Model of Partial-body Irradiation with Minimal Bone Marrow Sparing." Health Physics **116**(3): 426-446
- Parker, G. A., et al. (2019). "Lung and Heart Injury in a Nonhuman Primate Model of Partial-body Irradiation with Minimal Bone Marrow Sparing: Histopathological Evidence of Lung and Heart Injury." Health Physics **116**(3): 383.
- Penning, T. M. (1997). "Molecular Endocrinology of Hydroxysteroid Dehydrogenases." Endocrine Reviews **18**(3): 281-305.
- Phillips, F., et al. (2015). "Are bile acid malabsorption and bile acid diarrhoea important causes of loose stool complicating cancer therapy?" Colorectal Disease **17**(8): 730-734.
- Puri, P., et al. (2018). "The presence and severity of nonalcoholic steatohepatitis is associated with specific changes in circulating bile acids." Hepatology **67**(2): 534-548.
- Raselli, T., et al. (2019). "Elevated oxysterol levels in human and mouse livers reflect nonalcoholic steatohepatitis." Journal of Lipid Research **60**(7): 1270-1283.
- Rees, D. O., et al. (2017). "Comparison of the composition of bile acids in bile of patients with adenocarcinoma of the pancreas and benign disease." The Journal of Steroid Biochemistry and Molecular Biology **174**: 290-295.
- Ressom, H. W., et al. (2012). "Utilization of metabolomics to identify serum biomarkers for hepatocellular carcinoma in patients with liver cirrhosis." Analytica Chimica Acta **743**: 90-100.
- Ridlon, J. M., et al. (2016). "Taurocholic acid metabolism by gut microbes and colon cancer." Gut Microbes **7**(3): 201-215.

- Rudling, M. (2016). "Understanding mouse bile acid formation: Is it time to unwind why mice and rats make unique bile acids?" Journal of Lipid Research **57**(12): 2097-2098.
- Saeed, A., et al. (2014). " $7\alpha$ -hydroxy-3-oxo-4-cholestenoic acid in cerebrospinal fluid reflects the integrity of the blood-brain barrier." Journal of Lipid Research **55**(2): 313-318.
- Sagar, N. M., et al. (2020). "The pathophysiology of bile acid diarrhoea: differences in the colonic microbiome, metabolome and bile acids." Scientific Reports **10**(1): 20436.
- Scanff, P., et al. (2004). "Alteration of the enterohepatic recirculation of bile acids in rats after exposure to ionizing radiation." Canadian journal of physiology and pharmacology **82**(2): 114-124.
- Schadt, H. S., et al. (2016). "Bile acids in drug induced liver injury: Key players and surrogate markers." Clinics and Research in Hepatology and Gastroenterology **40**(3): 257-266.
- Schmid, A., et al. (2016). "Bile Acid Metabolome after an Oral Lipid Tolerance Test by Liquid Chromatography-Tandem Mass Spectrometry (LC-MS/MS)." PLOS ONE **11**(2): 1-13.
- Schonewille, M., et al. (2016). "Bile salts in control of lipid metabolism." Curr Opin Lipidol **27**(3): 295-301.
- Setchell, K. D., et al. (1997). "Bile acid concentrations in human and rat liver tissue and in hepatocyte nuclei." Gastroenterology **112**(1): 226-235.
- Shao, Y., et al. (2021). "Comprehensive metabolic profiling of Parkinson's disease by liquid chromatography-mass spectrometry." Molecular Neurodegeneration **16**.
- Shapiro, H., et al. (2018). "Bile acids in glucose metabolism in health and disease." The Journal of Experimental Medicine **215**(2): 383.
- Shi, J., et al. (2018). "Comparison of protein expression between human livers and the hepatic cell lines HepG2, Hep3B, and Huh7 using SWATH and MRM-HR proteomics: Focusing on drug-metabolizing enzymes." Drug Metabolism and Pharmacokinetics **33**(2): 133-140.
- Shiffka, S. J., et al. (2020). "Quantification of common and planar bile acids in tissues and cultured cells." Journal of Lipid Research **61**(11): 1524-1535.

- Shiffka, S. J., et al. (2017). "Planar bile acids in health and disease." Biochimica et Biophysica Acta (BBA) - Biomembranes **1859**(11): 2269-2276.
- Shoda, J., et al. (1993). "Formation of 7 $\alpha$ - and 7 $\beta$ -hydroxylated bile acid precursors from 27-hydroxycholesterol in human liver microsomes and mitochondria." Hepatology **17**(3): 395-403.
- Singh, V. K. and A. O. Olabisi (2017). "Nonhuman primates as models for the discovery and development of radiation countermeasures." Expert Opinion on Drug Discovery **12**(7): 695-709.
- Sjovall, J. and G. Meurant (1985). Sterols and bile acids. Amsterdam, Elsevier Science.
- Song, X., et al. (2013). "Mechanistic insights into isoform-dependent and species-specific regulation of bile salt export pump by farnesoid X receptor." Journal of Lipid Research **54**(11): 3030-3044.
- Souidi, M., et al. (2007). "Effects of ionizing radiation on the activity of the major hepatic enzymes implicated in bile acid biosynthesis in the rat." Comptes rendus biologies **330**(12): 861-870.
- Stärkel, P., et al. (2009). "Foetal 'flat' bile acids reappear during human liver regeneration after surgery." European Journal of Clinical Investigation **39**(1): 58-64.
- Sturman, J., et al. (2019). "Growth, Development and Aging Tissue Taurine Content, Activity of Taurine Synthesis Enzymes and Conjugated Bile Acid Composition of Taurine-Deprived and Taurine-Supplemented Rhesus Monkey Infants at 6 and 12 mo of Age."
- Suzuki, M., et al. (1997). "Determination of 3-oxo- $\Delta^4$ - and 3-oxo- $\Delta^{4,6}$ -bile acids and related compounds in biological fluids of infants with cholestasis by gas chromatography-mass spectrometry." J. Chrom. B **693**: 11-21.
- Swaan, P. W. (2017). Structural biology of the apical bile acid transporter, National Institute of Diabetes and Digestive and Kidzney Diseases.
- Tadano, T., et al. (2006). "Studies of serum and feces bile acids determination by gas chromatography-mass spectrometry." Rinsho Byori. The Japanese Journal Of Clinical Pathology **54**(2): 103-110.
- Takahashi, S., et al. (2016). "Cyp2c70 is responsible for the species difference in bile acid metabolism between mice and humans." Journal of Lipid Research **57**(12): 2130-2137.

- Thakare, R., et al. (2018). "Species differences in bile acids I. Plasma and urine bile acid composition." Journal of Applied Toxicology **38**(10): 1323-1335.
- Thakare, R., et al. (2018). "Species differences in bile acids II. Bile acid metabolism." Journal of Applied Toxicology **38**(10): 1336-1352.
- Wahlström, A., et al. (2017). "Induction of farnesoid X receptor signaling in germ-free mice colonized with a human microbiota." Journal of Lipid Research **58**(2): 412-419.
- Wang, L., et al. (2020). "Mechanism of Asbt (Slc10a2)-related bile acid malabsorption in diarrhea after pelvic radiation." International Journal of Radiation Biology **96**(4): 510-519.
- Xiao, J. F., et al. (2012). "LC-MS Based Serum Metabolomics for Identification of Hepatocellular Carcinoma Biomarkers in Egyptian Cohort." Journal of Proteome Research **11**(12): 5914-5923.
- Xie, G., et al. (2015). "Profiling of Serum Bile Acids in a Healthy Chinese Population Using UPLC-MS/MS." Journal of Proteome Research **14**(2): 850-859.
- Yaping Shao, Y. O. T. L. X. L. X. X. S. L. G. X. W. L. (2020). "Alteration of Metabolic Profile and Potential Biomarkers in the Plasma of Alzheimer's Disease." Aging and disease **11**(6): 1459-1470.
- Zhang, C. Y. K., et al. (2020). "Bronchoalveolar bile acid and inflammatory markers to identify high-risk lung transplant recipients with reflux and microaspiration." Journal of Heart & Lung Transplantation **39**(9): 934-944.
- Zheng, X., et al. (2009). "Computational Models for Drug Inhibition of the Human Apical Sodium-Dependent Bile Acid Transporter." Molecular Pharmaceutics **6**(5): 1591-1603.